Carnegie Mellon University

CARNEGIE INSTITUTE OF TECHNOLOGY

THESIS

SUBMITTED IN PARTIAL FULFILLMENT OF THE REQUIREMENTS

FOR THE DEGREE OF Doctor of Philosophy

TITLE **Reducing Carbon Intensity in Restructured Markets: Challenges and Potential Solutions**

PRESENTED BY **Roger Alan Lueken**

ACCEPTED BY THE DEPARTMENT OF

Engineering & Public Policy

_____ _____

MAJOR PROFESSOR DATE

_____ _____

DEPARTMENT HEAD DATE

APPROVED BY THE COLLEGE COUNCIL

_____ _____

DEAN DATE

Reducing Carbon Intensity in Restructured Markets: Challenges and Potential Solutions

SUBMITTED IN PARTIAL FULFILLMENT OF THE REQUIREMENTS FOR

THE DEGREE OF

DOCTOR OF PHILOSOPHY

IN

ENGINEERING & PUBLIC POLICY

Roger Alan Lueken

B.S., Mechanical Engineering, Purdue University

M.S., Engineering and Public Policy, University of Maryland

Carnegie Mellon University

Pittsburgh, PA

September 2014

ACKNOWLEDGEMENTS

This work was supported in part by the Doris Duke Charitable Foundation, the Richard King Mellon Foundation, The Heinz Endowments, and the Carnegie Mellon Electricity Industry Center. This research was also supported in part by the Climate and Energy Decision Making (CEDM) center, created through a cooperative agreement between the National Science Foundation (SES-0949710) and Carnegie Mellon University. A portion of this research was also supported by the U.S. Department of Energy's National Energy Technology Laboratory.

For their advice and helpful conversations over the course of my research I would like to thank my fellow students, including Jared Moore, David Luke Oates, Todd Ryan, Allison Weis, Eric Hittenger, Kyle Siler-Evans, Jinhyok Heo, and Steve Rose. I would also like to thank Kelly Klima, Mike Griffin, Fallaw Sowell, Peter Adams, and Paulina Jaramillo. I am grateful to PJM, the EPA, and the EIA for making significant amounts of data publically available.

I would also like to thank Patti Steranchak, Victoria Finney, Barbara Bugosh, Adam Loucks, and the rest of the EPP staff for all of their help and support.

I am grateful for the support and guidance of my advisor Jay Apt, and the rest of my committee: Granger Morgan, Kathleen Spees, and Gabriela Hug.

Finally, I would like to thank my friends and family, especially my wife Colleen Lueken and my parents, Geriann and Paul Lueken.

ABSTRACT

The U.S. electric power sector is in the early stages of transitioning from a reliance on carbon intensive generation sources to a system based on low-carbon sources. In this thesis, I present analyses of four different aspects of this transition, with an emphasis on the PJM Interconnection.

The effects of bulk electricity storage on the PJM market

I analyze the value of three storage technologies in the PJM day-ahead energy market, using a reduced-form unit commitment model with 2010 data. I find that large-scale storage would increase overall social welfare in PJM. However, the annualized capital costs of storage would exceed social welfare gains. Consumers would save up to $4 billion annually, largely at the expense of generator surplus. Storage modestly increases emissions of CO_2 and other pollutants.

The external costs and benefits of wind energy in PJM

Large deployments of wind create external costs and benefits that are not fully captured in power purchase agreements. I find that wind's external costs in the PJM market are uncertain but significant when compared to levelized PPA prices. Pollution reduction benefits are very uncertain but exceed external costs with high probability.

The climate and health effects of a USA switch from coal to gas electricity generation

I analyze the emission benefits created by a hypothetical scenario in which all U.S. coal plants are switched to natural gas plants in 2016. The net effect on warming is unclear; results are highly sensitive to the rate of fugitive methane emissions and the efficiency of replacement gas plants.

However, the human health benefits of such a switch are substantial. The costs of building and operating new gas plants likely exceed the health benefits.

Robust resource adequacy planning in the face of coal retirements

Over the next decade, many U.S. coal-fired power plants are expected to retire, posing a challenge to system planners. I investigate the resource adequacy requirements of the PJM Interconnection, and how procuring less capacity may affect reliability. I find that PJM's 2010 reserve margin of 20.5% was sufficient to achieve the stated reliability standard with 90% confidence. PJM could reduce reserve margins to 13% and still achieve levels of reliability accepted by other power systems.

TABLE OF CONTENTS

LIST OF TABLES

List of Figures

Chapter 1: INTRODUCTION

The U.S. electric power sector is currently undergoing one of the most significant transformations in its history. The risks posed by climate change are increasingly apparent to the public, policymakers, and regulators. Pressure to reduce greenhouse gas emissions, as well as criteria pollutants that harm public health, is growing. In response, the industry has begun to shift how electricity is generated and consumed in fundamental ways.

This transformation poses many challenges. Large deployments of intermittent renewables will make grid operations and planning more difficult. Significant retirements of heavily polluting coal plants will challenge the ability of system planners to provide reliable service. However, potential solutions exist. Abundant shale gas resource have made generating power from natural gas much more economical over the past decade. Emerging technologies, such as grid-scale electricity storage and demand response, may also be viable solutions.

The PJM Interconnection is an interesting microcosm of this transformation. PJM is the nation's largest independent system operator, serving more than 60 million people [1]. As of 2010, PJM had 78 GW of installed coal capacity, which made up 41% of total capacity [2]. PJM has identified 11 GW of this capacity "at high risk" of retirement, and an additional 14 GW "at some risk" of retirement [2]. At the same time, PJM member states have established renewable portfolio standards that are expected to lead to a tenfold increase in PJM's generation from wind and solar from 1.2% of total generation in 2010 to 14% of total generation by 2026 [3,4]. As a restructured market, PJM must manage these and other challenges through market designs that are fair and transparent to participants.

This thesis contains four studies into different aspects of the challenges the power sector will face over the coming years while transitioning to a low-carbon future. The focus of these analyses is

the PJM Interconnection, due to its relative importance, size, and leadership status amongst U.S. grid operators.

In Chapter 2, I investigate the potential for bulk electricity storage to participate in the PJM wholesale energy market. Widespread deployment of storage could assist in managing the intermittency of renewable sources, and in meeting peak load. Storage profits on energy markets by charging during low price hours, typically at night, and discharging at peak hours when prices are high. Several technologies have been proposed for the bulk storage of electricity, including pumped hydropower storage, compressed air storage, and chemical batteries. I find that storage would reduce prices at peak hours on PJM's energy market. This in turn would create large savings for consumers, and a net reduction in system costs. However, the capital costs of storage are likely to exceed the benefits they provide.

In Chapter 3, I explore the external costs and benefits of wind power in PJM. Large deployments of wind create costs and benefits that accrue to entities other than the owner. Wind creates external benefits by offsetting emissions of greenhouse gases and criteria pollutants that would otherwise come from fossil generation. External costs are due to the intermittency and variability of wind, which can force other plants to operate less efficiently and can require significant grid expansion and reinforcement. I find that the external costs of wind are uncertain, but may be significant when compared to the levelized cost of wind. External benefits due to pollution reduction are very uncertain but exceed external costs with very high probability.

In Chapter 4, I present an analysis of the potential climate and health benefits of switching the U.S. coal plant fleet to either gas plants or zero emission plants. The advent of low cost shale gas has made generation from natural gas increasingly economical. This has prompted industry and politicians to welcome gas as a 'bridge fuel' to a low carbon grid. I analyze the effect of retiring all

U.S. coal plants in 2016, and replacing them with either natural gas generation or zero emission plants such as renewables or nuclear. I find that the effect this switch would have on warming is unclear; results are highly sensitive to rate of fugitive emissions from the production and transportation of natural gas. However, the switch would significantly reduce criteria pollutant emissions and benefit public health.

In Chapter 5, I analyze the effects that significant retirements of coal plants may have on the reliability of the PJM system. PJM procures sufficient capacity to ensure that supply shortages only occur once per ten years. I find that PJM correctly sets its capacity target to meet this standard. However, PJM procures more capacity than needed to meet the target, suggesting PJM is risk averse and wants to meet the standard with 90% confidence. The reliability standard set by PJM is more stringent than the standards used by several other systems in the U.S. and abroad. Switching to a different reliability standard would reduce PJM's needed level of capacity by 10 GW, equal to the amount of coal capacity that PJM deems "at high risk" of retirement.

The work in this thesis is intended to better inform policies associated with reducing emissions in restructured markets. The challenges of transitioning to a low-carbon electricity system are multifaceted; this thesis contains studies into four aspects of these challenges. With carefully designed policies and market rules, system operators will be able to reduce emissions in intelligent and cost-effective ways.

1.1 References

[1] PJM Interconnection. *PJM 2013 Annual Report*; Norristown, PA, **2013.**

[2] PJM Interconnection. *Coal Capacity at Risk of Retirement in PJM: Potential Impacts of the Finalized EPA Cross State Air Pollution Rule and Proposed National Emissions Standards for Hazardous Air Pollutants*; Norristown, PA, **2011**.

[3] PJM Interconnection. *2010 State of the Market Report for PJM, Volume 2*; Norristown, PA. Prepared by Monitoring Analytics, LLC. **2011**.

[4] PJM Interconnection. PJM Renewable Integration Study; Norristown, PA. Prepared by GE Energy Consulting. **2014**.

Chapter 2: THE EFFECTS OF BULK ELECTRICITY STORAGE IN THE PJM MARKET

Abstract

Recent advancements in battery technologies may make bulk electricity storage economically feasible. We analyze the value of two electrochemical storage technologies and traditional pumped hydropower storage in the 2010 PJM day-ahead energy market, using a reduced-form unit commitment model. We find that large-scale storage would increase overall social welfare in PJM. However, the annualized capital costs of storage would exceed social welfare gains. Consumers would save up to $4 billion annually due to reduced peak prices and reduced reliance on expensive peaking generators. These savings are equivalent to ~10% of sales in the PJM day-ahead energy market. Savings come largely at the expense of generator surplus. Existing market mechanisms are insufficient to encourage the socially optimal quantity of storage. Storage reduces the profitability of generators and the need for peaking generation capacity. Storage modestly increases emissions of CO_2 and other pollutants in a system with 2010 PJM characteristics.

This paper was published as Lueken, R.; Apt, J. The effects of bulk electricity storage on the PJM market. *Energy Systems*. ***2014***, DOI: 10.1007/s12667-014-0123- 7.

I. Introduction

Electric power systems today have limited storage capacity. Both in the USA and worldwide, storage makes up less than 3% of generation capacity [1]. This lack of storage forces grid operators to continuously balance generation and load, and prevents the electricity sector from operating as a conventional competitive market that relies on inventory.

Pumped hydropower storage (PHS) is the predominant storage technology today, making up 99% of all deployed storage capacity. The Federal Energy Regulatory Commission (FERC) has issued preliminary permits to an additional 55 PHS facilities, with a combined capacity of 47 GW [2]. R&D investments have led to rapid improvements in advanced battery technologies. Recent advancements suggest batteries with long cycle life may approach cost parity with pumped hydropower [1].

Inexpensive electricity storage has the potential to transform electricity markets. Storage can provide a variety of high-value services, including ancillary services such as frequency regulation [3]. Although profitable, these relatively small market opportunities are expected to saturate quickly: in PJM, average hourly regulation procurement is less than 1 GW, or ~1% of total load [4]. At that point, storage operators and manufacturers will consider larger volume, lower value applications. One such application is arbitrage in wholesale energy markets.

In wholesale markets, storage profits by buying electricity when prices are low and selling at peak hours. For small amounts of storage, this arbitrage will not affect prices or generator dispatch order. A large body of research exists on how small, price-taking storage devices can maximize profits in wholesale markets. This research has looked at storage in several applications, including the value of electric vehicle batteries for grid storage [5] and the economics of storage in the New York state electricity market [6].

How large amounts of storage will change wholesale markets is less well understood. Existing studies have found that the benefits of 1 GW of storage are 10% - 20% less than price-taking storage in PJM, assuming a linear relationship between load and electricity price [7]. Recent research [8] used a unit commitment model to study the effect of up to 800 MW of electricity storage on the Irish power system (12% of peak annual demand), finding that storage reduces production costs, but increases average electricity prices due to storage capital costs. Using a game-theoretic approach, Schill and Kemfert find that while the utilization of storage depends on the operator's market power, storage generally increases consumer welfare and reduces producer surplus in the German market [9]. Sioshansi analyses the value of large-scale wind and energy storage deployments in the ERCOT (Texas) market and the effects of market power [10].

Here we analyze the effect of bulk storage on the PJM's day-ahead wholesale energy market and capacity market. Storage has the potential to effectively provide power at peak load hours, which would reduce wholesale energy prices and expenditures on capacity markets. We estimate the value of large storage deployments in the PJM Interconnection's day-ahead energy market and capacity market with a reduced-form unit commitment model. The viability of storage in PJM is likely to be representative, as PJM is the world's largest competitive electricity market with $35 billion in transactions and 167 GW of installed capacity in 2010 [4].

We build upon existing research by investigating the feasibility of three different storage technologies: pumped hydropower storage, aqueous hybrid ion (AHI) batteries (an example of the class of aqueous intercalation batteries), and sodium sulfur (SS) batteries. We investigate how storage will affect overall consumer welfare. We also investigate the effect on consumer costs on the day-ahead wholesale market and capacity market, the profitability of bulk storage, and its effect on the revenues of generators. We constrain the analysis to short-term effects; we assume storage does not cause changes to the PJM generation fleet or net load (we do include the additional load imposed by

charging the storage). Finally, we investigate how bulk storage will affect emissions of CO_2, nitrous oxides (NO_X), and sulfur dioxide (SO_2).

2.1 Methods

2.1.1 Unit commitment and economic dispatch model

We developed a reduced-form unit commitment and economic dispatch (UCED) model, called PHORUM, to simulate the 2010 PJM day-ahead market. This software is open source and freely available online[1]. PHORUM is a mixed integer linear program (MILP) that calculates the least-cost combination of generators and storage to meet load at each hour on the day-ahead market, subject to generator and transmission constraints. We assume that under a scenario with large capacities of storage, system operators will control the dispatch of storage to maintain grid reliability.

PJM calculates locational marginal prices (LMPs) for more than 10,000 nodes [4]. The nodal pricing system allows PJM to account for transmission constraints that result from locational variation in supply and demand. In general, transmission constrains the flow of power from Midwestern states to coastal load centers, resulting in higher LMPs along the coast. Congestion costs make up approximately 5% of costs in the PJM day-ahead energy market [4]. Details of transmission assets are designated as Critical Energy Infrastructure Information and not publically available. However, PJM provides hourly data on the capacity of seven transmission interfaces, each made up of multiple 500 kV lines, which form critical congestion paths that made up 49% of all congestion costs in 2010 [4].

Based on the seven transmission interfaces, we divided PJM into five transmission buses to account for transmission constraints (Figure 2-1). We aggregated the seven PJM interfaces into six

[1] PHORUM can be downloaded at https://github.com/rlueken/PHORUM

transmission lines between regions. We ignored other transmission constraints, and assumed lossless power flow between buses. We assumed that within each bus, transmission is unconstrained and all LMPs are equal. 2010 LMP data shows that within our defined buses, zonal LMPs are highly correlated (Figure A-3), supporting this assumption. Other researchers have used this technique of dividing PJM into regions [11]. More details can be found in Appendix A.

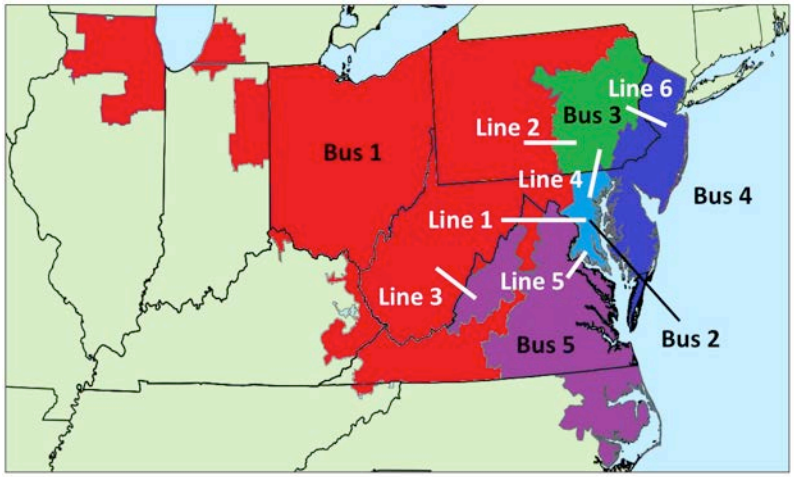

Figure 2-1. Reduced form model of the PJM Interconnection

We simulated 1,017 generators and four existing PJM pumped hydroelectric storage (PHS) facilities: Bath County (VA, 2.8 GW), Yards Creek (NJ, 400 MW), Muddy Run (PA, 1 GW), and Smith Mountain (VA, 240 MW). These facilities total 4.5 GW of capacity, approximately 2.5% of total generation capacity [12]. Generators smaller than 5 MW were excluded. We assumed demand is perfectly inelastic; the short-term elasticity of demand is highly inelastic [13]. We constrained the analysis to short-term effects; we assumed storage does not cause changes to the PJM generation fleet or net load.

PHORUM tracks emissions of CO_2, NO_X, and SO_2 from each generator, using emission rate data from the EPA Emissions & Generation Resource Integrated Database (eGRID) [12]. We assumed emission rates are linear with output level and independent of time of year or ambient temperature. We also did not account for variations in NO_X output for ozone season. We tracked

emissions associated with generator startups [14]; however, startup emissions are less than 1% of total emissions.

We ran 365 daily optimizations, each minimizing costs over a 48-hour period. The optimizations were rolled over, with the 25th hour of the previous optimization becoming the first hour of the next. This rollover ensured that minimum runtime/downtime constraints held between days. Storage state of charge is constrained to 50% for the first hour of the first optimization and the 48th hour of each optimization. PJM's actual dispatch process minimizes costs over one day only; cross-day decisions are made manually by the day-ahead operator [15]. Appendix A contains more details on how variables are passed across day boundaries.

We assumed perfect information over the 48-hour optimization. In reality, the system operator has perfect information for the first 24 hours of each period (the day ahead forecast), but not hours 25-48 (the day ahead forecast for the second day). The assumption of perfect information inflates the value of storage; in reality, forecast error in load and wind generation will lead to suboptimal use of storage. Optimizing storage operations over a longer period of time would increase the value of storage; however, accurately predicting load more than 48 hours out may be difficult. The relatively high charging and discharging speed of storage gives system operators the ability to flexibly respond to unforeseen forecast errors in real time [3]. We do not simulate the real time market, and therefore do not capture this value.

Two types of data were used: hourly data and generator data. Hourly data from PJM were used to calculate net hourly load at each bus and transmission limits between buses. Net hourly load considers such factors as imports, exports, and must-take wind generation. Generator data were used to characterize each generator, and were derived from multiple sources, including eGRID, EPA National Electric Energy Data System (NEEDS) database, and PJM reports. Data on fuel

prices, aggregated by state and by month, were from the Energy Information Agency. Appendix A contains details on all data sources.

To maintain reliability, PJM co-optimizes the day-ahead energy market and a separate day-ahead scheduled reserve (DASR) market. Rather than co-optimizing the energy and DASR markets, we approximated hourly reserve requirements by adding 3.6 GW to hourly load. 3.6 GW is equivalent to PJM's hourly synchronized reserve requirement: the total capacity of largest unit in RFC (bus 1), the largest unit in the Mid-Atlantic control zone (buses 2-4), and the largest unit in Dominion (bus 5) [16]. This approximation overstates the load each hour, and therefore increases hourly LMPs. However, the error caused by this approximation is minimal; compared to a scenario in which reserve requirements are not added to load, average LMPs increase by less than 5%. When compared to actual 2010 LMPs, including reserves as load also results in lower error than not including reserves as load. Section 3 contains more details on model validation. Mean hourly LMP error is 0%, suggesting this approximation does not induce bias into our results. The approximation was necessary to keep computation time manageable.

Table 2-1. Model Nomenclature

Constants			
$D_r(t)$	Consumer demand at time t in bus r [MW]	$P_i(0)$	Initial level of generator i [MW]
$IMP_r(t)$	Net imports from other regional transmission operators (RTOs) at time t to bus r [MW]	$\dot{P}_i$	Ramp rate of generator i [MW/h]
$ND_r(t)$	Net load demand at time t in bus r [MW]	S_i	Startup cost of generator i [$]
$SR_r(t)$	Spinning reserve requirement at time t for bus r [MW]	$U_i(0)$	Initial state of generator i (1 if online, 0 otherwise)
$WG_r(t)$	Wind generation at time t in bus r [MW]	UT_i, DT_i	Minimum uptime / downtime of generator i
$\overline{P_{rm}}(t)$	Max power flow on interface rm [MW]	**Variables**	
$\overline{C}_k$	Max SoC of storage unit k [MWh]	$p_{r,rm}(t)$	Power imported (+) or exported (-) from bus r via interface rm [MW]
$C_k(0)$	Initial SoC of storage unit k [MWh]	$c_k(t)$	SoC of storage unit k at time t [MWh]
$\overline{P_k}$	Max charge/discharge rate from storage unit k [MW]	$pd_k(t)$, $pc_k(t)$	Power discharged or charged by storage unit k at time t [MW]
P	Round trip efficiency of storage units [%]	$p_i(t)$	Power generated by generator i at time t [MW]
FC_i	Fuel cost of generator i [$/MMBtu]	$s_i(t)$	Startup cost of generator i at period t [$]
G_i	Number of periods generator i must be initially online due to its minimum up time constraint	$u_i(t)$	State of generator i at time t (1 if online, 0 otherwise)
HR_i	Heat rate of generator i [MMBtu/MWh]	**Sets**	
L_i	Number of periods generator i must be initially offline due to its minimum down time constraint	I_r	Set of indices of the generators in bus r
OM_i	Variable O&M costs of generator i [$/MWh]	K_r	Set of indices of the storage units in bus r
$\overline{P_i}, \underline{P_i}$	Max and min output from generator i [MW]	R	Set of buses
		RM	Set of indices of the transmission interfaces
		T	Set of indices of the time periods

Table 2-2. Model Formulation

Minimize

$$\sum_{t\in T}\sum_{r\in R}\sum_{i\in I_r} 1.1 p_i(t) * (HR_i * FC_i + OM_i) + s_i(t) \quad (2\text{–}1)$$

System Constraints

$$ND_r(t) = \sum_{i\in I_r} p_i(t) + \sum_{k\in K_r} (pd_k(t) - pc_k(t)) + \sum_{rm\in RM} p_{r,rm}(t) \quad \forall t \in T, \forall r \in R \quad (2\text{–}2)$$

$$-\overline{P_{rm}}(t) \le p_{r,rm}(t) \le \overline{P_{rm}}(t) \quad \forall r \in R, \forall rm \in RM, \forall t \in T \quad (2\text{–}3)$$

Storage Constraints

$$c_k(t+1) = c_k(t) + \sqrt{\rho} * pc_k(t) - \frac{pd_k(t)}{\sqrt{\rho}} \quad \forall k \in K, \forall t \in T \quad (2\text{–}4)$$

$$0 \le c_k(t) \le \overline{C_k} \quad \forall k \in K, \forall t \in T \quad (2\text{–}5)$$

$$0 \le pd_k(t) \le \overline{P_k} \quad \forall k \in K, \forall t \in T \quad (2\text{–}6)$$

$$0 \le pc_k(t) \le \overline{P_k} \quad \forall k \in K, \forall t \in T \quad (2\text{–}7)$$

$$c_k(0) \le C_k(0) \quad \forall k \in K \quad (2\text{–}8)$$

Generator Constraints

$$p_i(0) = P_i(0) \quad \forall i \in I \quad (2\text{–}9)$$

$$u_i(0) = U_i(0) \quad \forall i \in I \quad (2\text{–}10)$$

$$s_i(t) \ge S_i * (u_i(t) - u_i(t-1)) \quad \forall i \in I, \forall t \in T \quad (2\text{–}11)$$

$$s_i(t) \ge 0 \quad \forall i \in I, \forall t \in T \quad (2\text{–}12)$$

$$\underline{P_i} * u_i(t) \le p_i(t) \le \overline{P_i} * u_i(t) \quad \forall i \in I, \forall t \in T \quad (2\text{–}13)$$

$$p_i(t) \le p_i(t-1) + \dot{P}_i * u_i(t-1) + \underline{P_i} * (u_i(t) - u_i(t-1)) \quad \forall i \in I, \forall t \in T \quad (2\text{–}14)$$

$$p_i(t-1) - p_i(t) \le \dot{P}_i * u_i(t) + \underline{P_i} * (u_i(t-1) - u_i(t)) \quad \forall i \in I, \forall t \in T \quad (2\text{–}15)$$

$$\sum_{t=1}^{G_i} [1 - u_i(t)] = 0 \quad \forall i \in I \quad (2\text{–}16)$$

$$\sum_{n=t}^{t+UT_i-1} u_i(n) \ge UT_i [u_i(t) - u_i(t-1)] \quad \forall i \in I, \forall t \in G_i + 1 \ldots T - UT_i + 1 \quad (2\text{–}17)$$

$$\sum_{n=t}^{T} \{u_i(n) - [u_i(t) - u_i(t-1)]\} \ge 0 \quad \forall i \in I, \forall t \in T - UT_i + 2 \ldots T \quad (2\text{–}18)$$

$$\sum_{t=1}^{L_i} u_i(t) = 0 \quad \forall i \in I \quad (2\text{–}19)$$

$$\sum_{n=t}^{t+DT_i-1} [1 - u_i(n)] \ge DT_i [u_i(t-1) - u_i(t)] \quad \forall i \in I, \forall t \in L_i + 1 \ldots T - DT_i + 1 \quad (2\text{–}20)$$

$$\sum_{n=t}^{T} \{1 - u_i(n) - [u_i(\mathrm{t}-1) - u_i(\mathrm{t})]\} \ge 0 \quad \forall i \in I, \forall t \in T - DT_i + 2 \ldots T \quad (2\text{–}21)$$

$$ND_r(t) = D_r(t) + SR_r(t) - WG_r(t) + IMP_r(t) \quad \forall t \in T \quad (2\text{–}22)$$

Our formulation owes much to earlier work [17, 18] and is similar to the model used by PJM to dispatch power on the day-ahead market [19]. The objective function, (2–1), minimizes the total social cost of providing electricity, which includes the variable costs and startup costs. The equation includes the 10% cost adder that PJM allows all generators to add to their hourly bid [20]. (2–2) sets separate supply/demand constraints for each bus. The LMPs at each bus are the negative Lagrange multiplier (shadow price) of these constraints.

(2–3) sets transmission limits between buses. Equations (2–4) to (2–8) are storage constraints that limit the capacity, charge/discharge rates, and set initial charge levels. (2–9) and (2–10) set initial conditions for generators. Equations (2–11) and (2–12) trigger startup costs when a generator turns on, and (2–13) constrains generation capacity while the generator is online. Equations (2–14) and (2–15) constrain generator ramp rates. Equations (2–16) to (2–18) ensure generators satisfy uptime constraints: (2–16) sets initial uptimes, (2–17) constraints uptimes for subsequent hours, and (2–18) forces generators that turn on near the end of the day to stay on over the final time periods. Equations (2–19) to (2–21) are analogous to (2–16) to (2–18), but for generator downtimes. Equation (2–22) calculates net hourly load in each region, considering wind generation and imports/exports to PJM.

2.1.2 Storage modeling

We modeled three storage technologies: pumped hydropower, aqueous hybrid ion (AHI) batteries, and sodium sulfur (SS) batteries. We modeled each technology with four parameters: capacity (in GW), round-trip efficiency (RTE), duration (how long storage can provide the rated capacity before going flat), and location (bus 1-5). We varied capacity from 0.5 – 80 GW (0.4% - 60% of peak annual demand).

Data on storage technologies is uncertain for three reasons. First, AHI and SS battery technologies are relatively new and extensive commercial data are not yet available. Second, performance and cost of large storage projects vary greatly. Third, the RTE of electrochemical batteries depends on how quickly they are charged and discharged; charging more slowly improves efficiency [21]. To incorporate these uncertainties, we modeled two cases for each technology, as shown in Table 2-3. The lower bound scenario assumes pessimistic technical assumptions and fast charging/discharging (low RTE, low duration, high capital cost); the upper bound scenario assumes optimistic technical assumptions and slow charging/discharging (high RTE, high duration, low capital cost). Cycle counts are held constant between upper and lower bound scenarios. Parameter assumptions are from [1, 22, 23].

Table 2-3. Modeled storage technologies [1, 22, 23]. Costs in 2010 dollars

Technology	Duration [hours]	% Round trip efficiency	Maximum cycle count	Cost [$/kWh]
Aqueous hybrid ion (AHI) battery				
Lower bound	4	80%	10,000	300
Upper bound	20	90%	10,000	300
Sodium sulfur (SS) battery				
Lower bound	6	75%	4,500	550
Upper bound	8	86%	4,500	535
Pumped hydropower				
Lower bound	4	70%	>13,000	430
Upper bound	12	85%	>13,000	250

We deployed storage to each of the five buses in proportion to fraction of total annual load on that bus (45% bus 1, 10% bus 2, 8% bus 3, 24% bus 4, 14% bus 5). We assumed storage could be deployed in any grid location and in any capacity. We also assumed storage is dispatched by the system operator, who has perfect information of prices over the 48-hour optimization. We made several simplifying assumptions in our model of storage devices, ignoring storage degradation,

minimum depth of discharge, operational costs, and standby losses. By ignoring these complications, we somewhat overestimated the value of storage. We set storage state of charge to 50% for the first hour of the year and the last hour of each optimization.

We calculated the lifespan of each storage technology with (2–23). We assumed one 'cycle' is equivalent to discharging energy equal to the device's capacity. We assumed all devices are decommissioned after 40 years, putting an upper bound on lifespan.

$$Lifespan = \min\left(\frac{total\ cycle\ count * kWh\ capacity}{annual\ kWh\ discharged}, 40\right) \quad (2–23)$$

2.1.3 Effects of storage on market participants

We modeled the effect of bulk storage by first simulating a 'business as usual' case, the actual operations of the 2010 PJM day-ahead energy market. We then added bulk storage and examine how prices, dispatch order, and emissions changed. From the annual simulations, we quantified the following effects that storage has on participants in the PJM wholesale market.

Consumer benefits

We analyzed the benefits that storage provides to consumers on the PJM day-ahead wholesale energy market and capacity market. We quantified energy market savings as the reduction in total annual consumer expenditures on the energy market, as calculated by Equation (2–24).

$$Consumer\ energy\ costs = \sum_{hour}\sum_{bus} LMP_{hour,bus} * Load_{hour,bus} \quad (2–24)$$

In PJM, generators receive payments on the capacity market for providing firm capacity towards reliability. Bulk storage reduces the amount of capacity that is needed; as more storage is deployed, fewer peaking plants are needed and could in theory be decommissioned. We quantified the savings to consumers if these unused plants are decommissioned with the 2010/2011 PJM capacity auction

price of $175/MW-day [24]. We did not endogenously model effects of storage on capacity auction clearing prices, but performed sensitivity analyses on the benefits under a range of clearing prices (see section 5). Storage is currently ineligible for capacity payments in PJM [25]. Other research has estimated the capacity value of storage by using other methods [26, 27, 28].

Finally, we calculated the net consumer benefits of storage: changes in the money transacted on the wholesale energy and capacity market minus the annualized cost of storage. A positive net consumer benefit means consumers are made better off by storage on the wholesale and capacity markets. We annualized capital cost using an 8% cost of capital and storage lifespan calculated with Equation (2–22).

Effect on generators

Bulk storage changes the dispatch of generators, altering how much electricity generators produce and how much revenues they receive. For each generator in PJM, we compared annual electricity production and revenues for a scenario with storage to the business as usual scenario.

Storage profitability

Storage profits in this application by arbitraging between high and low prices on the wholesale energy market. Storage profits were calculated as in (2–25).

$$StorageProfit = \sum_{buses} \sum_{hours} (LMP_{bus,hour} * Discharge_{bus,hour} - LMP_{bus,hour} * Charge_{bus,hour}) - AnnualCost \quad (2–25)$$

Overall social welfare

We define changes in overall social welfare as reductions in total energy market costs minus the annualized capital cost of storage. Reductions in total energy market costs, measured as improvements to the system operator's cost minimization (2–1), are the net effect of storage on consumers, generators, and storage operators. Changes in the capacity market are excluded, as any consumer savings in the capacity market are a direct transfer from generators. Our social welfare

analysis excludes implications of adding storage on other markets and the effects of changes in emissions of CO_2, NO_X, and SO_2.

Emissions

We quantified the change in annual emissions of CO_2, NO_X, and SO_2 due to storage by comparing the total annual emissions from each PJM generator in a scenario with storage to the business as usual scenario.

2.2 Validation

To validate that PHORUM captures the salient factors that determine electricity price and dispatch order, we constructed a business as usual (BAU) scenario that simulates the market as it was in 2010. We then compared the LMPs from the BAU simulation to the actual 2010 day-ahead market LMPs, aggregated by bus. We measured accuracy with two metrics: hourly error and daily arbitrage error. The first tracks the model's accuracy in predicting prices each hour (2–26). The second tracks how well PHORUM predicts the minimum and maximum daily prices (2–27).

The model consistently modestly under-predicts arbitrage and therefore under-predicts the value of storage. We investigated the implications by comparing the total annual revenue a price-taking storage device would receive under the simulated LMPs and the actual 2010 LMPs. Annual revenue to storage with a two-hour duration (charges the two lowest priced hours and discharges the two highest priced hours each day) is 3% less under the simulated LMPs than the actual 2010 LMPs; revenue for 20-hour duration storage is 10% less. We conclude that although our results will be biased to somewhat under-predict the value of storage, results are close enough to the observed data to validate the model's usefulness for this application.

Table 2-4. Validation equation and variables

Equation		Variables	
$Hourly\ Error = \frac{LMP_{modeled} - LMP_{actual}}{LMP_{actual}}$	(2–26)	$LMP_{modeled}$	Modeled hourly LMP
		LMP_{actual}	Actual 2010 hourly LMP
$Daily\ Aritrage\ Error = \frac{\Delta LMP_{max,modeled} - \Delta LMP_{max,actual}}{\Delta LMP_{max,modeled}}$	(2–27)	$\Delta LMP_{max,modeled}$	Modeled maximum daily difference in hourly LMPs
		$\Delta LMP_{max,actual}$	Actual 2010 maximum daily difference in hourly LMPs

Table 2-5 Validation Results

	Bus 1	Bus 2	Bus 3	Bus 4	Bus 5	Average
Hourly Error (%)						
Mean	1%	0%	8%	5%	-15%	0%
Standard Deviation	24%	24%	24%	23%	21%	23%
Arbitrage Error (%)						
Mean	4%	-6%	9%	15%	-34%	-2%
Standard Deviation	72%	64%	68%	71%	52%	65%

2.3 Results

2.3.1 Consumer benefits

Storage benefits consumers in two ways: by reducing costs in the wholesale energy market, and by reducing reliance on expensive peaking generators. Table 2-6 shows how consumer benefits increase as more storage is deployed.

Storage reduces wholesale energy costs by lowering locational marginal prices (LMPs) at high-load hours. Annual wholesale energy savings reach $2 billion. More than 75% of total savings are reached with 20 GW of storage. These savings are up to 6% of total 2010 PJM wholesale energy

costs of $35 billion. Storage also reduces LMP volatility; large deployments reduce volatility by more than 50%.

Storage reduces consumer capacity costs by replacing peaking plants, which in theory could be decommissioned. Up to 30 GW, or 20% of total PJM capacity, could be retired (Figure 2-2). Capacity savings approach $2 billion, assuming the 2010/2011 PJM capacity auction price of $175/MW-day [24]. The majority of these benefits are achieved by 20 GW of storage.

Decommissioning plants due to bulk storage would not significantly affect PJM reserve margins. According to the North American Electric Reliability Corporation (NERC), any storage primarily used for energy (not regulation or transmission) qualifies as reserves [29]. Therefore, PJM reserve margins do not fall below 15% for any level of storage deployment, as additions in storage capacity offset the generation capacity that is decommissioned.

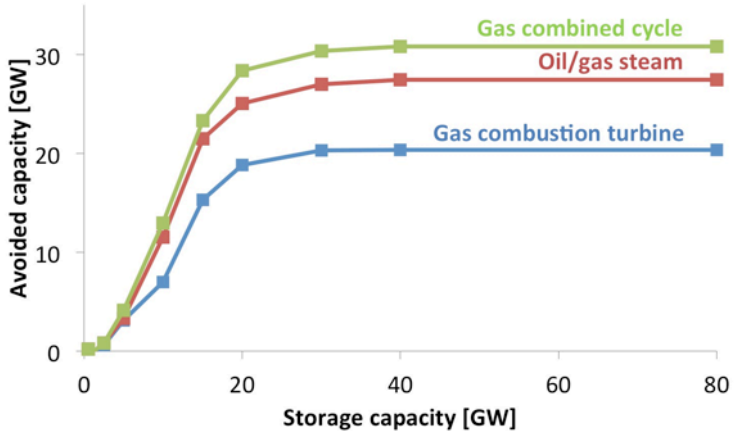

Figure 2-2. Cumulative peaking capacity that is never needed due to storage, and could in theory be decommissioned. Storage technology is AHI battery, 90% round trip efficiency, 20-hour duration

Table 2-6. Consumer savings due to storage. Energy savings are savings in the wholesale day-ahead energy market. Capacity savings are the avoided capacity payments to plants that storage has replaced, valued at the 2010/2011 capacity auction price of $175/MW-day. Ranges represent lower and upper bounds. 2010 dollars

	Storage Capacity [GW]				
Savings [$B]	**1**	**10**	**20**	**40**	**80**
Sodium sulfur batteries					
Energy	0.2	1.2 – 1.7	1.6 – 2.2	1.7 – 2.0	1.7 – 1.9
Capacity	0.0 – 0.1	0.7 – 0.8	1.5 – 1.7	1.6 – 1.8	1.7 – 1.9
Total	0.2 – 0.3	1.9 – 2.5	3.1 – 3.9	3.3 – 3.8	3.4 – 3.8
Aqueous hybrid ion batteries					
Energy	0.1 – 0.4	0.8 – 1.7	1.4 – 2.0	1.9 – 2.0	1.8 – 2.0
Capacity	-0.1 – 0.0	0.5 – 0.8	1.0 – 1.8	1.7 – 2.0	1.7 – 2.0
Total	0.0 – 0.4	1.3 – 2.5	2.4 – 3.8	3.6 – 4.0	3.5 – 4.0
Pumped hydropower					
Energy	0.1 – 0.4	0.7 – 1.4	1.2 – 2.0	1.5 – 1.9	1.6 – 1.7
Capacity	-0.1 – 0.0	0.5 – 0.8	0.9 – 1.7	1.6 – 1.9	1.6 – 1.9
Total	0.0 – 0.4	1.2 – 2.6	2.1 – 3.7	3.1 – 3.8	3.2 – 3.8

We next calculated net consumer benefit, defined as total consumer benefit minus annualized storage costs. Figure 2-3 shows that AHI batteries can provide positive net consumer benefits depending on parameter assumptions, while the net benefit of SS batteries is always negative. Under optimistic technical assumptions and operating conditions (slow, high efficiency charging and discharging), AHI can provide positive net benefits up to 35 GW of deployment. First movers provide large benefits, as they displace the most inefficient and expensive peaking generators. The net benefits of AHI are similar to that of traditional pumped hydropower. Differences in capital costs are the primary driver of the variation in net consumer benefit (Section 5.2).

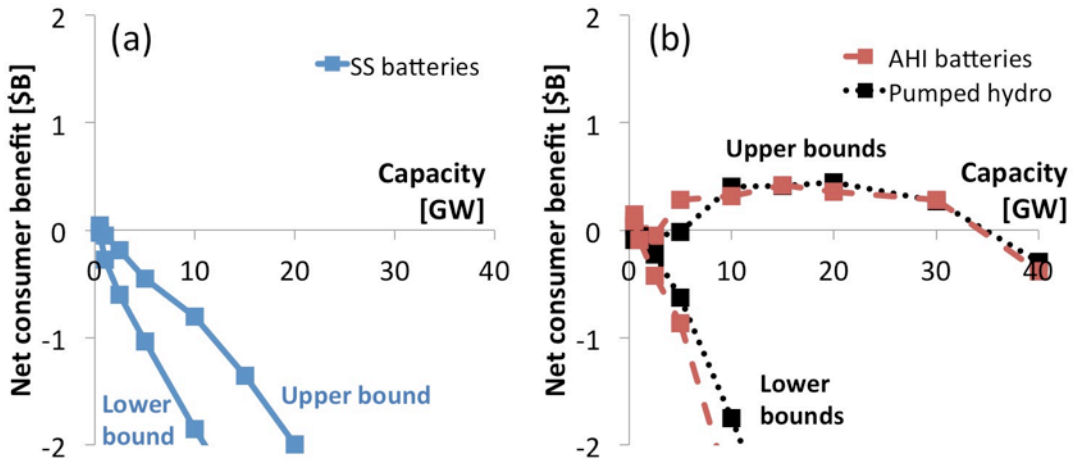

Figure 2-3. Net annual consumer benefit (total consumer benefit – annualized storage cost). (a): sodium sulfur (SS) batteries; (b): aqueous hybrid ion (AHI) batteries and pumped hydropower. Net benefits vary depending on assumptions of storage parameters and cost. Net benefits of AHI batteries similar to that of conventional pumped hydro. 2010 dollars

2.3.2 Effect on generators

By reducing prices on the wholesale energy market and reducing reliance on peakers, storage reduces generator revenues. As shown in Table 2-7, generation from peaking plants (combustion turbine, oil/gas steam, and combined cycle) falls as they are displaced by storage. Output from coal plants increases as they charge storage at off-peak hours. Revenues to all generators on the wholesale energy market fall as storage capacity increases; total revenues fall by more than 10% in high storage cases. In addition, generator revenues on the capacity market are reduced by an amount equal to the consumer savings on the capacity market (Table 2-6). Our findings agree with other research that shows the increases in consumer welfare due to storage come with significant reductions in producer surplus accruing to generators [7, 30].

Table 2-7. Generator output and energy market revenue, business as usual (BAU) scenario and a scenario with 80 GW of aqueous hybrid ion (AHI) storage (90% round trip efficiency, 20-hour duration). Revenues in 2010 dollars

	Generation [TWh]		Energy Market Revenues [$M]	
Generator type	**BAU**	**AHI storage**	**BAU**	**AHI storage**
Nuclear	260	260	$9,200	$8,950
Hydropower	8	8	$380	$370
Coal steam	420	432	$5,350	$4,820
Natural gas combined cycle	48	42	$650	$20
Natural gas combustion turbine	4	0	$131	$0
Oil/gas steam	1	0	$20	$0

2.3.3 Storage profits

Figure 2-4 shows that storage revenues peak with considerably less than 20 GW of storage deployed; as more storage is deployed, less arbitrage opportunities are available, and revenues drop. If used only for arbitrage, net annual profits are negative, regardless of the technology used or capacity deployed. For both AHI and SS batteries, debt service on capital costs greatly exceeds wholesale energy market revenues (Table 2-8).

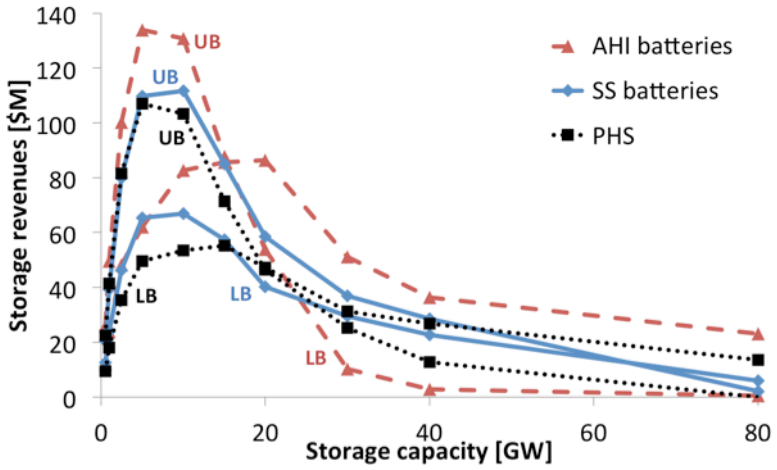

Figure 2-4. Annual wholesale market arbitrage revenues to storage operators. Revenues vary depending on upper bound (UB) or lower bound (LB) assumptions of storage parameters and cost. Revenues peak with less than 20 GW of storage deployed. 2010 dollars

Table 2-8. Annual net profits of storage technologies to storage operator. Ranges represent lower and upper bounds. 2010 dollars

Capacity [GW]	AHI battery profit [$B]	SS battery profit [$B]	PHS profit [$B]
1	[0, 0]	[0, -1]	[0, 0]
10	[-5, -1]	[-4, -3]	[-2, -1]
80	[-40, -8]	[-28, -20]	[-20, -7]

2.3.4 Overall social welfare

Adding storage to the system increases overall social welfare on the wholesale energy market. Total energy market savings monotonically increase as more storage is deployed (Figure 2-5). Total market savings are much smaller than improvements in consumer welfare (Table 2-6), as the majority of consumer welfare benefits are transfers from generators. Although storage increases total social welfare, the annualized capital costs of storage exceed these savings (Table 2-9).

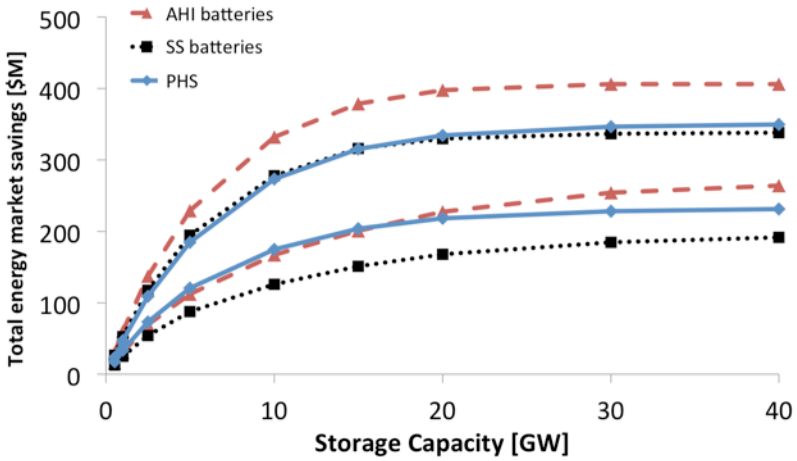

Figure 2-5. Total savings on the wholesale energy market due to storage. 2010 dollars

Table 2-9. Change in overall social welfare on the energy market minus annualized storage capital cost. Ranges represent lower and upper bounds. 2010 dollars

Capacity [GW]	AHI battery [$B]	PHS [$B]	SS battery [$B]
1	[0, 0]	[0, 0]	[0, 0]
10	[-5, -1]	[-4, 0]	[-4, -3]
20	[-10, -2]	[-9, -2]	[-8, -5]
40	[-20, -4]	[-17, -3]	[-15, -10]
80	[-40, -8]	[-35, -7]	[-30, -21]

2.3.5 Effect on emissions

Storage modestly increases emissions (Table 2-10). This is for two reasons. First, storage is primarily charged off-peak by coal plants, which have higher emissions than the peaking gas plants they replace. Second, additional electricity must be generated to compensate for the losses inherent in storing electricity. However, the effect of storage on emissions will depend on underlying market dynamics (see section 5).

Table 2-10. Annual emission increases and associated damages due to storage in the 2010 PJM wholesale energy market. Storage technology is aqueous hybrid ion (AHI) batteries, 90% round trip efficiency, 20-hour duration.

AHI battery capacity [GW]	Change in Emissions [MT] (%)		
	CO_2	NO_X	SO_2
1	2,400,000 (0.5%)	2,500 (0.6%)	16,600 (0.9%)
10	5,400,000 (1.2%)	4,700 (1.2%)	58,000 (3.0%)
80	6,600,000 (1.5%)	5,600 (1.4%)	71,800 (3.7%)

2.4 Sensitivity Analysis

We tested the robustness of our results with four sensitivity analyses:

- Sensitivity of consumer benefits to storage round trip efficiency and duration
- Sensitivity of net consumer benefits to the capital cost and lifespan of storage
- Sensitivity of consumer benefits to capacity market prices
- Sensitivity of consumer benefit and emissions to fuel prices and the amount of wind deployed.

2.4.1 Sensitivity to round trip efficiency and duration parameters

To test for sensitivity to RTE and duration, we performed a one-way sensitivity analysis. We varied the RTE of a generic storage device from 64%-100% and duration from 4-20 hours. These ranges capture the majority of storage technologies being discussed today. Figure 2-6 shows that increasing storage RTE increases total consumer savings on the wholesale energy and capacity markets. Increasing duration does not increase savings, but allows a given level of savings to be reached with less storage capacity.

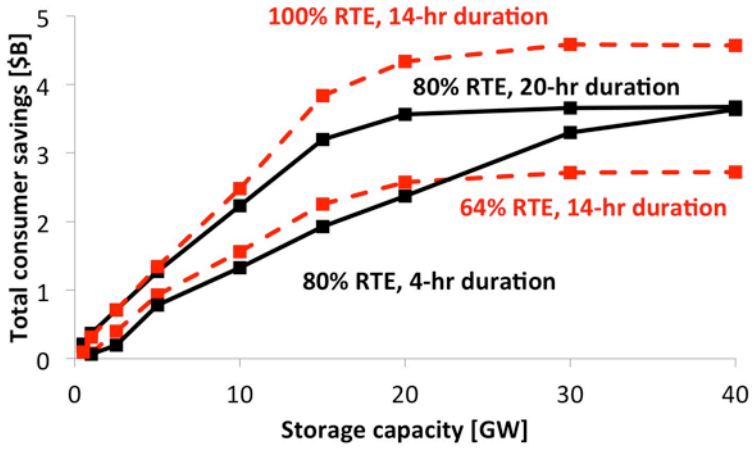

Figure 2-6. Sensitivity of total annual consumer savings to storage round trip efficiency (RTE) and duration. 2010 dollars

2.4.2 Sensitivity to capital costs and lifespan

We next tested for sensitivity to the capital cost and lifespan of storage technologies. We fixed the capital cost at $300/kWh for both SS and AHI battery technologies and analyzed the resulting net consumer benefit. Because the lifespan of SS batteries varies from 14 – 40 years depending on the amount deployed, we examined sensitivity of net consumer benefit to SS battery lifespan by setting lifespan to 40 years, the same as AHI batteries. Variations in net consumer benefit are solely due to differences in technology parameters (efficiency and duration). Figure 2-7 shows that SS batteries become competitive with AHI batteries if equal capital costs are assumed. Improving SS battery lifespan to 40 years increases net consumer benefit by up to 20% for deployments less than 20 GW. Because the RTE and duration parameters of AHI vary greatly depending on how the battery is operated, the range of net consumer benefits is wider than SS.

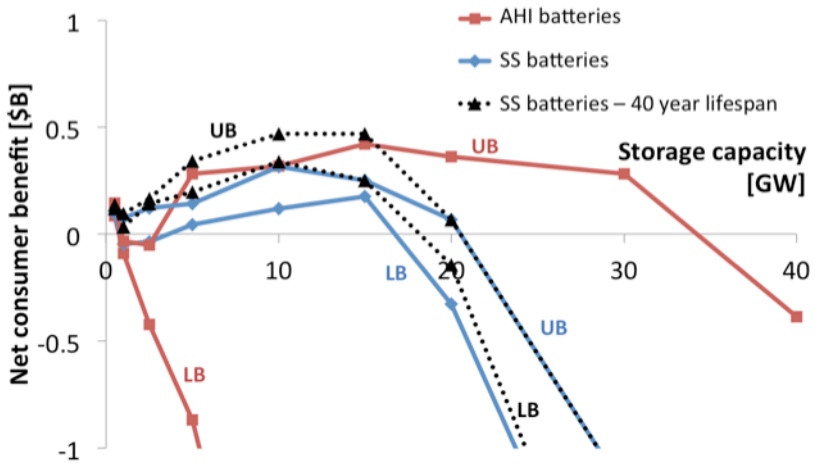

Figure 2-7. Net annual consumer benefit for sodium sulfur (SS) and aqueous hybrid ion (AHI) batteries, assuming a capital cost of $300/kWh for both technologies. Dashed lines are SS net annual consumer benefits, assuming 40-year lifespan. Net benefits vary between upper bound (UB) and lower bound (LB) depending on assumptions of storage parameters. 2010 dollars

2.4.3 Sensitivity to capacity market prices

Capacity prices in PJM have varied significantly since capacity auctions were established in 2007. Prices have varied from a high of $174/MWh in the 2010/2011 auction to a low of $16/MWh in

the 2012/2013 auction [24]. The value of storage to consumers is highly dependent on capacity market prices, as half of the total consumer benefits of storage are due to reductions in capacity market expenditures (Table 2-6). Reducing the modeled capacity market price from $174/MWh to $16/MWh would reduce modeled total consumer benefits by half.

Future capacity prices are highly uncertain, and historic prices show no clear trend. Environmental regulations such as the Clean Air Interstate Rule are expected to put upward pressure on capacity prices; PJM projects 20 GW of coal capacity will be forced to retire due environmental regulations [31]. However, the rapid growth of demand response (DR) will put downward pressure on capacity prices. DR's participation in the PJM capacity market has expanded from 700 MW in 2008/2009 to 19 GW in 2015/2016 [24]. How these and other forces will affect capacity prices in the coming years will significantly affect the consumer benefits of storage.

2.4.4 Sensitivity to fuel price

The above analysis uses 2010 fuel prices. However, fuel prices have changed dramatically since 2010 due to the expansion of the shale gas industry. In particular, the average delivered price of natural gas to PJM generators has dropped by roughly 30% (as of late 2012) [32]. To test the robustness of our results, we ran a simulation with fuel prices from August 2011 – July 2012. All other variables were left unchanged.

Without storage, changing from 2010 to 2011/2012 fuel prices reduces total consumer expenditures in the energy market from $35B to $30B. The new fuel prices also cause the generator dispatch order to change. Coal generation decreases by 14%; this drop is filled primarily by combined cycle gas generation (our model results match the observed switch from coal to gas well).

Storage provides greater benefits under the 2011/2012 fuel price scenario; on average, benefits are 10% higher. The increased benefits are due to higher savings in the wholesale energy market;

capacity savings are largely unchanged. Based on this analysis, the conclusion that storage provides substantial benefits to consumers is robust to variations in fuel price, including current low natural gas prices.

Without storage, emissions of CO_2, NO_X, and SO_2 are lower in the 2011/2012 fuel price scenario than the 2010 scenario due to the decrease in coal generation. Adding storage increases emissions of CO_2 and SO_2 in both scenarios, although increases are smaller in the 20111/2012 fuel price scenario (Table 2-11). Storage increases emissions of NO_X in the 2010 scenario, but does not change NO_X emissions in the 2011/2012 fuel price scenario. Adding storage to the 2011/2012 fuel price scenario increases emissions from coal generators, which are largely offset by decreased emissions from peaking generators. NO_X emissions are unchanged, as reductions from peaking plants are as large as increases from coal plants.

2.4.5 Sensitivity to amount of wind deployed

Finally, we investigated how the benefit of storage changes in a scenario with high penetrations of wind. Over the next decade, PJM anticipates a large expansion of wind in order to meet state renewable portfolio standards. We investigated the benefits of deploying 40 GW of 90% RTE, 20-hour duration AHI storage in two scenarios: the base 2010 scenario (1.5% of energy supplied by wind), and a scenario with 20% of energy from wind. For the 20% wind scenario, we used the data from the Eastern Wind Integration and Transmission Study [33] to identify hourly generation from likely wind sites in PJM member states. We then added sites in order of decreasing capacity factor until total wind generation was 20% of load.

In the base scenario, storage induces $3.2 billion in consumer benefits; in the 20% wind scenario, total benefits increase ~10% to $3.6 billion. This increase is due to reductions in wind curtailment. Without storage, 5% of wind energy is curtailed; with storage, no wind is curtailed.

Therefore, we conclude that the benefits of storage are unlikely to increase dramatically in high wind scenarios.

Without storage, emissions are significantly lower in the 20% wind scenario than the base scenario. Adding storage in the 20% wind scenario increases CO_2 and SO_2 emissions by less than 1%; NO_X emissions slightly decrease (Table 2-11). The net CO_2 emission increase is due to a 2% increase in CO_2 emissions by coal plants, which is largely offset by a 93% reduction in CO_2 emissions from peaking combustion turbine and oil/gas steam plants. Although researchers have shown that hybrid wind/storage systems can provide low emission baseload power [34], our findings agree with studies that show adding storage into high-wind systems can increase emissions. Tuohy and O'Malley find that storage increases the level of carbon emissions at wind penetrations less than 60% in the Irish system [26, 27]. Sioshansi finds that adding large amounts of storage (10 GW) to the ERCOT system in the presence of high wind (10 GW) increases emissions of CO_2, NO_X, and SO_2, assuming a competitive market [35].

Table 2-11. Emissions of CO_2, NO_X, and SO_2 in the business as usual (BAU) scenario - 2010 fuel prices, a scenario with 2011/2012 fuel prices, and a scenario with 20% of energy from wind. Storage is 40 GW aqueous hybrid ion (AHI) batteries (90% RTE, 20-hr duration)

	BAU [Million tons]			2011/2012 fuel prices [Million tons]			20% wind [Million tons]		
	CO_2	NO_X	SO_2	CO_2	NO_X	SO_2	CO_2	NO_X	SO_2
No storage	466	0.43	2.09	432	0.36	1.71	337	0.31	1.46
Storage	473	0.44	2.16	434	0.36	1.73	338	0.30	1.46

2.5 Discussion

Although storage increases overall social welfare on the wholesale energy market, the annualized capital cost of storage exceeds these benefits. However, storage creates large benefits for consumers, ~10% of the value transacted in PJM's day-ahead energy market. These benefits are primarily transfers from generators on the wholesale and energy markets. Net consumer benefits, or

total benefit on wholesale energy and capacity markets minus annualized capital costs, are positive under optimistic technical and operating assumptions for AHI batteries but negative for SS batteries. The positive benefits of AHI batteries could be distributed in three ways: they could be given to consumers as reduced energy costs, to generators to compensate for revenue losses, or to storage operators as profit. Even if all net benefits are given to generators, they are insufficient to completely compensate for lost revenues.

Due to the high capital costs, operating storage on wholesale markets is unprofitable for storage operators if used solely for arbitrage. Figure 2-8 illustrates that under current market design, storage revenues are much smaller than total welfare increases, and therefore the socially optimal amount of storage is not achieved. Other researchers have noted the limitations of existing market designs in signaling the value of energy storage [36].

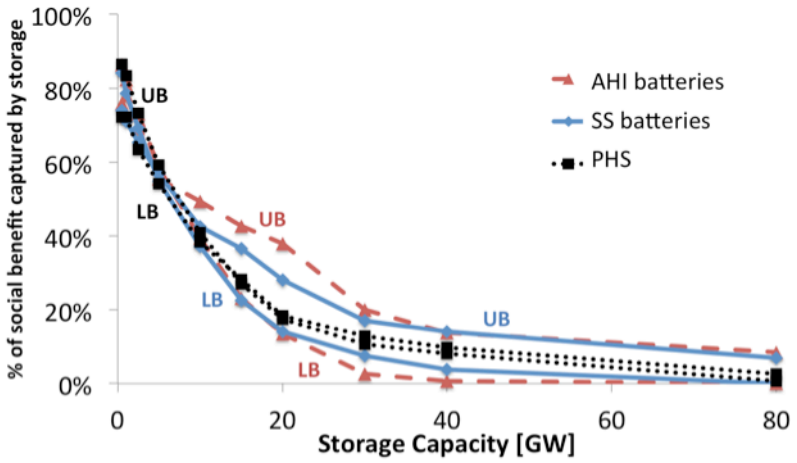

Figure 2-8. Percentage of the total social welfare benefits captured by storage operators. Storage operators capture only a small fraction of the benefits they create at high levels of deployment. Results vary between upper bound (UB) and lower bound (LB) depending on assumptions of storage parameters.

Sioshansi has shown that consumer or generator ownership of storage is not welfare maximizing [37]. Consumers overuse storage, as they neglect the producer surplus losses the storage creates. Generators underuse storage, as they seek to minimize producer surplus losses. Merchant operated

storage does result in social welfare maximization, assuming perfectly competitive storage and generation. We propose four strategies that might be used in various combinations to encourage storage deployment closer to the societally optimal level by merchant operators.

First, regional transmission operators (RTOs) should ensure that storage assets are eligible for capacity market payments, where such markets exist.

Second, RTOs could establish rules that allow profit maximizing behavior. For example, storage operators could be permitted to bid into the market the prices at which they are willing to charge or discharge. Our analysis assumes RTOs will dispatch storage in order to minimize total social costs, as they currently dispatch generators.

Third, RTOs or governments could directly subsidize storage operators. This subsidy would be based on the overall social welfare benefits that storage provides.

Finally, system operators could attempt to incentivize storage by removing all price caps and allowing for high price spikes. During these few hours of very high prices, some argue that storage could possibly recoup enough money to be profitable [38].

2.6 Conclusion

Storage increases overall social welfare on the wholesale energy market. However, the annualized capital cost of storage exceeds these benefits. Storage provides substantial benefits to consumers in two ways: by reducing prices in the wholesale energy market, and by reducing the need for peaking generators. 20 GW of storage would reduce consumer expenditures by more than $2.5 billion annually and allow 30 GW of peaking capacity to be retired. However, storage reduces the profitability of all generators. Generation from peaking gas and oil plants decreases, while generation from coal plants increases. Storage modestly increases system emissions of CO_2 and

other pollutants in the 2010 PJM market. No current storage technologies are profitable if solely used for arbitrage on the PJM day-ahead market.

The current market design results in merchant storage operators receiving only a small fraction of the total social welfare they create at high levels of deployment. Four strategies might be used by PJM and the public utilities commissions and governments in its territory to encourage storage deployment closer to the socially optimal level: (1) ensure storage is eligible for capacity payments; (2) establish rules that allow profit-maximizing behavior for storage; (3) directly subsidize storage for the overall social welfare benefits it provides; and (4) remove all price caps and allow for high price spikes if this is shown to be effective.

Future research could improve the accuracy with which storage is modeled in the unit commitment model framework by (1) modeling transmission congestion within each of the 5 buses; (2) considering wind uncertainty by using a stochastic unit commitment model; and (3) co-optimizing the energy and reserve markets.

2.7 References

[1] Electric Power Research Institute: Electric Energy Storage Technology Options: A White Paper Primer on Applications, Costs, and Benefits (2010)

[2] U.S. Federal Energy Regulatory Commission: Issued Preliminary Permits. http://www.ferc.gov/industries/hydropower/gen-info/licensing/issued-pre-permits.xls. Accessed Jan 10, 2014

[3] Eyer, J., Corey, G.: Energy Storage for the Electricity Grid: Benefits and Market Potential Assessment Guide. SAND2010-0815. (2010)

[4] Monitoring Analytics: PJM State of the Market report, 2010. http://www.monitoringanalytics.com/reports/PJM_State_of_the_Market/2010.shtml (2011). Accessed June 2013

[5] Kempton, W., Tomić, J.: Vehicle-to-grid Power Fundamentals: Calculating Capacity and Net Revenue. Journal of Power Sources 144, 1, 1268–279 (2005)

[6] Walawalkar, R., Apt, J., Mancini, R.: Economics of Electric Energy Storage for Energy Arbitrage and Regulation in New York. Energy Policy, 35,4, 2558–2568 (2007)

[7] Sioshansi, R., Denholm, P., Jenkin, T., Weiss, J.: Estimating the Value of Electricity Storage in PJM: Arbitrage and Some Welfare Effects. Energy Economics 31, 2, 269–277 (2009)

[8] Nyamdash, B., Denny, E.: The impact of electricity storage on wholesale electricity prices. Energy Policy 58, 6-16 (2013)

[9] Schill, W.P., Kemfert, C.: Modeling Strategic Electricity Storage: The Case of Pumped Hydro Storage in Germany. The Energy Journal, Vol 32 (2011)

[10] Sioshansi, R.: Increasing the Value of Wind with Energy Storage. The Energy Journal, Vol 32, (2011)

[11] London Economics International LLC: A Comparative Analysis of Actual Locational Marginal Prices in the PJM Market and Estimated Short-run Marginal Costs: 2003-2006. (2007)

[12] US Environmental Protection Agency: eGRID 2012. http://www.epa.gov/cleanenergy/energy-resources/egrid/index.html (2012). Accessed Aug 2012

[13] Spees, K., Lave, L.: Demand response and electricity market efficiency. The Electricity Journal 20, 3, 69-85 (2007)

[14] Oates, D.L., and Jaramillo, P.: Production cost and air emissions impacts of coal cycling in power systems with large-scale wind penetration. Environmental Research Letters 8.2 024022 (2013)

[15] Ward, M.: Resource Commitment and Dispatch in the PJM Wholesale Electricity Market. http://www.ferc.gov/eventcalendar/Files/20110628072854-Jun28-SesA2-Ward-PJM.pdf (2011). Accessed Aug 2012

[16] PJM: Reserves Scheduling, Reporting, and Loading. http://www.pjm.com/~/media/training/core-curriculum/ip-ops-101/ops-101-reserves.ashx (2011). Accessed Aug 2012

[17] Guan X., Luh, P., Yen, H., Rogan, P.: Optimization-based Scheduling of Hydrothermal Power Systems with Pumped-storage Units. Power Systems, IEEE Transactions On, 9, 2, 1023–1031 (1994)

[18] Carrión, M., Arroyo, J.: A Computationally Efficient Mixed-integer Linear Formulation for the Thermal Unit Commitment Problem. Power Systems, IEEE Transactions On 21, 3, 1371–1378 (2006)

[19] Streiffert, D., Philbrick, R., Ott, A.: A Mixed Integer Programming Solution for Market Clearing and Reliability Analysis. Power Engineering Society General Meeting, IEEE 2724–2731 (2005)

[20] PJM: A Review of Generation Compensation and Cost Elements in the PJM Markets. http://www.pjm.com/~/media/committees-groups/committees/mrc/20100120/20100120-item-02-review-of-generation-costs-and-compensation.ashx (2009). Accessed Aug 3, 2012

[21] Whitacre, J. F., et al.: An aqueous electrolyte, sodium ion functional, large format energy storage device for stationary applications. Journal of Power Sources, 213, 255-265 (2012)

[22] Connolly, D: A Review of Energy Storage Technologies. University of Limerick (2009)

[23] Wiley, T.: Update on Aquion Energy. 2013 Carnegie Mellon Electricity Industry Center Advisory Committee Meeting (2013)

[24] PJM: PJM 2016/2017 RPM Base Residual Auction Results. http://www.pjm.com/~/media/markets-ops/rpm/rpm-auction-info/2016-2017-base-residual-auction-report.ashx (2013). Accessed Oct 2013

[25] PJM: Energy Storage Resources in RPM. http://www.pjm.com/~/media/committees-groups/committees/mrc/20130829/20130829-item-11-energy-storage-participation-in-rpm-proposed-problem-statement.ashx (2013). Accessed Oct 2013

[26] Tuohy, A., O'Malley, M.: Impact of Pumped Storage on Power Systems with Increasing Wind Penetration. Proceedings of the IEEE Power & Energy Society General Meeting (2009)

[27] Tuohy, A., O'Malley, M.: Pumped storage in systems with very high wind penetration. Energy Policy, Vol 39 (2011)

[28] Sioshansi, R., Madaeni, S. H., Denholm, P.: A Dynamic Programming Approach to Estimate the Capacity Value of Energy Storage. IEEE Transactions on Power Systems, Vol 29 (2014)

[29] Moura, J.: Personal communication, North American Electric Reliability Corporation (NERC) (2012)

[30] R. Sioshansi: When Energy Storage Reduces Social Welfare. Energy Economics, Vol 41 (2014)

[31] PJM: Coal Capacity at Risk of Retirement in PJM: Potential Impacts of the Finalized EPA Cross State Air Pollution Rule and Proposed National Emissions Standards for Hazardous Air Pollutants (2011)

[32] US Department of Energy, Energy Information Agency: Electric Power Monthly. http://205.254.135.7/electricity/monthly/index.cfm (2012). Accessed Nov 2012

[33] Corbus, D., King, J., Mousseau, T.: Eastern wind integration and transmission study. US Department of Energy, National Renewable Energy Laboratory. (2010)

[34] Denholm, P.; Kulcinski, G.L.; Holloway, T.: Emissions and energy efficiency assessment of baseload wind energy systems. Environmental Science and Technology, Vol 39 (2005)

[35] Sioshansi, R.: Emissions Impacts of Wind and Energy Storage in a Market Environment. Environmental Science and Technology, Vol 45 (2011)

[36] Sioshansi, R., Denholm, P., Jenkin, T.: Market and Policy Barriers to Deployment of Energy Storage. Economics of Energy and Environmental Policy, Vol 1 (2012)

[37] Sioshansi, R.: Welfare impacts of electricity storage and the implications of ownership structure. Energy Journal, *31*(2), 173 (2010)

[38] Hogan, W.: On an Energy Only Electricity Market Design for Resource Adequacy. Working paper, Center for Business and Government, Harvard University. http://www.ferc.gov/EventCalendar/files/20060207132019-hogan_energy_only_092305.pdf (2005). Accessed June 2013

A Appendix: Detailed model description

Our analysis used a five-bus model of PJM. Each of the five buses consists of one or more of the 19 PJM zones (Figure A-1). When defining buses, more data are now available than were available to earlier researchers, so we were able to incorporate additional granularity. The London Economics International (LEI) analysis [1] includes three transmission interfaces (Western, Central, and Eastern), and five regions. PHORUM includes three additional transmission interfaces: Bedington – Black Oak, AEP-DOM and AP South. Figure A-2 shows all PJM transmission interfaces. We added one more bus than the LEI study, bus 5 (Dominion/VA), but did not model Delmarva Power and Light (DPL) as a separate region. Finally, we did not divide the METED zone across multiple regions, as did LEI. DUK (Duke Energy) zone was integrated into PJM Jan 1, 2012 and was not included in the analysis.

We made three modifications when dividing the PJM transmission interfaces into PHORUM's transmission lines: (1) the Western Interface is made up of four 500kV lines, each connecting different buses. Therefore, we divided the Interface's capacity into quarters and apportion the capacity to lines as appropriate; (2) the 500X(5004+5005) Interface is made up of two 500kV lines that are contained within the Western Interface. Therefore, we did not model the 500X(5004+5005) interface as it is included in the Western Interface; and (3) we combined the Bedington-Black Oak, AP South, and AEP-DOM Interfaces into a single line between buses 1 and 5. We made the simplifying assumption that the capacity of each line is independent of how much current it carries. Table A-1. Assignment of PJM zones to PHORUM buses and PJM interfaces to PHORUM transmission lines. Table A-1 summarizes the assignment of PJM zones and interfaces to PHORUM buses and transmission lines. 2010 LMP data shows that within our defined buses, zonal LMPs are highly correlated, supporting our assumptions of bus locations and unconstrained

transmission within each bus (Figure A-3). Aggregating PJM into five transmission buses will obscure the high arbitrage potential, and therefore storage revenue, at a few localized nodes. However, we assume large deployments of storage will saturate these localized opportunities and act to equalize LMPs at all nodes within the bus.

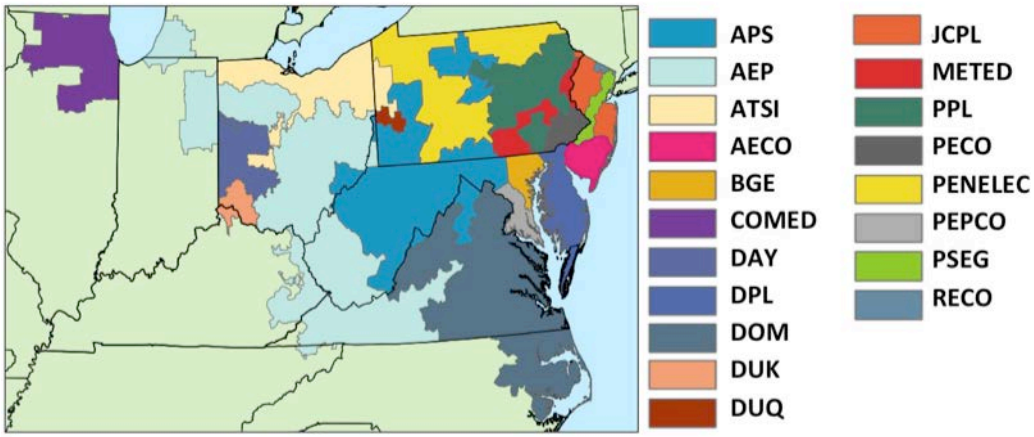

Figure A-1. The PJM Interconnection and its constituent zones [2]

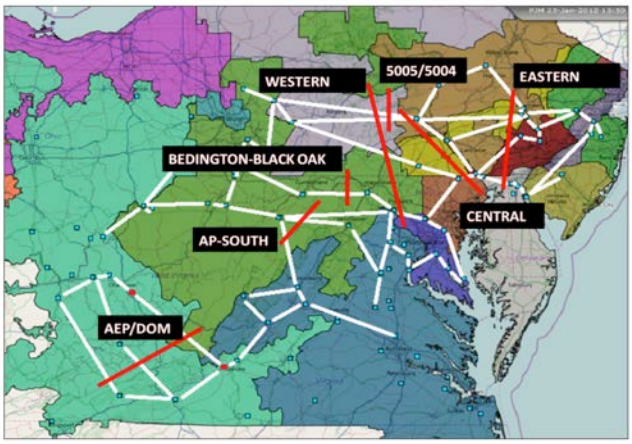

Figure A-2. PJM 500kV transmission lines (white lines) and transmission interfaces (red lines) [3, 4]. Most interfaces contain multiple 500kV lines

Table A-1. Assignment of PJM zones to PHORUM buses and PJM interfaces to PHORUM transmission lines.

Bus	PJM Zones
Bus 1	AEP, APS, COMED, DAY, DUQ, PENELEC, ATSI
Bus 2	BGE, PEPCO
Bus 3	METED, PPL
Bus 4	JCPL, PECO, PSEG, AECO, DPL, RECO
Bus 5	DOM
Line	**PJM Interface**
Line 1	¼ of Western Interface capacity
Line 2	½ of Western Interface capacity
Line 5	¼ of Western Interface capacity
Line 3	Bedington-Black Oak, AP South, AEP-DOM
Line 4	Central Interface
Line 6	Eastern Interface
Not modeled	500X(5004+5005)

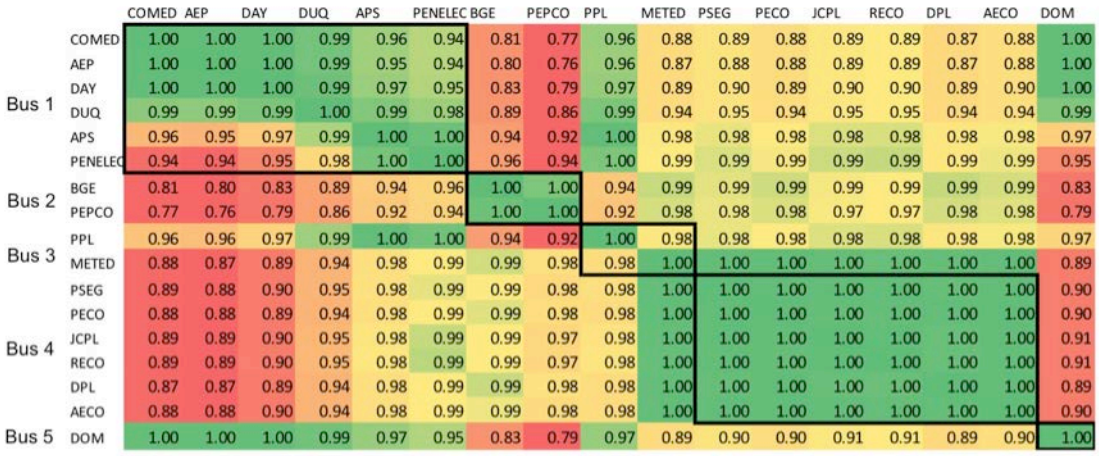

		COMED	AEP	DAY	DUQ	APS	PENELEC	BGE	PEPCO	PPL	METED	PSEG	PECO	JCPL	RECO	DPL	AECO	DOM
Bus 1	COMED	1.00	1.00	1.00	0.99	0.96	0.94	0.81	0.77	0.96	0.88	0.89	0.88	0.89	0.89	0.87	0.88	1.00
	AEP	1.00	1.00	1.00	0.99	0.95	0.94	0.80	0.76	0.96	0.87	0.88	0.88	0.89	0.89	0.87	0.88	1.00
	DAY	1.00	1.00	1.00	0.99	0.97	0.95	0.83	0.79	0.97	0.89	0.90	0.89	0.90	0.90	0.89	0.90	1.00
	DUQ	0.99	0.99	0.99	1.00	0.99	0.98	0.89	0.86	0.99	0.94	0.95	0.94	0.95	0.95	0.94	0.94	0.99
	APS	0.96	0.95	0.97	0.99	1.00	1.00	0.94	0.92	1.00	0.98	0.98	0.98	0.98	0.98	0.98	0.98	0.97
	PENELEC	0.94	0.94	0.95	0.98	1.00	1.00	0.96	0.94	1.00	0.99	0.99	0.99	0.99	0.99	0.99	0.99	0.95
Bus 2	BGE	0.81	0.80	0.83	0.89	0.94	0.96	1.00	1.00	0.94	0.99	0.99	0.99	0.99	0.99	0.99	0.99	0.83
	PEPCO	0.77	0.76	0.79	0.86	0.92	0.94	1.00	1.00	0.92	0.98	0.98	0.98	0.97	0.97	0.98	0.98	0.79
Bus 3	PPL	0.96	0.96	0.97	0.99	1.00	1.00	0.94	0.92	1.00	0.98	0.98	0.98	0.98	0.98	0.98	0.98	0.97
	METED	0.88	0.87	0.89	0.94	0.98	0.99	0.99	0.98	0.98	1.00	1.00	1.00	1.00	1.00	1.00	1.00	0.89
Bus 4	PSEG	0.89	0.88	0.90	0.95	0.98	0.99	0.99	0.98	0.98	1.00	1.00	1.00	1.00	1.00	1.00	1.00	0.90
	PECO	0.88	0.88	0.89	0.94	0.98	0.99	0.99	0.98	0.98	1.00	1.00	1.00	1.00	1.00	1.00	1.00	0.90
	JCPL	0.89	0.89	0.90	0.95	0.98	0.99	0.99	0.97	0.98	1.00	1.00	1.00	1.00	1.00	1.00	1.00	0.91
	RECO	0.89	0.89	0.90	0.95	0.98	0.99	0.99	0.97	0.98	1.00	1.00	1.00	1.00	1.00	1.00	1.00	0.91
	DPL	0.87	0.87	0.89	0.94	0.98	0.99	0.99	0.98	0.98	1.00	1.00	1.00	1.00	1.00	1.00	1.00	0.89
	AECO	0.88	0.88	0.90	0.94	0.98	0.99	0.99	0.98	0.98	1.00	1.00	1.00	1.00	1.00	1.00	1.00	0.90
Bus 5	DOM	1.00	1.00	1.00	0.99	0.97	0.95	0.83	0.79	0.97	0.89	0.90	0.90	0.91	0.91	0.89	0.90	1.00

Figure A-3. Correlation coefficients between zones for 2010 hourly day-ahead LMPs. High correlation within a bus supports the model's simplifying assumption that transmission is unconstrained within the bus

PJM operates several electricity markets, the largest of which are the day-ahead (DAH) and real-time energy markets. We modeled the DAH market instead of the real-time market for two reasons. First, the DAH market is larger, with generally lower and less volatile prices, serving as a conservative lower bound on storage profits [5]. Secondly, prices in the real-time market are highly

influenced by factors outside the capability of PHORUM, such as sudden changes in the weather, forced generator outages, transmission outages, and strategic behavior. According to PJM, "The price difference between the Real-Time and the Day-Ahead Energy Markets results, in part, from volatility in the Real-Time Energy Market that is difficult, or impossible, to anticipate in the Day-Ahead Energy Market" [5]. We assumed all available generators participate in the DAH market. In reality, 2010 PJM DAH load was met by a combination of bilateral contracts (4.9%), self-supply from the load-serving entity's own generation (75.8%), and spot purchases on the DAH market (19.3%) [5]. This assumption is equivalent to assuming that bilateral contracts and self-supply do not cause out-of-merit-order dispatch.

We ran 365 optimizations, each minimizing costs over 48 hours. Each 48-hour optimization was initialized with four variables from the last hour of the previous day's optimization:

- The on/off state of each generator
- How much longer each generator must remain on/off
- The power output of each generator
- The state of charge for each storage unit

Figure A-4 illustrates how cross-day variables are handled by PHORUM. In addition, the state of charge of each storage device at hour 48 is constrained to be the same as the each 48-hour optimization constraints.

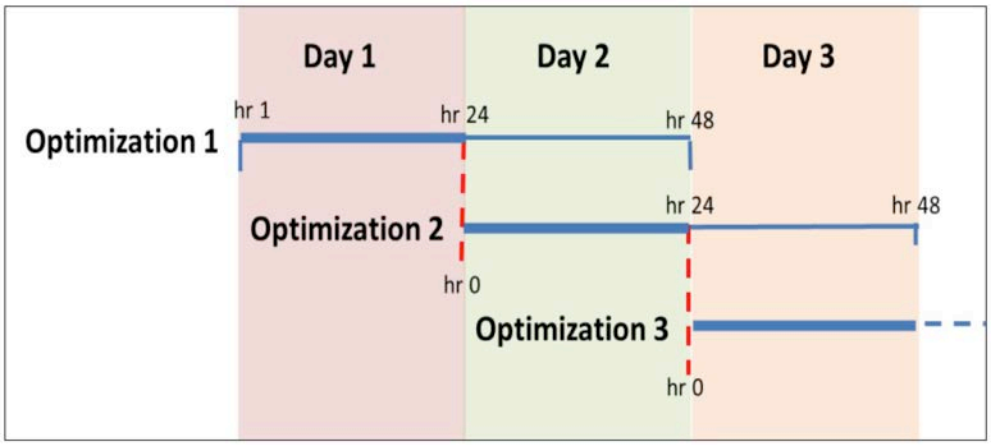

Figure A-4. Illustration of how PHORUM handles day boundaries. Each optimization runs for a full 48 hours, but only the first 24 hours of results are retained. Variables are passed from the 24th hour of the first optimization to hour 0 of the second.

Table A-2 details each data element used in PHORUM. We made several modifications to the generator data in order to improve accuracy. First, for generators in the PJM EIA-411 generator database but not in the NEEDS database, we assumed values for NEEDS and eGRID data elements. These assumptions are based on values for similar plants. Similarly, the PJM database occasionally combines two generators that NEEDS calls out separately. In these cases, we combined the generators as in the PJM database and assumed values based on the constituent generators. We assumed generators have linear heat rates, variable O&M costs, ramp rates, and emission factors over their operating range. Better data could further improve accuracy. In particular, better information on when generators are offline for maintenance, more detailed transmission constraints, and more refined buses would improve the model.

Table A-2. PHORUM data sources

Data Element	Source
Generator Data	
Plant type	[6]
State & county[1]	[6]
Heat Rate [Btu/kWh]	[6]
Fuel	[6]
Capacity [MW] (Summer & winter)[2]	[7]
Variable O&M Cost [$/MWh][3]	[8]
Monthly Fuel Price: Jan – Dec 2010 [$/MMBtu][4]	[9, 10]
Ramp Rate [MW/hr][5]	[11]
Min uptime & downtime [hrs][6]	[12]
Startup cost adder [$][7]	[13, 14]
Minimum Generation [% of maximum generation]	[15]
Monthly Equivalent Availability Factor: Jan – Dec 2010[8]	[16, 17]
Stack Height [ft]	[18]
CO_2 emission rate [lb/MMBtu]	[19]
NO_x & SO_2 emission rates [lb/MWh]	[19]
Hourly Data	
Load[10]	[20]
Imports/Exports [MW][11]	[21]
Zonal Locational Marginal Prices (LMPs) [$/MWh]	[22]
Transmission Capacity [MW]	[23]
Wind Generation [MW][12]	[24]
Reserve Requirement [MW][13]	[25]

1. Plants are assigned to zones by state and county codes.

2. Generator capacities listed for different databases (PJM EIA-411, eGRID, and NEEDS) vary widely. We use data listed in the PJM EIA 4-11 report. Hydro generator capacities are derated by their annual capacity factor.

3. Variable O&M costs are 2010 values. LFG and MSW costs are based on [27].

4. Fuel prices are aggregated by state and by month for each fuel. This aggregation captures both location and seasonal variation in fuel price. Prices are primarily based on the EIA's Electric Power Monthly data for coal, petroleum liquids, and natural gas delivered price. These databases intentionally exclude some entries in order to maintain anonymity for data providers. Excluded prices are assumed to be the Census Division average, with the exception of West Virginia coal prices, which are derived from the EIA-423 reporting. Prices are assumed to be the same for all types of coal (BIT, SUB, waste coal, etc) and liquid petroleum (DFO, RFO). Fuel price for LFG, MSW, and NUC are assumed to be zero.

5. Ramp rates are derived from the GADS database [11]. Ramp rates are assumed to be equal for up-ramping and down-ramping. The GADS data was used to identify how the ramp rate of each plant type was correlated to the plant's capacity. We used an OLS regression of ramp rate against generator capacity. Results are as follows:

- Combined cycle: 0.22 MW/h ramp / MW capacity
- Steam Turbine: 0.14 MW/h ramp / MW capacity

- Gas Turbine: 0.34 MW/h ramp / MW capacity
- Combustion Turbine: 0.33 MW/h ramp / MW capacity

6. Minimum runtime for small (<150MW) coal plants have been adjusted to account for the fact that these plants are used within PJM as shoulder plants. Runtimes for LFG and MSW plants are assumed to be equal to combined cycle plants.

7. Based on InterTek and CAISO data, startup costs are assumed at $25/MW for combustion turbine, $50/MW for combined cycle, $100/MW for coal, and $500/MW for nuclear

8. PJM provided monthly 2010 EAF data, aggregated by generator type (coal 0-249 MW, coal 250-499 MW, coal 500+MW, gas CC, and gas CT). PJM-provided estimates were divided in half to roughly account for the effect of monthly averaging. Nuclear EAF was derived from NRC data, using generators in PJM. EAF for LFG and MSW was assumed to be equal to natural gas combustion turbine plants.

9. NEI contains data on total pollutant emissions from each generator. Data was cross-referenced with total annual power output numbers from eGRID to find pollutant emission rates in units of tons/MWh.

10. PJM sums the DAH load for all zones within the MIDATL region (PENELEC, BGE, PEPCO, METED, PPL, JCPL, PECO, PSEG, AECO, DPL, and RECO) into one entry. Therefore, we divide MIDATL load into its constituent zones. We do this by analyzing the Real Time load data, which is provided separately for all MIDATL zones. For each MIDATL zone, we find the percentage of MIDATL total its load contributes. We then assume that this percentage is the same for DAH and RT loads. Finally, we use that percentage to find the DAH load for each MIDATL zone.

11. Imports and export data is provided for each interface. We assign these interfaces to the appropriate zones as follows. We assume imports and exports do not change based on PJM prices.

Zone	Interfaces
AEP	ALTE, ALTW, CPLW, CWLP, DUK, EKPC, IPL, LGEE, MEC, MECS, NIPS, OVEC, TVA, WEC
PENELEC	FE
PSEG	NEPT, NYIS, LIND
DOM	CPLE
DAY	CIN

12. PJM provides hourly wind generation for WEST & MIDATL PJM regions. All WEST wind generation is assigned to bus 1, all MIDATL wind is assigned to bus 3, which is the location of most Mid-Atlantic wind capacity [27]. We assume wind generation is must take, and subtract it from load.

13. For RFC (bus 1), DOM (bus 5) and Mid-Atlantic (buses 2-4), the synchronized reserve requirement is the single largest unit. This is 1300 MW for bus 1, 1170 MW for buses 2-4, and 1170 MW for bus 5. The 1170 MW reserve for buses 2-4 is apportioned among the buses based on their loads. Reserve requirements are added to zonal loads.

To investigate the accuracy with which the model dispatches generators, we compared the simulated capacity factors of several PJM generators to their actual 2010 capacity factors. To find the generation and of PJM plants in 2010, we used data from the EPA's Air Market Program

Database (AMPD), which tracks generation and emissions from all plants regulated by the Clean Air Interstate Rule [28]. Because AMPD tracks generation at the plant level, we summed the power generation from all generators at the same plant in our simulation. In total, we compared the generation from 196 plants in PJM. Figure A-5 shows the simulated and actual generation from all plants. The mean error in capacity factor, weighted by plant capacity, was 3.6%. The root mean squared error in capacity factor, weighted by plant capacity, was 15.9%.

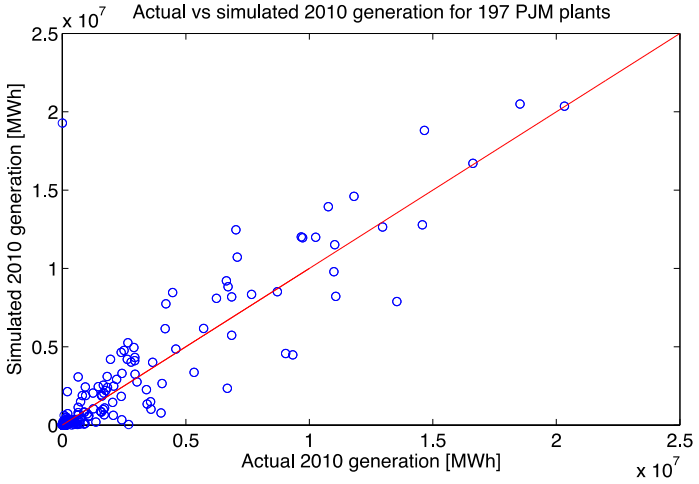

Figure A-5. Actual vs simulated 2010 generation for 197 PJM plants

References

[1] London Economics International LLC: A Comparative Analysis of Actual Locational Marginal Prices in the PJM Market and Estimated Short-run Marginal Costs: 2003-2006. (2007)

[2] PJM: Zone Map. http://www.pjm.com/about-pjm/how-we-operate/~/media/about-pjm/pjm-zones.ashx (2013). Accessed June 2013

[3] PJM: eData. https://edata.pjm.com/eContour/#app=ecca&e929-selectedIndex=2 (2012). Accessed June 2012

[4] PJM: Transmission and Voltage Emergencies. http://pjm.com/training/~/media/training/core-curriculum/ip-ops- 101/ops101-transemer.ashx (2011). Accessed Aug 6, 2012

[5] Monitoring Analytics: PJM State of the Market report, 2010. http://www.monitoringanalytics.com/reports/PJM_State_of_the_Market/2010.shtml (2011). Accessed June 2013

[6] US Environmental Protection Agency: National Electric Energy Data System (NEEDS) v.4.10. http://www.epa.gov/airmarkt/progsregs/epa-ipm/BaseCasev410.html#needs (2012). Accessed Aug 2012

[7] PJM: EIA 411 Report. http://www.pjm.com/documents/reports/~/media/documents/reports/2006-pjm-411-data.ashx (2010). Accessed Aug 2012

[8] Beaty, H. W., Mahrous, H., Seidman, A. H.: Handbook of electric power calculations. New York: McGraw-Hill. (2001)

[9] US Department of Energy, Energy Information Agency: EIA-423 Monthly Nonutility Fuel Receipts and Fuel Quality Data, 2010. http://www.eia.gov/cneaf/electricity/page/eia423.html (2011). Accessed Aug 2012

[10] US Department of Energy, Energy Information Agency: Electric Power Monthly. http://205.254.135.7/electricity/monthly/index.cfm (2012). Accessed Nov 2012

[11] North American Electric Reliability Corporation: 2012 Generating Availability Data System (GADS). http://www.nerc.com/page.php?cid=4%7C43 (2012). Accessed Aug 2012

[12] Bowring, J.: Updated Operating Parameter Matrix. http://www.monitoringanalytics.com/reports/Presentations/2007/011107-rmwg.pdf (2007). Accessed Aug 2012

[13] California Independent System Operator: MRTU Market Power Mitigation: Options for Bid Caps for Start-Up and Minimum Load Costs. http://www.caiso.com/1b87/1b87a5451d380.pdf (2007). Accessed Aug 2012

[14] InterTek: Estimating Power Plant Cycling Costs. http://www.wecc.biz/Lists/Calendar/Attachments/3868/11082011_WECC_DWG_Lower.pdf (2011). Accessed Aug 2012

[15] PJM: Scheduling Process and eMKT. http://www.pjm.com/~/media/training/core-curriculum/ip-gen-201/gen-201-scheduling-process.ashx (2011). Accessed Aug 2012

[16] US Nuclear Regulatory Commission. Power Status Reports 2010. http://www.nrc.gov/reading-rm/doc-collections/event-status/reactor-status/2010/2010PowerStatus.txt (2012). Accessed Aug 2012

[17] Bresler, S.: Personal communication, PJM. (2012)

[18] US Environmental Protection Agency: National Emissions Inventory. http://www.epa.gov/ttnchie1/net/2005inventory.html (2005). Accessed Aug 2012

[19] US Environmental Protection Agency: eGRID 2012. http://www.epa.gov/cleanenergy/energy-resources/egrid/index.html (2012). Accessed Aug 2012

[20] PJM: Historical Load Forecasts. http://www.pjm.com/markets-and-operations/~/media/markets-ops/ops-analysis/2010-rto-forecasts-zip.ashx (2011). Accessed Aug 2012

[21] PJM: Interchange Actual/Schedule Summary Report. http://www.pjm.com/markets-and-operations/~/media/markets-ops/ops-analysis/2010-act-sch-summary.ashx (2010). Accessed Aug 2012

[22] PJM: Monthly Locational Marginal Pricing. http://www.pjm.com/markets-and-operations/energy/real-time/monthlylmp.aspx (2010). Accessed Aug 2012

[23] PJM: Historical RTO Transfer Limit and Flows. http://www.pjm.com/markets-and-operations/~/media/markets-ops/ops-analysis/2010-flows.ashx (2010). Accessed Aug 2012

[24] PJM: Hourly Wind. http://www.pjm.com/markets-and-operations/~/media/markets-ops/ops-analysis/2010-hourly-wind.ashx (2010). Accessed Aug 2012

[25] PJM: Reserves Scheduling, Reporting, and Loading. http://www.pjm.com/~/media/training/core-curriculum/ip-ops-101/ops-101-reserves.ashx (2011). Accessed Aug 2012

[26] US Department of Energy, Energy Information Agency: Levelized Cost of New Generation Resources in the Annual Energy Outlook. http://www.eia.gov/oiaf/aeo/electricity_generation.html (2011). Accessed Aug 2012

[27] Schweizer, D.: Curtailment of Wind Farms Output Breakout Session, Illinois Wind Working Group 5th Annual Conference (2011)

[28] U.S. EPA. Air Markets Program Data. http://ampd.epa.gov/ampd/ (accessed Jan 8, 2014).

Chapter 3: THE EXTERNAL COSTS AND BENEFITS OF WIND ENERGY: A CASE STUDY IN THE PJM INTERCONNECTION

Abstract

Large deployments of wind create external costs and benefits that are not fully captured in power purchase agreements. External costs are due to the inherent variability and unpredictability of wind power and its negative effects on the local environment. Reduced greenhouse gases and criteria pollutants from fossil plants are external benefits. We investigate the external costs and benefits of wind in the PJM Interconnection for two scenarios: a 2012 scenario with 1.5% of energy from wind, and a high wind scenario with 20% of energy from wind. We find that external costs are uncertain but significant when compared to levelized PPA prices. The expected value of external costs is $23/MWh in both scenarios. Pollution reduction benefits are very uncertain but exceed external costs with high probability. For the low wind scenario, expected pollution reduction benefits exceed expected external costs by $97/MWh, with a 90% confidence range of $40/MWh - $160/MWh. In the high wind scenario, expected pollution reduction benefits exceed expected external costs by $114/MWh, with a 90% confidence range of $50/MWh - $190/MWh. Pollution reduction benefits may decrease in the future if criteria pollutant emission rates from PJM fossil plants continue to drop. If EPA cross-state air pollution regulations result in binding emission caps, policies that incentivize wind will not reduce criteria pollutant emissions and wind's external costs may exceed its external benefits. If caps bind at anticipated permit prices, state renewable portfolio standards may have less benefits than if they do not bind.

This paper was coauthored with Jared Moore and Jay Apt.

3.1 Introduction

In the United States, a variety of government subsidies and falling capital costs have resulted in nationwide deployments of more than 60 GW of wind capacity since 2002 [1]. However, low wholesale electricity prices, driven by falling demand and the expansion of domestic gas production, have eroded support for wind subsidies. The federal production tax credit expired at the end of 2013 [2] and several state legislatures have considered repealing or limiting state renewable portfolio standards [3]. This debate is underpinned by the following question: are policies incentivizing wind justified?

Wind developers typically sign long-term power purchase agreements (PPAs) to sell the energy produced by wind projects. The price of a PPA is determined by the private costs of developing a wind project, which include turbine costs, installed project costs, transmission connection costs, taxes, subsidies, operations and maintenance costs, and other development costs. PPA prices are also influenced by market characteristics, such as avoided costs on wholesale markets, and do not directly represent project costs [1].

Levelized PPA prices can be useful for comparing the competitiveness of wind to other electricity technologies. However, levelized PPA prices are not a useful metric for fully accounting for the costs and benefits of wind power relative to other electricity technologies [1]. Evaluating wind's effect on overall social welfare requires a full accounting of private costs and the costs and benefits that accrue to entities other than the PPA holder. PPA prices "do not fully reflect integration, resource adequacy, or transmission costs" [1]. These external costs, along with wind's environmental costs and benefits, accrue to third parties.

Wind power has several characteristics that create external costs and benefits (ECBs) that are different than those of traditional power plants. Managing wind's inherent variability can require operating other plants less efficiently and can require significant grid expansion and reinforcement. Wind may be harmful to ecosystems and wildlife, and may be a nuisance to local communities [4 – 6]. Finally, wind turbines emit no greenhouse gases (GHG) or criteria pollutants (CP), benefiting public health and the climate.

ECBs vary across different systems, and depend on system size, location, and level of wind penetration. Several studies have investigated individual ECB categories [7 – 14]. These studies are difficult to compare, as the methods, assumptions, and systems they study vary greatly. Few studies have attempted to comprehensively measure wind's external costs and benefits. The OECD analyzes the comprehensive costs of wind for several developed countries [7], but focuses on national-level costs and excludes the benefits of wind.

In this paper, we quantify the external costs and benefits of wind power in the PJM Interconnection. Our accounting of these costs and benefits is meant to contribute to the evaluation of existing and future incentives for wind energy in PJM. We considered the major ECB categories discussed in literature (Table 3-1). We levelized the ECBs so they can be directly compared to levelized PPA prices. We analyzed average expected ECBs for two scenarios: a low wind scenario representative of PJM as it was in 2010 with 1.5% of energy from wind, and a high wind scenario with 20% of energy from wind. These two scenarios can be viewed as lower and upper bounds of wind's penetration in PJM for the foreseeable future. ECBs are highly uncertain and cannot be calculated with a high level of precision. Therefore, we did not attempt to find the marginal ECB nor the optimal level of wind deployment that satisfies the first order condition. Rather, our goal was to identify if wind's ECBs are significant, and therefore if policies to incorporate these costs and benefits into private decision making are warranted. Due to this inherent uncertainty, our results are

presented as probability density functions. Accounting for the full range of uncertainty is necessary for a robust evaluation of the appropriateness of current and future wind incentives.

We do not quantify the damages that wind can cause to the local environment and stakeholders. Wind can harm biodiversity and ecosystems, cause bird and bat collisions, visual pollution, and noise pollution. We provide a discussion of these issues, but do not quantify them as they are highly uncertain and difficult to quantify rigorously.

The participation of wind on energy and capacity markets will create second-order effects for other market participants. Wind provides energy at very low marginal costs, offsetting more expensive generation and lowering energy prices. Wind also provides equivalent load carrying capability, which will affect prices on the capacity market. We do not quantify these effects in this analysis. Doing so would require a detailed analysis of the interplay between energy and capacity markets, which is beyond the scope of this paper. The Methods section contains a more thorough discussion of this topic.

Table 3-1. Definitions of External Cost and Benefit (ECB) categories quantified in this analysis

Cost and benefit categories	Definition
External costs	
Operational costs	The cost of ensuring stable grid operations, distributed across different markets (unit commitment, load following, regulation, and reserves)
Grid reinforcement and expansion	The cost of expanding and reinforcing the grid to support distant and variable wind plants
External benefits	
Greenhouse gas reduction	The societal benefit of reducing CO_2 and other greenhouse gas pollutants by displacing fossil-fueled generation with wind
Criteria pollutant reduction	The societal benefit of reducing criteria pollutant emissions (NO_X, SO_2, particulate matter) that harm human health and the environment, by displacing fossil-fueled generation with wind
Local environmental damages	The harm to biodiversity and local stakeholders from wind farm development. This includes harm to ecosystems such as bird and bat collisions, visual pollution, and noise pollution.

3.2 Methods

We investigated the external costs and benefits of wind in the PJM Interconnection. We separately analyzed the six categories most discussed in literature (Table 1). We analyzed these categories for PJM under a low wind scenario with 1.5% of energy from wind, as it was in 2010, and a high wind scenario with 20% of energy from wind, as is possible under the renewable portfolio standards of PJM member states [2].

Because estimates of each ECB category are uncertain, we treated wind's ECBs probabilistically with Monte Carlo simulation [15]. For each category, we estimated a lower bound, upper bound, and mode for triangular distributions in the low wind and high wind scenarios. We then used Monte Carlo simulation to calculate the probability density function of total external costs and external benefits.

Our estimates for each category are based on existing literature and our internal modeling using a unit commitment and economic dispatch model (UCED) of the PJM Interconnection. ECB estimates are highly dependent on the makeup of the electricity grid, generator technologies, location and quality of wind resources, and fuel costs. Most importantly, estimates vary due to differences in methods among studies. By combining prior research and the present modeling with multivariate Monte Carlo analysis, we investigated a large range of possible values for each ECB category.

Our UCED, the PHORUM model, uses mixed integer linear optimization to find the least-cost combination of generators to meet load at each hour of the year [16]. The optimization considers each plant's fuel costs and variable operations and maintenance costs. PHORUM also tracks emissions from each plant. PHORUM uses 2010 data to simulate PJM's day-ahead energy market. We updated the emission rates of CO_2, NO_X, and SO_2 for each plant to 2012 levels (see Pollution reduction benefits section). We used PHORUM to estimate operational costs and pollution

reductions because we found no other study or model that allowed us to simulate system-level costs and emissions at different levels of wind penetration in PJM. The high wind scenario, with 20% of energy from wind, used data from the Eastern Wind Integration and Transmission Study (EWITS) to characterize likely locations for new wind plants in PJM states [8].

3.2.1 Operational costs

Operational costs are the costs of maintaining grid stability by continuously balancing total generation with total load, given the variability and unpredictability of renewable energy. Operational costs occur from the next 48 hours to real-time [17]. The net effect of these costs is increased prices in markets run by the independent system operator (ISO), including the energy market, regulation market, and reserve markets. Compensating for wind variability requires ramping other generators in the system, which in turn can cause generators to operate inefficiently and increase the frequency of generator cycling. The variability of wind also leads to forecasting errors that increase reserve requirements and, when realized, may force system operators to use fast-ramping but inefficient generation instead of more cost-effective generators. Day-ahead wind forecast errors are typically 8% - 14% (RMS error) [18].

Calculating increases in operational costs requires both a statistical model of wind generation and a model of the electricity grid. Wind models use either measured or simulated wind speed data. Grid simulations vary in complexity from simple unit commitment models to more sophisticated models that capture forecast uncertainty and electrical dynamics of the grid. To isolate the costs of wind variability and unpredictability, it is common to use the 'flat-block' approach, in which a scenario with wind is compared not to a scenario without wind, but rather to a scenario in which the wind generation is constant and perfectly known [8].

Figure 3-1 shows operational cost estimates of several published studies [8 – 14] and our modeling with PHORUM. The studies vary in the costs they include, but generally find that unit commitment and load following costs are larger than regulation and reserve costs. The exception is Lueken et al. [14], which used historical California regulation market price data instead of simulation techniques to estimate operational costs. The high resulting costs suggest that either simulation methods may be biased to under-predict regulation costs, or that the observed California price data may be unrepresentative of areas used in simulations.

The published studies we review are for systems other than PJM. Our internal modeling with PHORUM enabled us to directly assess the effect of wind on the PJM system. Our findings are similar to those of other studies (Figure 3-1). Increases in operational costs depend on the generation technology displaced by wind. Our simulations show that in the low wind scenario, the generation offset by wind in PJM was 77% coal and 20% combined cycle. For the high wind scenario, the generation offset was 91% coal and 4% combined cycle. If gas prices were to fall from the 2010 fuel prices used in PHORUM and make combined cycle generation more competitive with coal, we expect that wind could be integrated more inexpensively, as the higher ramp rates and flexibility of combined cycle plants match well with the variability of wind.

The low wind scenario operational costs range from $0 - $4.3/MWh, with a mode of $1.2/MWh, and high wind scenario costs range from $1.9 - $9.7/MWh, with a mode of $4.0/MWh. For both scenarios, bounds were derived from existing literature and mode values from PHORUM simulations.

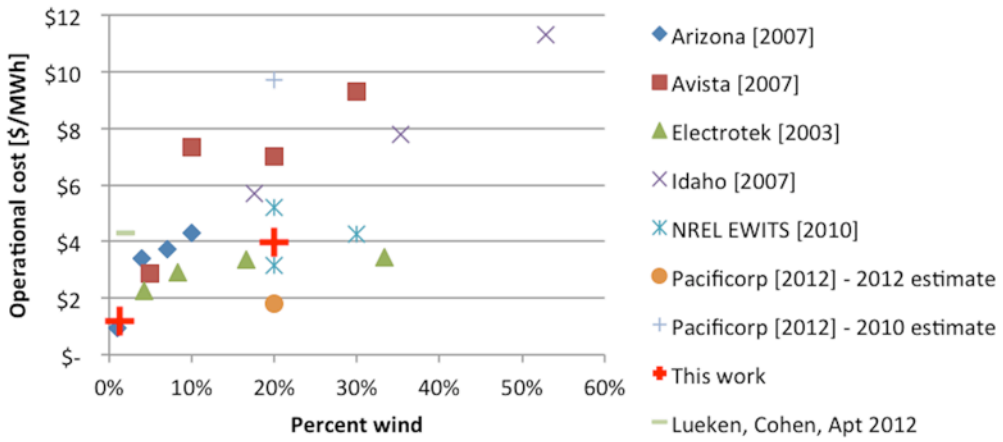

Figure 3-1. Estimates of operational integration costs from previous literature and this work (2010 dollars).

3.2.2 Grid reinforcement and expansion costs

The cost of connecting electricity produced by distant and variable renewables to load is an appreciable cost for wind energy. The allocation of these costs is also subject to extensive debate, leading FERC to issue Order No. 1000 [19]. Order No. 1000 requires local transmission providers to participate in the regional transmission planning process. It specifically requires transmission providers to devise cost allocation methods that, "…consider transmission needs driven by public policy requirements established by state or federal laws or regulations" [19].

FERC's order recognizes that transmission is a large impediment to wind energy development and could keep states from realizing renewable portfolio standards [20]. Transmission lines typically require far more time to develop than wind projects, and, once developed, there is a "free-rider" problem. Regions benefit from new transmission through eased transmission congestion or increased grid reliability by connecting dispatchable generators.

Fully allocating the costs and benefits of transmission that is necessary to enable wind development is beyond the scope of this study. For purposes of this research, we will follow the

allocation method set by PJM in response to FERC Order No. 1000. PJM has allocated the costs to ratepayers for large transmission lines (above 345 kV) [21].

The Lawrence Berkeley National Laboratory (LBNL) reviewed a sample of 40 transmission planning studies from across the country to assess the range of costs allocated to wind for transmission [22]. The vast majority of transmission lines in the sample were above 345 kV and the majority of these costs would be socialized among ratepayers according to PJM's new transmission allocation cost method [21]. Therefore, we use the LBNL study for the external costs of transmission for wind at low penetrations of wind.

LBNL found that transmission has a median cost of $300/kW of wind capacity. We converted these numbers to a levelized cost ($/MWh of wind) assuming a 28% capacity factor for PJM wind projects [1] and a fixed charged factor of 15% as assumed by the LBNL authors. A histogram of the costs is shown below in Figure 3-2.

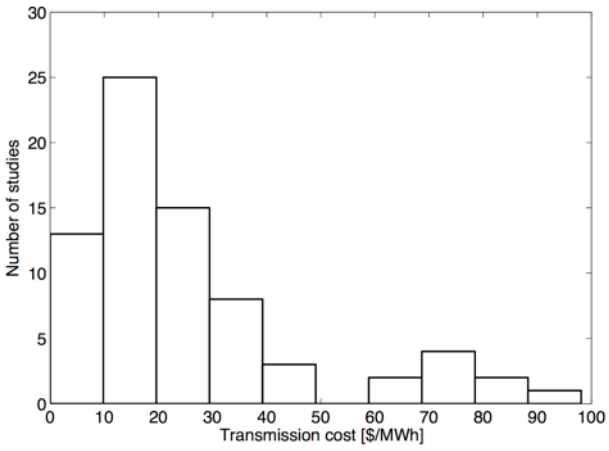

Figure 3-2. Histogram of transmission line costs from LBNL [22], assuming a wind capacity factor of 28% and fixed charge factor of 15%.

Transmission costs varied from $0/MWh to $98/MWh with a median of $18/MWh. Cost estimates at the high end are due to projects with transmission oversized for future plant development. Ignoring these projects, we assumed transmission costs range from $0/MWh -

$48/MWh with a mode of $16/MWh. The study also examined the case in which costs were not allocated to fossil plants on the same transmission line. This made a small difference increasing the cost allocated to wind by $30/kW ($2/MWh). We did not include these co-benefits or costs in this analysis, but note that they may be appreciable [8, 23].

In order to realize 20% penetration of renewable energy, a significant "top-down" expansion of the transmission grid may be necessary [8]. Table 3-2 shows capital cost estimates from studies of very large transmission expansions across the country in order to incorporate high wind penetrations. Based on these studies, we assumed bounds of $4 - $35/MWh of wind for the high wind scenario, with a most likely value of $15/MWh. Transmission costs for these studies are in the range found in the LBNL report, and agree with LBNL's finding that, "Unit transmission costs of wind … do not appear to increase significantly with higher levels of wind addition" [22].

Table 3-2. Capital Costs from Various Large Transmission Studies and Calculated Levelized Cost, assuming 28% Wind Capacity Factor and 15% Fixed Charge Factor

Cost per kW of Wind [$/kW]	Levelized Cost Per MWh of Wind [$/MWh]	Study
150 - 300	9 – 18	LBNL from AEP [22]
207	13	NREL [8]
316	19	LBNL from NEMS [22]
67-367	4 – 22	Holttinen [24]
350-570	21 – 35	DOE for ERCOT [25]
-	9	Dobesova et al. [26]

3.2.3 Resource adequacy

In this section, we discuss the resource adequacy (capacity) implications of wind. Wind energy provides relatively little capacity during times of peak load, as computed by the metric Equivalent Load Carrying Capability (ELCC) [27]. In PJM, wind receives an ELCC rating of 13% [27], meaning that 100 MW of nameplate wind capacity, its capacity contribution would be rated at 13 MW.

Some researchers have quantified the cost of procuring capacity so wind generators would have similar ELCC ratings as dispatchable generators [28]. In this research, we do not consider this point of view because we are not comparing wind to generator options. Here, we are examining the externalized costs not included in PPA contracts for wind so that policymakers may make a more informed decision about whether or not to implement wind.

In the sections above, we quantified transmission and ancillary services because wind increases the demand for these services and the costs are born by stakeholders other than the PPA holder. The addition of wind by itself does not increase the demand for capacity [29]. On the contrary, wind increases the supply of capacity, albeit in a relatively small amount. To first order, the net effect of wind is increased energy and capacity supply. How the cost of energy and capacity supplied by wind compares with the cost of energy and capacity it would displace is beyond the scope of this research.

It is worth noting that wind energy may have adverse second order effects on capacity market *prices* because it supplies a disproportionate amount of energy compared to capacity. Bids in capacity markets are driven by fixed costs less profits made in energy markets [30]. The addition of wind undercuts the profits of fossil generators in energy markets and causes them to increase their bids in capacity markets. However, these changes affect the revenue source (i.e. energy or capacity markets) for producers and not the overall social costs of capacity.

3.2.4 Curtailment costs

Curtailment occurs when wind plants intentionally reduce power output due to transmission constraints or market conditions. Wind curtailment has been reported for only six months in PJM and has been insignificant [1]. Curtailment costs could become significant at higher penetrations of wind as they were in ERCOT when 17% of wind energy was curtailed in 2009. Assuming a large

expansion of the transmission grid necessary to support 20% wind, EWITS estimated that curtailments would range from 3.6% to 10% [8].

Some PPA contracts compensate wind generators for curtailed wind via make-whole payments to wind generators, although rules vary by region [31]. We did not include curtailment payments here as an ECB, as reduced capacity factors due to weak wind resources, curtailment, or any other reason should not be included in the PPA. Sustained compensation for curtailment would not incentivize wind developers to develop in areas that are most cost effective per unit of electricity actually delivered to the grid. This is the precedent set for fossil fuel plants whose compensation is based on delivered electricity or delivered capacity.

3.2.5 Local environmental damages

Wind energy development has environmental costs that include fragmentation of local ecosystems, bird and bat collisions, noise pollution, and visual pollution. Developers may indirectly internalize mitigation costs for some of these damages through PPAs. For example, local landowners are compensated through lease payments for tolerating visual and noise pollution on their property. Ecological damages may be quantified through mitigation costs for habitat destruction. In California, developers pay to set aside some amount of land per acre disturbed based on the ecological sensitivity of the land affected. However, "no obvious compensation ratio will offset bird and bat collisions with wind turbines" [32]. Therefore, California advises developers to "consult with the California Department of Fish and Game (CDFG), U.S. Fish and Wildlife Service (USFWS), and species experts in the development of site-specific ratios and fees to use in establishing compensation formulae" [32].

Social costs such as visual and noise pollution and wildlife effects are real costs of wind power. However, because these damages are site specific, may be internalized in PPAs, and

have "no obvious compensation" method, we omitted these damages in our quantifications for ECBs.

3.2.6 Pollution reduction benefits

A primary benefit of wind energy is pollution reduction. Because wind has very low short-run marginal costs, it is dispatched before more expensive generators. If wind displaces fossil-fueled generators, it reduces net grid emissions. We assume that the addition of wind will result in a net reduction in GHG and criteria pollutants, providing external benefits that can be valued by the social damages that would have been caused by these avoided pollutants. This may not be true if emissions are subject to a binding cap; this is not currently the case in PJM, and is unlikely to be in coming years (see Results & Discussion section below).

Emission reductions are typically given as pounds of emissions avoided per MWh of electricity produced by wind. We monetized the benefit of pollution reductions with the estimated external cost of each pollutant. We modeled pollution reduction benefits in the low wind and high wind scenarios as triangular distributions. We used PHORUM to simulate how adding wind to PJM in 2012 would have changed each plant's annual power generation and emissions. We find that wind offsets predominantly coal generation. In the low wind scenario, 77% of the generation offset was coal; in the high wind scenario, coal was 91% of the generation offset. If gas prices were to fall significantly such that combined cycle plants operated as baseload in place of coal, we would expect pollution reduction benefits to decrease.

CO_2 emission reductions are valued with a social cost of carbon (SCC) of \$12 - \$114/ton, with a mode of \$39/ton (2010 dollars), the US government's estimates of SCC for 2015. The low and mode cases are average damage estimates for 5% and 3% discount rates, respectively. The high

damage case is the 95th percentile of damages under a 3% discount rate [33]. These are the bounds for our distribution of GHG reduction benefits (Table 3).

We valued criteria pollutant reductions (NO_X, SO_2, 2.5 micrometer particulate matter ($PM_{2.5}$)) with the AP2 model, a reduced form, integrated assessment model that links emissions of criteria pollutants to human health and environmental damages for all U.S. counties [34]. AP2 uses Monte Carlo analysis to provide uncertainty estimates for all damages, accounting for variations in value of statistical life, dose-response functions, and the air transport model. We estimated the uncertainty of damages caused by emissions from PJM plants using AP2's raw Monte Carlo results, which were provided by the model's developer. For each of AP2's Monte Carlo cases, we found the location-specific damage rate for each plant, which we summed to find total damages caused by PJM plants. We identified the 5th, 50th, and 95th percentiles of the resulting distribution as the bounds for our distribution of wind's criteria pollutant benefits.

In the high wind scenario, it might be argued that AP2's baseline emissions are affected enough so that the human health effects are no longer accurate. In the case of SO2, there is clear evidence that PM2.5 formation is linear, no threshold with reduced SO2 emissions [35]. Large cohort studies have found PM2.5 concentration-response functions and mortality are also linear with no threshold [36, 37]. Thus, for our high wind case at 20% wind the AP2 model predictions are justified.

Since 2010, the year for which our base data are available, emissions of CO_2 and criteria pollutants have dropped significantly in PJM due to lower natural gas prices, the Clean Air Interstate Rule (CAIR) [38], and the Mercury and Air Toxics Standard (MATS) [39]. 2012 emissions of SO_2 were 42% lower than 2010 levels in PJM states, and NO_X and CO_2 emissions have both dropped 15% [40]. To compensate for these reductions, we reduced the simulated 2010 emissions and associated damages from each plant by 42% for SO_2, 15% for NO_X, and 15% for CO_2. This

adjustment ignores any changes to the dispatch order that may have occurred since 2010. We have applied this adjustment in the results that follow.

3.3 Results and discussion

Table 3-3 summarizes the parameters used in our Monte Carlo analysis of external costs and benefits in PJM. External costs are significant when compared to private costs – the average PPA price in 2012 was ~$50/MWh in the PJM region [1]. However, external costs are much smaller than both GHG emission reduction benefits and criteria pollutant emission reduction benefits (Figure 3-3). Emission reduction benefits are higher in PJM than other ISOs due to the combination of PJM's reliance on high emitting fossil-fueled generators and high population, resulting in increased pollution exposure compared to other ISOs.

Table 3-3. External cost and benefit parameters used in Monte Carlo simulation

Cost and benefit categories	Low wind scenario ($/MWh)			High wind scenario ($/MWh)		
	Lower bound	Median	Upper bound	Lower bound	Median	Upper bound
Operational costs	$0	$2	$4	$2	$4	$10
Grid reinforcement and expansion	$0	$16	$48	$4	$15	$35
Greenhouse gas reductions	$9	$30	$87	$9	$31	$87
Criteria pollutant reductions	$15	$57	$164	$19	$70	$198

* Local environmental damages and curtailment costs were not monetized (see respective sections)

Monte Carlo simulation results are shown in Figure 3-3. Total external costs have an expected value of $23/MWh in both the low wind and high wind scenarios. The monetized external benefits from pollution reduction exceed the monetized external costs in both the low and high wind scenarios. For the low wind scenario, expected pollution reduction benefits exceed expected external costs by $97/MWh, with a 90% confidence range of $40/MWh - $160/MWh. In the high

wind scenario, expected pollution reduction benefits exceed expected external costs by $114/MWh, with a 90% confidence range of $50/MWh - $190/MWh. The probability that monetized external costs exceed pollution reduction benefits is less than 1% for both scenarios.

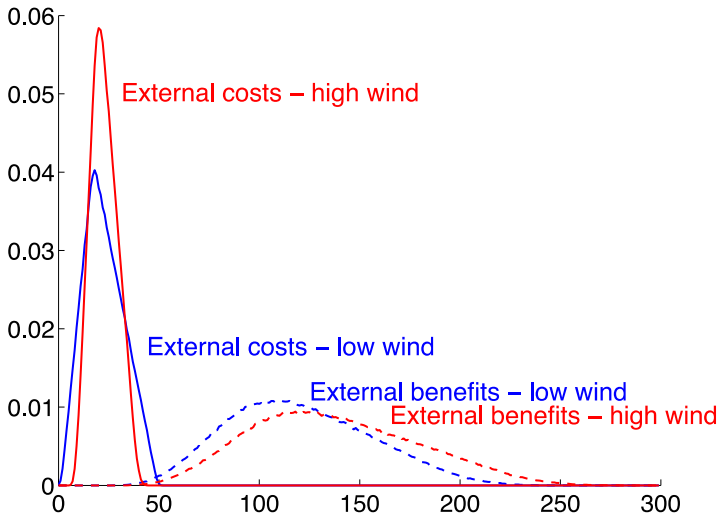

Figure 3-3. Distribution of total external costs and benefits. External costs and benefits are larger in the high wind scenario than the low wind scenario. Total external benefits are highly uncertain but have a very high probability of being significantly greater than costs.

The analysis presented here is of average ECBs under the high and low wind penetration scenarios, not ECBs at the margin. Other research has shown that marginal integration costs increase with increasing wind penetrations [1]. Therefore, the marginal external costs are likely higher than the average external costs we quantify here. It is less clear if emission reduction benefits increase or decrease on the margin. This will depend on if higher penetrations of wind increasingly offset high-emitting generation or low-emitting generation. Factors such as fuel price, the makeup of the generation fleet, and timing of wind generation will determine the marginal benefit of wind.

3.3.1 External benefits under a future, cleaner grid

Over the next decade, several rules by the U.S. Environmental Protection Agency (EPA) are expected to force many of PJM's coal generators to either retire or retrofit with improved emission

control technologies. Rules include the Clean Air Interstate Rule (CAIR), which capped emissions of NO_X and SO_2 [38]; the Acid Rain Program, which capped emissions of SO_2 and has since been superseded by CAIR [41]; the Mercury and Air Toxics Standard (MATS), which limits emissions of mercury and primary particulate matter [39]; and the forthcoming rules placing CO_2 restrictions on existing power plants [42]. The EPA has proposed the Cross-State Air Pollution Rule (CSPAR) to replace CAIR [43]. The U.S. Supreme Court recently upheld CSPAR, which will likely replace CAIR [44]. PJM anticipates as much as 20 GW of coal capacity is at risk of retirement by CAIR/CSAPR and MATS, or 25% of total coal capacity. An additional 29 GW of capacity may need at least two retrofits to comply with the rules [45].

Two future scenarios are possible under the EPA regulations. The first scenario is that the emission caps established by CAIR/CSPAR bind. In this case, total emissions of NO_X and SO_2 will be fixed at the emissions cap and new additions of wind will not result in a net reduction in emissions. Rather, wind will affect the price that other generators must pay for NO_X and SO_2 emission permits. The EPA anticipates permit prices will be \$1,300/ton for SO_2 and \$2,100/ton for NO_X in 2015 (2010 dollars) [38]. The anticipated SO_2 permit price is much lower than the health damages caused by SO_2 emissions from PJM plants. The AP2 model estimates the median damage per ton of SO_2 across all PJM coal plants has a 90% confidence range of \$9,000 - \$17,000 per ton, depending on location. If CAIR/CSPAR emission caps bind, significant amounts of wind would put downward pressure on permit prices. The external emission benefit of wind in this scenario would be the reduction in permit prices paid by other generators, due to the addition of wind to the system. This second order effect may be small relative to the EPA's anticipated permit prices.

In states subject to binding CAIR/CSPAR emission caps, additional wind does not reduce criteria pollutants. To simulate this effect, we repeat the analysis above but assume wind provides no external criteria pollutant emission benefits. In this context, wind's net external benefit is

reduced to an expected value of $19/MWh for both the high wind and low wind scenarios. Expected net benefits are positive because greenhouse gas reduction benefits exceed external costs. The probability of net benefits being negative is 18% in the low wind scenario and 16% in the high wind scenario. We therefore conclude that state renewable portfolio standards are still warranted in PJM states under binding emission caps, although their benefits will be significantly reduced.

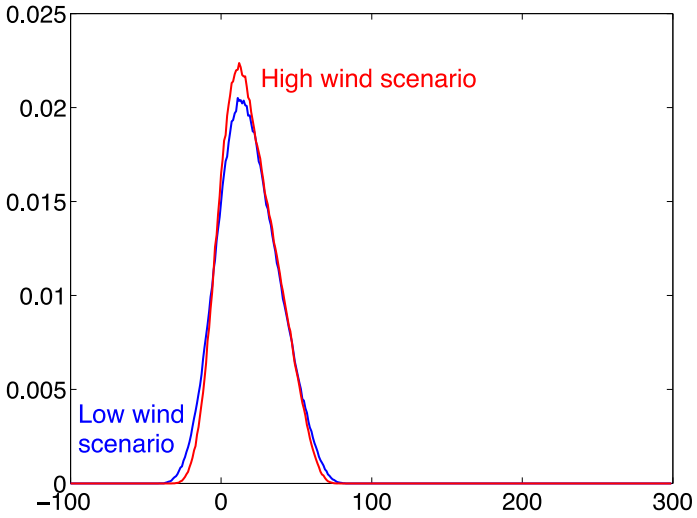

Figure 3-4. Distribution of wind's net external benefits under a scenario in which criteria pollutant emissions are subject to a binding cap, and wind provides no criteria pollutant emission reduction benefits.

The more likely scenario is that emission caps do not bind. Due to significant wind deployment, low natural gas prices, and tightened fossil plant emission regulations under MATS, caps are not expected to bind [46]. In this scenario, new additions of wind would reduce criteria pollutant emissions and should be valued by the human health benefits they induce. These benefits will be lower than those in Table 3 if criteria pollutant emission rates from coal and oil plants continue to drop as mandated by MATS. How much emission benefits fall will depend on the specifics of which plants retrofit or retire. Because our modeling shows ~85% of total health damages are due to SO_2, any reductions in the SO_2 emission rates of PJM plants will greatly reduce

the criteria pollutant benefits of wind. Halving current PJM SO_2 emission rates would result in expected pollution reduction benefits exceeding expected external costs by $64/MWh and $74/MWh for the low and high wind scenarios, respectively.

We also note that there is considerable uncertainty in health damages across different models. Levy et al. [47] find that median damages per ton across all U.S. coal plants in 1999 had a 90% confidence range of $6,000 to $50,000 per ton for SO_2; according to AP2 the median damages per ton of SO_2 are $9,000 - $17,000 per ton.

Two PJM member states, Maryland and Delaware, are subject to the Regional Greenhouse Gas Initiative (RGGI), a regional cap-and-trade program for CO_2. However, CO_2 emissions from plants in Maryland and Delaware are less than 10% of total PJM CO_2 emissions. Furthermore, the market clearing price for CO_2 permits has been much lower than the social cost of carbon estimates of the US government [48, 34]. Therefore, RGGI is unlikely to have a significant effect on PJM CO_2 emissions.

3.3.2 Market implications

The addition of wind to electric power systems creates external costs and benefits that are not priced in today's markets. These external costs and benefits (ECBs) are highly uncertain and vary between markets. We find that the external costs of wind are primarily due to grid reinforcement and expansion costs and resource adequacy costs. In PJM, our estimate of the expected value of total external costs is $23/MWh in both the low wind scenario and a high wind scenario with 20% of energy from wind. The external benefits wind creates by reducing GHG and criteria pollutant emissions are expected to exceed total external costs by $97/MWh for the low wind scenario and $114/MWh for the high wind. These net external benefits are significant compared to wind's traditional levelized cost ~$80/MWh [49]. We therefore recommend that policies be established to

incorporate the external costs and benefits of wind into the private decision making of wind developers.

Adding wind to PJM is anticipated to reduce criteria pollutant emissions and human health damages because existing emission caps are not expected to bind [46]. If caps do not bind but criteria pollutant emission rates from coal and oil plants continue to fall below 2012 levels, as mandated by MATS, the pollution reduction benefits of wind will be reduced. Under the scenario in which CAIR/CSPAR results in binding emission caps at anticipated permit prices, additional wind will not reduce criteria pollutant emissions and external costs may exceed external benefits. If these caps bind at anticipated permit prices, state renewable portfolio standards will have less benefits than if they do not bind.

3.4 References

[1] Wiser, R.; Bolinger, M. *2012 Wind Technologies Market Report;* DOE/GO-102013-3948; Lawrence Berkeley National Laboratory: Berkley, CA, **2013**.

[2] DSIRE – Database of State Incentives for Renewables and Efficiency. http://www.dsireusa.org/ (accessed March 1, 2014).

[3] Bloomberg News - U.S. States Turn Against Renewable Energy as Gas Plunges. http://www.bloomberg.com/news/2013-04-23/u-s-states-turn-against-renewable-energy-as-gas-plunges.html (accessed March 1, 2014).

[4] Saidur, R.; Rahim, N.; Islam, M.; Solangi, K. Environmental impact of wind energy. *Renewable and Sustainable Energy Review.* **2011***,* 15, 2423-2430.

[5] Leung, D.Y.; Yang, Y. Wind energy development and its environmental impact: A review. *Renewable and Sustainable Energy Review.* **2012***,* 16, 1031-1039.

[6] Premalatha, M.; Abbasi, T.; Abbasi, S.A. Wind energy: Increasing deployment, rising environmental concerns. *Renewable and Sustainable Energy Reviews.* **2014**, 31, 270-288.

[7] Organization for Economic Co-operation and Development. *Nuclear Energy and Renewables: System Effects in Low-carbon Electricity Systems;* Nuclear Energy Agency: Paris, **2012**.

[8] Corbus, D. *Eastern Wind Integration and Transmission Study*; NREL/SR-5500-47078; National Renewable Energy Laboratory: Golden, CO, 2010.

[9] Acker, T. Final Report: Arizona Public Service Wind Integration *Cost Impact Study*; Prepared for Arizona Public Service Company: Northern Arizona University, Flagstaff, AZ, **2007**.

[10] EnerNex Corporation. *Final Report: Avista Corporation Wind Integration Study;* Prepared for Avista Corporation: Knoxville, TN, **2007**.

[11] EnerNex Corporation. *Operational Impacts of Integrating Wind Generation into Idaho Power's Existing Resource Portfolio*; Prepared for Idaho Power Company: Knoxville, TN, **2007**.

[12] Electrotek Concepts. WE Energies Energy System Operations Impacts of Wind Generation Integration Study; Prepared for We Energies: Knoxville, TN, **2003**.

[13] PacifiCorp. PacifiCorp 2012 Wind Integration Resource Study – DRAFT For IRP Public Participants Review; Portland, OR, **2012**.

[14] Lueken, C.; Cohen, G.; Apt, J. Costs of Solar and Wind Power Variability for Reducing CO2 Emissions. *Environ. Sci. Technol.* **2012**, *46* (17), 9761-9767.

[15] Weber, C. L.; Clavin, C. Life cycle carbon footprint of shale gas: Review of evidence and implications. *Environ. Sci. Technol.* **2012**, *46* (11), 5688-5695.

[16] PHORUM is available at https://github.com/rlueken/PHORUM. For a description, see Lueken, R.; Apt, J. The effects of bulk electricity storage on the PJM market. *Energy Systems.* ***2014***, DOI: 10.1007/s12667-014-0123-7.

[17] North American Electric Reliability Corporation. *Task 2.4 Report. Operating Practice, Procedures and Tools*; Princeton, NJ, **2011**.

[18] Mauch, B., P.M.S. Carvalho and J. Apt, Can a Wind Farm with CAES Survive in the Day-ahead Market? *Energy Policy*. **2012**. 48: 584-593.

[19] Federal Energy Regulatory Commission. Order No. 1000 - Transmission Planning and Cost Allocation. **2011**. https://www.ferc.gov/industries/electric/indus-act/trans-plan.asp (Accessed May 18, 2014).

[20] Locke Lord Bissell and Liddell LLP. Transmission Access Challenges for Wind Generation: Developing solutions nationwide and in ERCOT. **2007**. http://www.lockelord.com/~/media/Files/NewsandEvents/News/2007/11/Transmission%20Access%20Challenges%20for%20Wind%20Generation/Files/Transmission%20Access/FileAttachment/transmission%20Access%20Challenges%20for%20Wind%20Generation.ppt (Accessed May 18, 2014).

[21] PJM Interconnection. *Order Conditionally Accepting and Suspending Cost Allocation Filing*; Docket No. ER 13-90-000. **2013**. http://www.pjm.com/~/media/documents/ferc/2013-orders/20130131-er13-90-000.ashx (accessed May 18, 2014)

[22] Mills, A.; Wiser, R.; Porter, K. *The Cost of Transmission for Wind Energy: A Review of Transmission Planning Studies;* LBNL-1471E; Lawrence Berkeley National Laboratory: Berkley, CA, **2009**.

[23] Black & Veatch. *Renewable Energy Transmission Initiative, Phase 2B Final Report*; RETI-1000-2010-002-F; Prepared for RETI Coordinating Committee: San Francisco, CA, **2010**.

[24] Holttinen, H.; Meibom, M.; Orths, A.; O'Malley, M.; Ummels, B.; Tande, J.O.; Estanqueiro, A.; Gomez, E.; Smith, J.C.; Ela, E. Impacts of large amounts of wind power on design and operation of power systems, results of IEA collaboration. *Wind Energy*. **2011***, 14(2)*, 179-192.

[25] U.S. Department of Energy. *20% Wind Energy by 2030: Increasing Wind Energy's Contribution to U.S. Electricity Supply*; DOE/GO-102008-2567; Office of Energy Efficiency and Renewable Energy: Washington, DC, **2008**.

[26] Dobesova, K.; Apt, J.; Lave, L. Are renewables portfolio standards cost-effective emission abatement policy? *Environ. Sci. Technol.* **2005**, 39.22, 8578-8583.

[27] Milligan, M.; Porter, K. *Determining the Capacity Value of Wind: An Updated Survey of Methods and Implementation*; NREL/CP-500-43433; National Renewable Energy Laboratory: Golden, CO, **2009**.

[28] Ueckererdt F.; Hirth L.; Luderer G.; Edenhofer O. "System LCOE: What are the costs of variable renewables?", *Energy, 63 (2013) 61-75*

[29] Smith J.; Milligan M.; DeMeo E.; Parsons B. "Utility wind integration and operating impact state of the art", Power Systems, IEEE Transactions on, 2007, 22(3): 900-908.

[30] Pfeifenberger J; Newell S; Spees, K; Murray A; Karkatsouli I. "Third Triennial Review of PJM's Variable Resource Requirement Curve," The Brattle Group, 2014.

[31] Rogers, J.; Fink, S.; Porter, K. *Examples of Wind Energy Curtailment Practices*; NREL/SR-550-48737; National Renewable Energy Laboratory: Golden, CO, 2010.

[32] California Energy Commission. *California Guidelines for Reducing Impacts to Birds and Bats from Wind Energy Development*; Report CEC-700-2007-008-SD; **2007**. http://www.energy.ca.gov/2007publications/CEC-700-2007-008/CEC-700-2007-008-SD.PDF (accessed May 18, 2014).

[33] U.S. Interagency Working Grop on the Social Cost of Carbon. Technical Support Document: Technical Update of the Social Cost of Carbon for Regulatory Impact Analysis Under Executive Order 12866, Revised Nov 2013; Washington, DC, **2013**.

[34] Muller, N. Linking policy to statistical uncertainty in air pollution damages. *The BE Journal of Economic Analysis & Policy*. 2011*, 11*, 1.

[35] Koo, B.; Wilson, G.; Morris, R.; Dunker, A.; Yarwood, G. Comparison of Source Apportionment and Sensitivity Analysis in a Particulate Matter Air Quality Model. *Environ. Sci. Technol.* **2009**, 43, 6669-6675.

[36] Krewski D.; Jerrett M.; Burnett R.T.; Ma R.; Hughes E.; Shi Y.; Turner M.C.; Pope C.A. 3rd.; Thurston G.; Calle E.E.; Thun M.J.; Beckerman B.; DeLuca P.; Finkelstein N.; Ito K.; Moore D.K.; Newbold K.B.; Ramsay T.; Ross Z.; Shin H.; and Tempalski B. *Extended follow-up and spatial analysis of the American*

Cancer Society study linking particulate air pollution and mortality. No. 140. Boston, MA: Health Effects Institute, **2009**.

[37] Lepeule, J.; Laden, F.; Dockery, D.; Schwartz, J. Chronic Exposure to Fine Particles and Mortality: An Extended Follow-up of the Harvard Six Cities Study from 1974 to 2009. *Environmental Health Perspectives*. **2012**, 120(7), 965–970.

[38] U.S. EPA. *Regulatory Impact Analysis for the Final Clean Air Interstate Rule*; Office of Air and Radiation: Washington, DC, **2005**.

[39] U.S. EPA. *Regulatory Impact Analysis for the Final Mercury and Air Toxics Standard*; Office of Air Quality Planning and Standards: Washington, DC, **2011**.

[40] U.S. EPA. Air Markets Program Data. http://ampd.epa.gov/ampd/ (accessed Oct 29, 2013).

[41] U.S. EPA. Interactions With Other Clean Air Act Requirements. *Fed Regist.* **2005**, 70 (91), 25289 – 25305.

[42] U.S. Executive Office of the President. The President's Climate Action Plan; Washington, DC, 2013. http://www.whitehouse.gov/sites/default/files/image/president27sclimateactionplan.pdf (accessed Oct 14, 2013).

[43] U.S. EPA. Regulatory Impact Analysis for the Federal Implementation Plans to Reduce Interstate Transport of Fine Particulate Matter and Ozone in 27 States; Office of Air and Radiation: Washington, DC, **2011**.

[44] Environmental Protection Agency v. EME Homer City Generation. 12-1182 (U.S. Supreme Court 2014). http://www.supremecourt.gov/opinions/13pdf/12-1182_bqm1.pdf (accessed May 1, 2014).

[45] PJM Interconnection. *Coal Capacity at Risk of Retirement in PJM: Potential Impacts of the Finalized EPA Cross State Air Pollution Rule and Proposed National Emissions Standards for Hazardous Air Pollutants*; Norristown, PA, **2011**. http://pjm.com/~/media/documents/reports/20110826-coal-capacity-at-risk-for-retirement.ashx (accessed Oct 14, 2013).

[46] Paul, A., Blair, B., Palmer, K. (2013). *Taxing Electricity Sector Carbon Emissions at Social Cost*; RFF DP 13-23; Resources For the Future: Washington, DC **2013**.

[47] Levy, J. I.; Baxter, L. K.; Schwartz, J. Uncertainty and Variability in Health- Related Damages from Coal- Fired Power Plants in the United States. *Risk Analysis*. **2009**, *29*(7), 1000-1014.

[48] RGGI Inc. *CO2 Allowances Sold at $3.00 at 22nd RGGI Auction*; New York, NY, **2013**. http://www.rggi.org/docs/Auctions/22/PR120613_Auction22.pdf (accessed May 1, 2014).

[49] U.S. Department of Energy. *Annual Energy Outlook 2014 Early Release*; Energy Information Administration: Washington, DC, **2013**. http://www.eia.gov/forecasts/aeo/pdf/0383(2014).pdf (accessed August 12, 2014).

Chapter 4: THE CLIMATE AND HEALTH EFFECTS OF A USA SWITCH FROM COAL TO GAS ELECTRICITY GENERATION

Abstract

Abundant natural gas at low prices has prompted industry and politicians to welcome gas as a 'bridge fuel' between today's coal intensive electric power generation and a future low-carbon grid. We used existing national datasets and publicly available models to investigate the upper limit to the emission benefits of natural gas in the USA power sector. As a limiting case, we analyzed a switch of all USA coal plants to natural gas plants, occurring in 2016. While the effect on global temperatures is small out to 2040, the USA power plant fleet's contribution could be changed by as much as -50% to +5%. By 2100, switching from coal would reduce global temperatures. The net effect on warming is highly sensitive to the rate of fugitive CH_4 emissions and efficiency of replacement gas plants. The human health benefits of such a switch are substantial: SO_2 emissions are reduced by more than 90%, and NO_X emissions by more than 60%. These reductions would reduce total national annual health damages by ~$20 billion annually. The costs of building and operating new gas plants likely exceed the health benefits; retrofitting coal plants with emission control technology is likely to be more cost effective.

This paper was coauthored with Kelly Klima, W. Michael Griffin, and Jay Apt.

4.1 Introduction

Over the past decade shale gas development has increased USA domestic gas production by 20% [1]. Abundant gas at low prices has prompted industry and politicians to welcome gas as a 'bridge fuel' between today's electric power generation system, whose largest single fuel is coal, and a future, low-carbon grid. In June 2013 President Obama released the USA Climate Action Plan, which included "actions to promote fuel switching from oil and coal to natural gas" [2].

Recently, a growing body of research has questioned the ability of domestic natural gas to substantially reduce USA greenhouse gas (GHG) emissions. Natural gas power plants typically emit 50% - 60% less carbon dioxide (CO_2) than coal plants due to their higher efficiency and lower carbon content of their fuel [3]. However, fugitive emissions from the production and transportation of natural gas (methane, CH_4), itself a potent GHG, may diminish these climate benefits [4 – 9].

The human health consequences of such a shift have not received as extensive discussion as the GHG effects. Compared to coal plants without emission controls, natural gas plants emit less SO_2 and NO_X, precursors of particulate matter. Natural gas also has lower primary emissions $PM_{2.5}$ and PM_{10} than coal. Exposure to $PM_{2.5}$ has been linked to human mortality and morbidity [10 – 14]. EPA regulations, including the Clean Air Interstate Rule (CAIR), the Cross-State Air Pollution Rule, and Mercury and Air Toxics Standard (MATS), are designed to reduce these emissions [10, 15, 16]. These regulations have been one cause of a switch from coal to natural gas plants [1, 17].

We investigated the potential for natural gas to reduce emissions of GHGs and criteria pollutants from the USA electric power sector. To establish an upper bound on the potential benefits, we analyzed a switch of all USA coal plants to natural gas or zero-emission plants

(renewables or nuclear), occurring in 2016. We quantified the reductions in total power sector emissions that would occur, as well as the associated climate and health benefits.

Our intent was not to quantify the cost effectiveness of switching to gas or the optimal generation fleet. Rather, the goal was to identify the limits to achieving U.S. pollution reduction goals through the use of natural gas power generation. This study differs from existing studies of the climate and health implications of U.S. coal plants [4, 7, 8, 18, 19], in that we attempted to quantify the maximum achievable benefit of switching the USA fleet of coal generators to gas or zero-emission sources. We also directly compare the magnitude of the reduction in GHG emissions to that of criteria pollutant emissions.

We used U.S. Department of Energy (DOE) forecasts of emissions and generation as the baseline for our analysis. From this baseline, we replaced all coal plants with either natural gas or zero-emission plants, starting in 2016. We varied the fugitive methane emission rate from 0% - 7%, a range that includes estimates from existing literature [9]. Using the Global Temperature Potential (GTP), we estimated how switching from coal to gas would affect the power plant fleet's contribution to global temperature until 2040, the last year for which EIA forecasts emissions and generation. The APEEP model [20] was used to compute the health benefits of such a switch.

4.2 Methods

4.2.1 Calculation of baseline emissions

We developed baseline emission scenarios for 2016 – 2040 based on the forecasts from the DOE's Energy Information Agency (EIA) [21]. EIA forecasts installed capacity by plant type; electricity generation by fuel type; and total NO_X and SO_2 emissions from the electric power sector. We used the EIA's Reference scenario as our analysis baseline; we also consider the EIA's Low Oil

and Gas Resource and High Oil and Gas Resource. Descriptions of each scenario are in Appendix B.

Baseline greenhouse gas emissions

EIA does not forecast CO_2 or CH_4 emissions. We calculated CO_2 emissions by multiplying EIA's forecast of total electricity production from each fuel by the 2012 capacity-weighted average CO_2 emission rate of plants of that fuel type. We used plant-level emission data from the EPA Air Market Program Database (AMPD) to identify 2012 CO_2 emission rates for plants in 27 eastern states regulated by the EPA Clean Air Interstate Rule (CAIR) [22]. These generators made up 70% of 2012 CO_2 emissions.

We calculated CH_4 emissions as the sum of combustion emissions and fugitive emissions from CH_4 production and transportation. Combustion CH_4 emissions for each fuel type are the capacity-weighted average CH_4 emission rates of plants in the EPA's Emissions & Generation Resource Integrated Database (eGRID), 2009 [3]. We parameterized the rate of fugitive CH4 emissions in a range of 0 - 7%, covering estimates from existing literature [9]. We multiplied the fugitive rate by forecasts of total gas to calculate total fugitive CH4 emissions. Total gas consumed was found by multiplying EIA's forecast of natural gas generation [21] by the capacity-weighted heat rate of existing gas plants in 2012 [3]. Other fugitive emissions (greenhouse gases, NO_X, SO_2, $PM_{2.5}$, PM_{10}) from the production and transportation of coal and natural gas did not qualitatively change our results and were excluded from the analysis.

Baseline NO_X and SO_2 emissions

EIA forecasts total electric power NO_X and SO_2 emissions out to 2040. It does not forecast emissions by fuel type. We therefore separated out the NO_X and SO_2 emissions associated with coal, oil, and gas plants. We first calculated NO_X and SO_2 emissions from oil and gas plants. Similar

to CO_2 emissions, we used the 2012 capacity-weighted average emission rate for oil and gas plants from AMPD [22].

Next, we multiplied these emission rates by EIA's forecast of electricity production to find total NO_X and SO_2 emissions from oil and gas plants. Finally, we calculated coal NO_X and SO_2 emissions as the difference between EIA's forecast of total NO_X and SO_2 emissions and total oil and gas plant emissions.

Baseline $PM_{2.5}$ and PM_{10} emissions

EIA does not forecast direct emissions of $PM_{2.5}$ and PM_{10} from power plants. We assumed that coal and oil plants emit 0.14 kg / MWh of $PM_{2.5}$ and PM_{10}, the limit imposed by the EPA's MATS [15]. Gas plants are not regulated by MATS, and therefore we used data from the 2005 National Emissions Inventory (NEI) [23] and eGRID 2005 [3] to identify gas plant $PM_{2.5}$ and PM_{10} combustion emissions rates. We found the capacity-weighted average emission rate of gas plants in the NEI database to be 0.06 kg/MWh for $PM_{2.5}$ and 0.07 kg/MWh for PM_{10}. For coal, oil and gas plants, we multiplied the assumed emission rates by EIA's forecast of annual electricity generation by each fuel.

4.2.2 Calculation of replacement plant emission rates

We modeled three scenarios to investigate the benefits of switching from coal to other fuels. Scenario a) retired all coal plants and built new, high-efficiency natural gas combined cycle (NGCC) plants. New NGCC plants were assumed to have a heat rate of 5,700 Btu/MWh achieved by state-of-the-art GE Flex-60 and Siemens Frame-H [24, 25]. The CO_2 emission rate was calculated by multiplying the heat rate by the carbon content of natural gas. Other emission rates were assumed to be the load-weighted average emission rates of 450 existing NGCC plants, as identified by the EPA's National Electric Energy Data System [26]. This assumption somewhat overstates emission

rates, as emission rates of new, high-efficiency NGCC will likely be lower than the existing NGCC fleet average. NO_X and SO_2 emission rates were based on 2012 emission rates (AMPD); CH_4 emission rates were from eGRID 2009; $PM_{2.5}$ and PM_{10} emission rates were based on NEI 2005.

Scenario b) retired all coal plants and built new natural gas plants with same heat rate and emission rates as the existing gas fleet's load-weighted average, considering both NGCC and combustion turbine plants. Heat rates, CO_2, NO_X and SO_2 emission rates were based on 2012 data (AMPD); CH_4 emission rates were from eGRID 2009; $PM_{2.5}$ and PM_{10} emission rates were based on NEI 2005. This scenario isolates the benefits of fuel switching from the benefits of switching to high-efficiency plants (scenario a).

Scenario c) retired all coal plants and built new plants that have zero emissions of all pollutants, either renewable or nuclear plants. We assumed the replacement plants could provide firm baseload power; in reality, variable renewables such as wind would need storage to serve as baseload.

We assumed replacement plants are built at the same location and have the same capacity as the coal plants they replace. We believe that this assumption is reasonable, as the sites will have much of the infrastructure needed for new plants, such as access to transmission. The location of renewable plants may be constrained by the availability of renewable resources (wind or solar). Our analysis ignored changes in the dispatch order that may occur due to fuel switching, or changes in load due to consumer price response.

4.2.3 Calculation of climate effects

We calculated resulting temperature changes using a metric used by the IPCC, Global Temperature Potential (GTP) [27, 28]. GTP is defined as the ratio between the global mean surface temperature change (ΔT) at a given future time horizon (TH) following an emission (pulse or sustained) of a compound x relative to an equivalent mass of CO_2 [29], or:

$$GTP_x^{TH} = \frac{\Delta T_x^{TH}}{\Delta T_{CO2}^{TH}} \tag{4–1}$$

Since power plant emissions are typically given at annual intervals, the total change in temperature (ΔT) due to emissions of all pollutant types [28] over the entire time horizon (*TH*) years can be approximated as:

$$\Delta T = \sum_{x=1}^{X} \sum_{t=1}^{TH} GTP_x(t) * \Delta T_{CO_2}(t) * M_x(t) \tag{4–2}$$

where M is the mass of the pollutant x emitted in year t (kg) and ΔT_{CO2} is the temperature response in year n due to a 1 kg pulse emission of pollutant emitted in year 0 (K/kg).

For the results shown in this paper, we calculate the temperature forcing due to carbon dioxide and methane. GTP_{CO2} is defined to be 1, and ΔT_{CO2} can be represented through empirical analysis [30]. Fossil methane, including climate change feedbacks, is estimated to have a GTP at 20 years (GTP20) of 68, and a GTP100 of 15, although estimates are highly uncertain (roughly ± 75%); the most recent IPCC report fully characterizes GTP_{CH4}^{TH} over a century [30]. A discussion of the global warming potential of CO_2 and CH_4 emissions can be found in Appendix B.

While this simple model can allow the user to intuitively understand the changes in CO_2 and CH_4, it does not take into account the effects of NO_X, SO_X, black carbon (BC), and organic carbon (OC). Due to the complex nature of the secondary chemistry involved in calculating temperature changes, we modeled climate change effects with the publicly available MAGICC6 model [31] a simple/reduced complexity climate model including an ocean, an atmosphere, a carbon cycle, and indirect aerosol effects; Appendix B contains a full model description and validation tests.

4.2.4 Calculation of health effects

Switching from coal to either gas or zero-emission plants reduces emissions of SO_2, NO_X, $PM_{2.5}$, and PM_{10}. We monetized the benefit to human health and the environment caused by this switch using the Air Pollution Emission Experiments and Policy (APEEP) model [20]. The model uses a reduced form air transport model and linear dose-response function to monetize the damages to human health and the environment caused by a marginal ton of emissions of NO_X, SO_2, $PM_{2.5}$, PM_{10}, volatile organic compounds (VOCs), and ammonia (NH_3) from each county in the USA. We excluded damages due to VOC and NH_3 from our analysis due to uncertainty in the atmospheric science surrounding these pollutants, and the relatively small damages they cause compared to SO_2, NO_X, and PM [35, 36].

Health effects, if valued at $6 million per statistical life, constitute 94% of the total APEEP damages, dominating environment damages (visibility loss, damages to forestry and agriculture, damage to manmade structures) [20]. APEEP was used in the National Academies' *Hidden Costs of Energy* report [18]; similar health models exist [19, 37] and have been used by the EPA to as technical support for major pollution regulations [10]. The APEEP model and our analysis exclude damages associated with emissions in Alaska and Hawaii.

Because the damages caused by emissions vary by location, we estimated individual coal plant emissions of SO_2, NO_X, $PM_{2.5}$, and PM_{10}. Although EIA forecasts total NO_X and SO_2 emissions, plant-level emissions out to 2040 are highly uncertain. We assumed the fraction of total coal SO_2 and NO_X emissions from each plant remains constant from 2012 levels through 2040 [3]. We assumed each coal plant emits 0.14 kg / MWh of $PM_{2.5}$ and PM_{10} [15].

Switching all coal plants to gas would have a significant effect on criteria pollutants, and it might be argued that APEEP's baseline emissions are affected enough so that the human health effects are

no longer good estimates. However, there is good evidence that the formation of $PM_{2.5}$ caused by SO_2 and NO_X is linear with reduced emissions, with no threshold [38]. Major cohort studies have found $PM_{2.5}$ concentration-response functions and mortality are linear with no threshold [39 – 41]. Since we find NO_X accounted for only 8% of total health damages from the electricity sector in 2012, we ignore the known second-order nonlinearities in $PM_{2.5}$ formation associated with NO_X emissions due to decreasing SO_2 emissions.

4.3 Results

Table 4-1 shows the load-weighted average emission rates and heat rates of coal plants in 2012, as well as the emission rates and heat rates for the coal replacement plants in scenarios a) – c). Switching to average gas reduces CO_2 emissions by half; switching to high-efficiency gas reduces CO_2 emissions by 2/3. Both average and high-efficiency gas plants emit an order of magnitude less SO_2 and NO_X than coal plants.

Table 4-1. 2016 load-weighted average emission rates for USA coal plants in EIA Reference Case, and replacement plants for scenarios a) – c).

Plant type	Combustion emission rates (kg/MWh)					
	CO_2	NO_X	SO_2	CH_4	$PM_{2.5}$	PM_{10}
Coal - 2016	910	0.69	0.72	0.010	0.14	0.14
Scenario a): High-efficiency gas	300	0.09	0.02	0.008	0.06	0.07
Scenario b): Average gas	450	0.17	0.02	0.009	0.06	0.07
Scenario c): Zero-emission plants	0	0	0	0	0	0

4.3.1 Change in emissions

As shown in Figure 4-1, switching all coal plants to natural gas would reduce annual electric power CO_2 emissions by 35% - 47% from the EIA's reference case; CH_4 emissions would be increase by 80% - 120%, assuming a 3% fugitive CH_4 emission rate. Switching to zero-emission plants would reduce CO_2 emissions by 70%. Table 4-2 shows that CH_4 reductions are highly

sensitive to the assumed fugitive CH_4 emission rate. Reductions in CO_2 and CH_4 emissions are similar for the EIA Reference Case, High Gas Resource Case, and Low Gas Resource Case (see Appendix B).

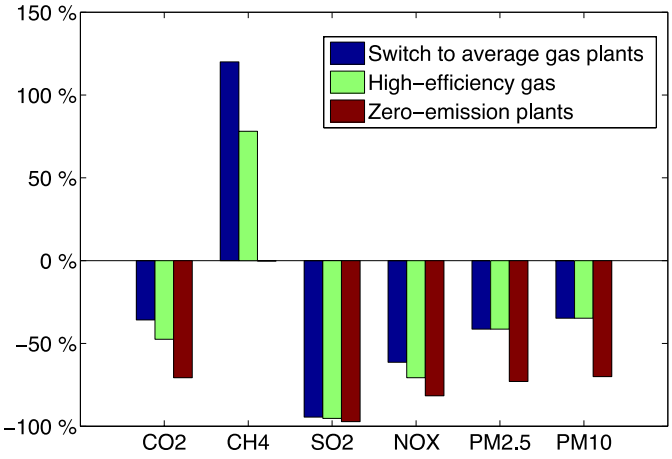

Figure 4-1. Percent change in total electric power GHG emissions (CO_2 and CH_4, 3% fugitive CH_4 rate), and criteria pollutants from the EIA Reference Case in 2025. Reductions are constant across years 2016 – 2040.

Switching from coal to gas or zero-emission sources reduces SO_2 emissions by more than 90%, NO_X emissions by more than 60%, and PM emissions by 40% - 70% (Figure B-3 to Figure B-6). Because coal plants are the primary source of criteria pollutant emissions, switching from coal has a larger effect on criteria pollutant emissions than GHG emissions. Emission reductions are insensitive to the EIA baseline case assumed (Appendix B).

Table 4-2. Sensitivity of CH_4 emissions in 2025 to fugitive CH_4 emission rate, EIA Reference Case.

Scenario	Percent change in CH_4 emissions			
	0% fugitive CH_4	3% fugitive CH_4	5% fugitive CH_4	7% fugitive CH_4
Baseline	0%	8%	13%	18%
A) Switch to high-efficiency gas	0%	14%	23%	33%
B) Switch to average gas	0%	17%	29%	40%
C) Switch to zero-emission plants	0%	8%	13%	18%

4.3.2 Effect on atmospheric concentrations of GHG emissions

In agreement with published literature [4 – 9], using the simple GTP model we find that climate benefits for a USA policy of switching from coal to natural gas are limited unless this action results in other major polluters reducing their GHG emissions. Figure 4-2 and Figure 4-3 show the change in temperature from business as usual minus the change in temperature for scenarios a) -c). Switching from coal to natural gas results in a difference of temperature change between -0.02 °C and + 0.03 °C, depending on the assumed fugitive CH_4 rate. Differences in temperature changes are insensitive to the baseline EIA case assumed. Switching to zero-emissions plants is more effective and less uncertain than switching to gas. As shown in Appendix B, the MAGICC6 model simulates a nearly identical contribution of CO_2 and CH_4 to temperature.

While a small change to global temperatures, these changes are a significant change to the temperature contributions from the US power plant fleet. Table 4-3 shows the fraction of change in temperature from scenarios a) –c) divided by the change in temperature from business as usual (EIA Reference Case). The table shows results for a $GTP20_{CH4}$ of 68, as well as the $GTP20_{CH4}$ uncertainty range of ± 75%. Assuming $GTP20_{CH4}$ is 68, we find that a switch to an average gas plant can change the power plant fleet's contribution to temperatures in 2040 by -40% to +30%, depending on fugitive emissions rate. A switch to high-efficiency plants is better for temperatures, and can change the power plant fleet's contribution to temperatures by –50% to +5%. A switch to zero-emissions plants changes the power plant fleet's contribution to temperatures by -70% to -40%. Results are insensitive to the baseline EIA case assumed.

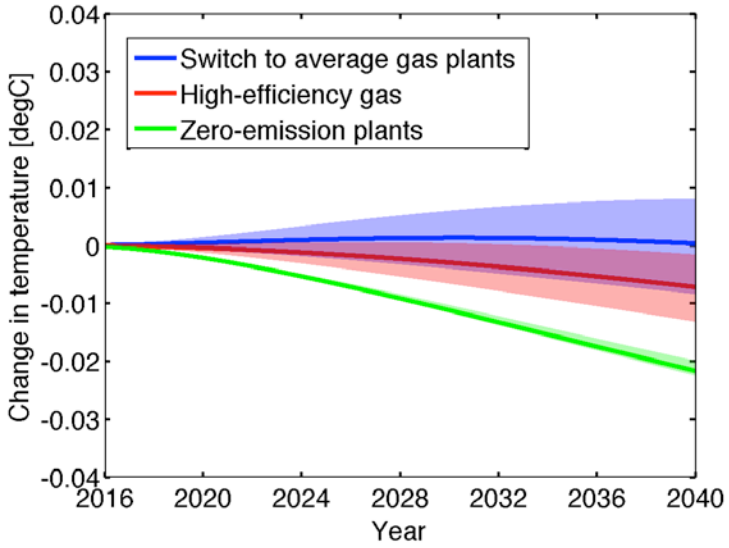

Figure 4-2. Change in temperature from scenarios (A) high-efficiency gas, (B) average gas, and (C) zero-emission plants minus change in temperature from business as usual. Temperature changes include contributions from CO_2 and CH_4 only. Solid line is 3% fugitive CH_4 rate for the EIA reference case; shaded area is range across EIA reference case, high gas resource case, and low gas resource case. Assumed $GTP20_{CH4}$ of 68 ± 75%.

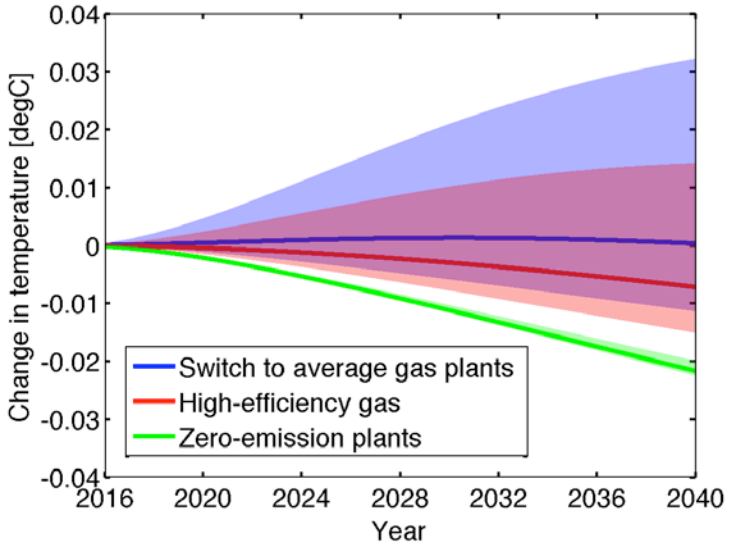

Figure 4-3. Effect of fugitive CH_4 rate uncertainty. Change in temperature from scenarios (A) high-efficiency gas, (B) average gas, and (C) zero-emission plants minus change in temperature from business as usual. Temperature changes include contributions from CO_2 and CH_4 only. Solid line is 3% fugitive CH_4 rate for the EIA reference case; shaded area is represents uncertainty across EIA reference case, high gas resource case, and low gas resource case and 0% - 7% fugitive CH_4 rate. Assumed $GTP20_{CH4}$ of 68 ± 75%.

Table 4-3. Fraction of change in temperature in 2040 from scenarios (A) high-efficiency gas, (B) average gas, and (C) zero-emission plants divided by the change in temperature from baseline EIA reference case. Temperature changes include contributions from CO_2 and CH_4 only. Reductions are constant across 2016 – 2040. Assumed $GTP20_{CH4}$ of 68; uncertainty range of ± 75% in parenthesis.

	Change in warming contributed by U.S. electric power sector, 2040			
Scenario	**0% fugitive CH_4**	**3% fugitive CH_4**	**5% fugitive CH_4**	**7% fugitive CH_4**
A) Switch to high-efficiency gas	**-47%**	**-18%** (-38%, -3%)	**-5%** (-33%, +11%)	**+5%** (-28%, +21%)
B) Switch to average gas	**-35%**	**+1%** (-24%, +18%)	**+16%** (-18% +36%)	**+28%** (-12%, +49%)
C) switch to zero-emission plants	**-70%**	**-53%** (-64%, -44%)	**-45%** (-61%, -36%)	**-40%** (-59%, -30%)

Previous literature assumes the base coal fleet emits a large amount of SO_2. Therefore, a shift from coal to gas would significantly reduce SO_2, offsetting both the climate forcing from the reduction in black carbon and some of the GHGs [6]. In our analysis, the baseline forecasts of SO_2 emissions account for mandated SO_2 emissions due to the MATS standard, and therefore already have low SO_2 emissions. Appendix B contains an analysis of the effects of SO_X, NO_X, BC, and OC on warming through 2100 using the publicly available MAGICC6 model.

4.3.3 Effect on human health

Switching from coal to gas or zero-emissions sources would significantly reduce SO_2, NO_X, and PM emissions (Figure 4-2). The monetized annual health and environmental damages of emissions, via the APEEP model, are shown in Figure 4-4. Damage reductions are $20 billion - $24 billion per year if switching to high-efficiency gas and $20 to $27 billion per year if switching to zero-emission plants. Damage reductions increase from 2016 – 2025, as the EIA forecasts increasing coal generation over that time period. More than 75% of damage reductions are due to reductions in SO_2; reductions in NO_X and $PM_{2.5}$ each make up 10% of damage reductions. Health and

environmental damages vary regionally (Figure 4-5). Most damages occur in the Ohio River Valley and Southeast due to the high concentration of coal plants and significant downwind population.

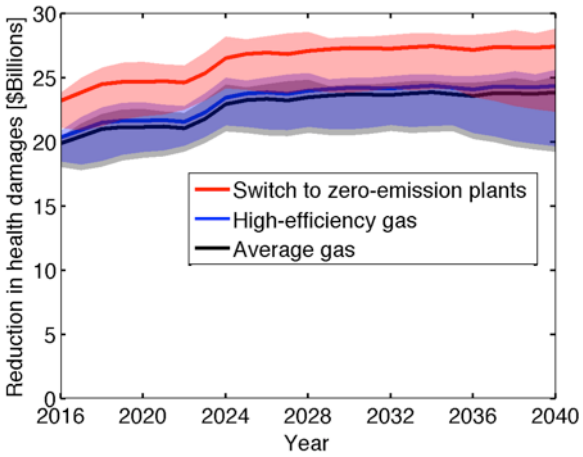

Figure 4-4. Reduction in annual health damages due to switching from coal. $6 million value of statistical life. Solid line is EIA reference case; shaded area is the range across EIA reference case, high gas resource case, and low gas resource case.

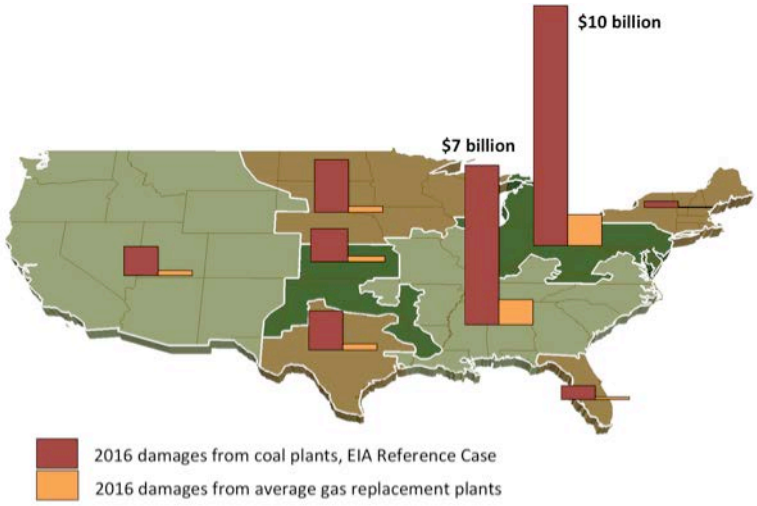

Figure 4-5. 2016 annual health and environmental damages due to emissions of criteria pollutants from coal plants, by NERC region. Replacing coal plants with average gas plants (scenario b) reduces damages most significantly in the Midwest and Southeast.

4.3.4 Costs of reducing emissions from coal

Although replacing all USA coal generation with new, high-efficiency NGCC plants would create health benefits of $20 - $24 billion annually, the costs of constructing and operating such plants are approximately twice as large as the created health benefits. The annual capital cost of

replacing all 375 GW of USA coal capacity would be $35 - $65 billion, assuming new NGCC plants cost $1,000/kW - $1,300/kW, have a facility life of 20 years [42] and a blended cost of capital of 7-12% [43].

Replacing coal plants with gas is only one option to mitigate SO_2 emissions, the primary source of health damages. Flue gas desulfurization and direct sorbent injection are two emission control technologies (ECTs) used to mitigate SO_2 in existing coal plants. Table 4-4 compares the costs and effectiveness of each ECT to building a new NGCC. ECTs have the potential to be a more cost effective SO_2 mitigation option than building new gas plants. Large deployments of these ECTs are anticipated by 2015, as utilities retrofit coal plants to comply with MATS [15, 17].

Table 4-4. Cost and effectiveness of different SO_2 control technologies. New NGCC costs and all fuel costs from [42]; FGD and DSI costs for a representative 500 MW coal unit [17]. Assumes natural gas cost of $4.50/MMBtu and coal cost of $1.70/MMBtu

SO_2 control technology	Capital cost ($/kW)	Fixed O&M ($/MW-yr)	Variable O&M ($/MWh)	Fuel cost ($/MWh)	SO_2 reduction
Build new NGCC	$1,000 - $1,300	$5,500 - $6,200	$2 - $3.5	$24 - $25	99%
Flue gas desulfurization (FGD)	$500	$8,100	$1.8	$15 - $20	98%
Direct sorbent injection (DSI)	$40	$590	$7.9	$15 - $20	50%

4.4 Discussion

In the short term, the potential for natural gas to reduce the USA power sector's contribution to global warming is highly sensitive to the CH_4 fugitive rate and efficiency of gas plants installed. Assuming 3% fugitive CH_4 emissions, switching all coal plants to high efficiency NGCC plants would reduce the power sector's contribution to warming by 20% in 2040. Assuming $GTP20_{CH4}$ of 68, a switch to high-efficiency NGCC plants can change the power sector's contribution to warming changes by -50% to +5% for fugitive CH_4 rates of 0% to 7%. Switching to average-efficiency plants can change warming contribution by -35% to +30% for fugitive rates of 0% to 7%.

Switching to zero-emission plants would change warming potential by -70% to -40%. Considering the uncertainty in $GTP20_{CH4}$ estimates further increases the uncertainty in our results. In all cases, the net effect on global temperatures by 2040 is inconsequential unless US leadership induces pollution control by other large nations. However, the same arguments can be made by every global region, which underscores the need for global coordinated efforts.

Human health in the United States can greatly benefit from policies that continue the reduction of criteria pollutant emissions from coal plants, by switching to gas, installing emissions controls, or switching to renewables or nuclear. Switching to gas would greatly reduce criteria pollutant emissions; SO_2 emissions would be reduced by more than 90%. Retrofitting existing coal plants with ECT is more cost effective than building gas plants in most cases (Table 4-4). It is likely that a combination of switching coal to gas and installations of ECT on coal plants will be the primary way utilities comply with MATS. Annual health damages could be reduced further by $18 - $24 billion if coal plants are either replaced with gas plants or fitted with flue gas desulfurization emission controls.

4.5 References

[1] U.S. Department of Energy. *Monthly Energy Review*; DOE/EIA-0035(2013/08); Energy Information Administration: Washington, DC, **2013**. http://www.eia.gov/totalenergy/data/monthly/pdf/mer.pdf (accessed Jan 8, 2014).

[2] U.S. Executive Office of the President. *The President's Climate Action Plan;* Washington, DC, **2013**. http://www.whitehouse.gov/sites/default/files/image/president27sclimateactionplan.pdf (accessed Jan 8, 2014).

[3] U.S. EPA. *eGRID2012 Version 1.0*; **2012**. http://www.epa.gov/egrid (accessed Jan 8, 2014).

[4] Hayhoe, K.; Kheshgi, H.S.; Jain, A.K.; Wuebbles, D.J. Substitution of natural gas for coal: climatic effects of utility sector emissions. *Climatic Change*. **2002**, *54*(1-2), 107-139.

[5] Jaramillo, P.; Griffin, W.M.; Matthews, H.S. Comparative life-cycle air emissions of coal, domestic natural gas, LNG, and SNG for electricity generation. *Environ. Sci. Technol.* **2007**, *41*(17), 6290-6296.

[6] Wigley, T. M. Coal to gas: the influence of methane leakage. *Climatic change*. **2011**, *108*(3), 601-608.

[7] Venkatesh, A.; Jaramillo, P.; Griffin, W.M.; Matthews, H.S. Implications of Near-Term Coal Power Plant Retirement for SO2 and NOX and Life Cycle GHG Emissions. *Environ. Sci. Technol.* **2012**, *46*(18), 9838-9845.

[8] Myhrvold, N.P.; Caldeira, K. Greenhouse gases, climate change and the transition from coal to low-carbon electricity. *Environmental Research Letters*. **2012**, *7*(1), 014019.

[9] Weber, C.L.; Clavin, C. Life cycle carbon footprint of shale gas: Review of evidence and implications. *Environ. Sci. Technol.* **2012**, *46*(11), 5688-5695.

[10] U.S. EPA. *Regulatory Impact Analysis for the Final Clean Air Interstate Rule*; Office of Air and Radiation: Washington, DC, **2005**.

[11] Pope CA III, Ezzati M, Dockery DW. 2009. Fine-particulate air pollution and life expectancy in the United States. New England J of Med 360:376-386.

[12] Bell ML, Ebisu K, Peng RD, Walker J, Samet JM, Zeger SL, Dominici F. 2008. Seasonal and Regional Short-term Effects of Fine Particles on Hospital Admissions in 2020 US Counties, 1999-2005. Am. J. Epidemiology 168(11): 1301-1310.

[13] Laden F, Schwartz J, Speizer FE, Dockery DW. 2006. Reduction in Fine Particulate Air Pollution and Mortality. Am J Respir Crit Care Med 173: 667–672.

[14] Bell ML and Dominici F. 2008. Effect Modification by Community Characteristics on the Short-term Effects of Ozone Exposure and Mortality in 98 US Communities. Am J Epidemiology 167(8): 986-997.

[15] U.S. EPA. *Regulatory Impact Analysis for the Final Mercury and Air Toxics Standard*; Office of Air Quality Planning and Standards: Washington, DC, **2011**.

[16] U.S. EPA. *Regulatory Impact Analysis for the Federal Implementation Plans to Reduce Interstate Transport of Fine Particulate Matter and Ozone in 27 States; Correction of SIP Approvals for 22 States*; Office of Air and Radiation: Washington, DC, **2011**.

[17] PJM Interconnection. *Coal Capacity at Risk of Retirement in PJM: Potential Impacts of the Finalized EPA Cross State Air Pollution Rule and Proposed National Emissions Standards for Hazardous Air Pollutants*; Norristown, PA, **2011**. http://pjm.com/~/media/documents/reports/20110826-coal-capacity-at-risk-for-retirement.ashx (accessed Jan 8, 2014).

[18] National Research Council (US). Committee on Health, Environmental, and Other External Costs and Benefits of Energy Production and Consumption. *Hidden Costs of Energy: Unpriced Consequences of Energy Production and Use*. National Academies Press., **2010**.

[19] Levy, J. I.; Baxter, L. K.; Schwartz, J. Uncertainty and Variability in Health- Related Damages from Coal- Fired Power Plants in the United States. *Risk Analysis*. **2009**, *29*(7), 1000-1014.

[20] Muller, N.Z.; Mendelsohn, R. Measuring the damages of air pollution in the United States. *Journal of Environmental Economics and Management*. 2007, *54*(1), 1-14.

[21] U.S. Department of Energy. *Annual Energy Outlook 2014 Early Release*; Energy Information Administration: Washington, DC, **2013**. http://www.eia.gov/forecasts/aeo/er/index.cfm (accessed Jan 8, 2014).

[22] U.S. EPA. Air Markets Program Data. http://ampd.epa.gov/ampd/ (accessed Jan 8, 2014).

[23] U.S. EPA. *2005 National Emissions Inventory (Version 2);* **2009**. http://www.epa.gov/ttnchie1/net/2005inventory.html (accessed Jan 8, 2014).

[24] General Electric. *FlexEfficiency 60 Portfolio*; **2012**. http://www.ge-flexibility.com/static/global-multimedia/flexibility/documents/FE60_Interactive_pdf_FINAL_9-25-12.pdf (accessed Jan 8, 2014).

[25] Siemens. *H-Class High Performance Siemens Gas Turbine SGT-8000H series*; **2011**. http://www.energy.siemens.com/us/pool/hq/power-generation/gas-turbines/SGT5-8000H/downloads/H%20class%20high%20performance.pdf (accessed Jan 8, 2014).

[26] U.S. EPA. *National Electric Energy Data System Version 5.13;* **2013**. http://www.epa.gov/airmarkets/progsregs/epa-ipm/BaseCasev513.html#needs (accessed Jan 8, 2014).

[27] Climate Change 2007: The Physical Science Basis. Contribution of Working Group I to the Fourth Assessment Report of the Intergovernmental Panel on Climate Change [Solomon, S., D. Qin, M. Manning, Z. Chen, M. Marquis, K.B. Averyt, M. Tignor and H.L. Miller (eds.)]. Cambridge University Press, Cambridge, United Kingdom and New York, NY, USA.

[28] IPCC, 2013: Climate Change 2013: The Physical Science Basis. Contribution of Working Group I to the Fifth Assessment Report of the Intergovernmental Panel on Climate Change [Stocker, T.F., D. Qin, G.-K. Plattner, M. Tignor, S.K. Allen, J. Boschung, A. Nauels, Y. Xia, V. Bex and P.M. Midgley (eds.)]. Cambridge University Press, Cambridge, United Kingdom and New York, NY, USA, 1535 pp.

[29] Climate Change 2007: The Physical Science Basis. Contribution of Working Group I to the Fourth Assessment Report of the Intergovernmental Panel on Climate Change [Solomon, S., D. Qin, M. Manning, Z. Chen, M. Marquis, K.B. Averyt, M. Tignor and H.L. Miller (eds.)]. Cambridge University Press, Cambridge, United Kingdom and New York, NY, USA. Section 2.10.4.2.

[30] Intergovernmental Panel on Climate Change, 2014. Climate Change 2014: Impacts, Adaptation, and Vulnerability. Working Group II Contribution to the Fifth Assessment Report of the Intergovernmental Panel on Climate Change, Supporting Material. As of April 7, 2014: http://ipcc-wg2.gov/AR5/

[31] Meinshausen, M.; Raper, S.C.B.; Wigley, T.M.L. Emulating coupled atmosphere-ocean and carbon cycle models with a simpler model, MAGICC6–Part 1: Model description and calibration. *Atmospheric Chemistry and Physics*. **2011**, *11*(4), 1417-1456.

[32] Hanrahan, P. L. The plume volume molar ratio method for determining NO2/NOx ratios in modeling—Part I: Methodology. *Journal of the Air & Waste Management Association*. **1999**, *49*(11), 1324-1331.

[33] Wang, X.; Williams, B. J.; Tang, Y.; Huang, Y.; Kong, L.; Yang, X.; Biswas, P. Characterization of organic aerosol produced during pulverized coal combustion in a drop tube furnace. *Atmospheric Chemistry & Physics*. **2013**, *13*(21).

[34] Goodarzi, F. Characteristics and composition of fly ash from Canadian coal-fired power plants. *Fuel*. **2006,** *85*(10), 1418-1427.

[35] Pinder, R.W.; Adams, P.J.; Pandis, S.N. Ammonia Emission Controls as a Cost-Effective Strategy for Reducing Atmospheric Particulate Matter in the Eastern United States. *Environ. Sci. Technol.* **2007**, *41*, 380–386.

[36] Robinson, A. L.; Donahue, N.M.; Shrivastava, M.K.; Weitkamp, E.A.; Sage, A.M.; Grieshop, A.P.; Pandis, S.N.Rethinking Organic Aerosols: Semivolatile Emissions and Photochemical Aging. *Science*. **2007**, 315(5816), 1259–1262.

[37] Fann, N.; Fulcher, C. M.; Hubbell, B. J. The influence of location, source, and emission type in estimates of the human health benefits of reducing a ton of air pollution. *Air Quality, Atmosphere & Health*. **2009**, *2*(3), 169-176.

[38] Koo, B.; Wilson, G.; Morris, R.; Dunker, A.; Yarwood, G. Comparison of Source Apportionment and Sensitivity Analysis in a Particulate Matter Air Quality Model. *Environ. Sci. Technol.* **2009**, 43, 6669-6675.

[39] Krewski, D.; Jerrett, M.; Burnett, R. T.; Ma, R.; Hughes, E.; Shi, Y.; Turner, M.; Pope, C.A.; Thurston, G.; Calle, E.E.; Thun, M.J.; Beckerman, B.; DeLuca, P.; Finkelstein, N.; Ito, K.; Moore, D.K.; Newbold, K.B.; Ramsay, T.; Ross, Z.; Shin, H.; Tempalski, B. *Extended follow-up and spatial analysis of the American Cancer Society study linking particulate air pollution and mortality* (No.140). Boston, MA: Health Effects Institute, **2009**.

[40] Lepeule, J.; Laden, F.; Dockery, D.; Schwartz, J. Chronic Exposure to Fine Particles and Mortality: An Extended Follow-up of the Harvard Six Cities Study from 1974 to 2009. *Environmental Health Perspectives*. **2012**, 120(7), 965–970.

[41] Correia, A. W.; Pope III, C. A.; Dockery, D. W.; Wang, Y.; Ezzati, M.; Dominici, F. Effect of air pollution control on life expectancy in the United States: an analysis of 545 US counties for the period from 2000 to 2007. *Epidemiology*. **2013,** *24*(1), 23-31.

[42] Lazard, Levelized Cost of Energy Analysis – Version 6.0 **2012**. https://www.misoenergy.org/Library/Repository/Meeting%20Material/Stakeholder/PAC/2012/20121221/20121221%20PAC%20Supplemental%20Levelized%20Cost%20of%20Energy%20Analysis.pdf (accessed June 20, 2014).

[43] Spees, K.; Newell, S.; Carlton, R.; Zhou, B.; Pfeifenberger, J. *Cost of New Entry Estimates For Combustion Turbine and Combined-Cycle Plants in PJM*; Prepared for PJM Interconnection by the Brattle Group: Norristown, PA, **2011**. http://www.pjm.com/~/media/committees-groups/committees/mrc/20110818/20110818-brattle-report-on-cost-of-new-entry-estimates-for-ct-and-cc-plants-in-pjm.ashx (accessed Jan 8, 2014).

B Appendix

Methods overview

A graphical representation of the model used in this work is shown in Figure B-1. We use existing national datasets of USA power plants, as well as forecasts of future energy production and emissions from the US Department of Energy's Energy Information Agency (EIA) [1]. In particular, we identify total annual combustion emissions of carbon dioxide (CO_2), CH_4, nitric oxide and nitrogen dioxide (NO_X), sulfur dioxide (SO_2), and 2.5 micrometer and 10 micrometer particulate matter ($PM_{2.5}$ & PM_{10}) for the years 2016 - 2040. We then examine the benefits of three replacement scenarios: a) coal is replaced by new, high-efficiency natural gas combined cycle (NGCC) plants; b) coal is replaced by a combination of new NGCC and natural gas combustion turbine (NGCT) generators that matches the current gas fleet; and c) all coal is replaced by plants with zero emissions, either renewables or nuclear plants. We investigate the effect of fugitive methane emissions from the production and transportation of natural gas (ranging from 0-7%).

We use the publicly available APEEP model with its empirical health damages as a function of particulate type and location [2] to value the reductions in damages to human health and the environment associated with NO_x, SO_2, $PM_{2.5}$, and PM_{10}. We calculate the change in temperatures in two ways: using a global temperature potential model under different EIA scenarios as described in the Main text Section 2, and the publicly available MAGICC6 climate model [3] under different representative concentration pathways (RCPs) as described below.

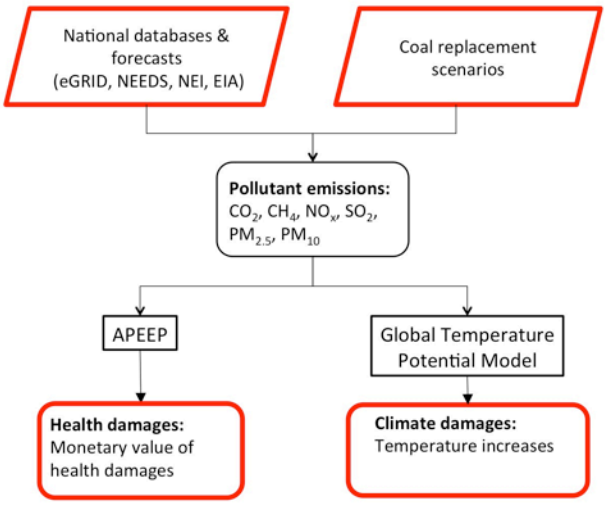

Figure B-1. Graphical representation of the model used in this work. Thick red parallelograms denote inputs we varied. Thick red ovals indicate outputs.

Definitions

As many different metrics have been applied to this problem, we briefly describe 1) what we mean by carbon dioxide equivalent, and 2) climate metrics.

What we mean by carbon dioxide equivalent

Combining different types of emissions and obtaining a value that is equivalent to carbon dioxide can be done in the following ways.

Carbon dioxide equivalent, or CDE, is a forward-looking measurement. This value is the **mass** of carbon dioxide that would have the same global warming potential as the **mass** in question when measured over a specified timescale. This value is calculated as:

$$CDE = \sum_n GWP_n m_n \tag{B-1}$$

where n is number of types of molecules or particles, m_n is the total mass of n, and GWP_n is the global warming potential of a unit of particle n.

Equivalent CO_2, or carbon dioxide equivalent concentrations (CO_2eq), is a snapshot in time. This value is the **concentration** of carbon dioxide that would have the same radiative forcing as the **concentration** in question when measured over a specified timescale. Usually it includes historical emissions. This value is calculated as:

$$CO_2eq = C_o e^{\frac{RF}{\alpha}} \quad \textbf{(B-2)}$$

where *Co* is the concentration of the pre-industrial concentration of carbon dioxide (278 ppm), *RF* is the radiative forcing of the concentration in question, and α is a constant (5.35 W/m^2).

CDE and CO_2eq depend on only the components of mass or concentration that are of interest. Most often, these values are calculated as a function of greenhouse gases only. Sometimes, these values include both greenhouse gases and land use changes. For instance, MAGICC's "KYOTO CO2EQ" is a function of CO_2, CH_4, N_2O, and halogenated gases regulated under the Kyoto protocol. MAGICC's "CO2EQ" is a function of CO_2, CH_4, N_2O, and halogenated gases regulated under both the Montreal and the Kyoto protocol. Another choice is to use CO_2eq as a function of CO_2 and CH_4 only. In other possible choices, these values also include aerosols.

Climate metrics

Radiative forcing, CO_2eq, and temperature have quite different uncertainties. A climate model such as MAGICC6 requires as input specifications the emissions of different constituents (e.g., CO_2, CH_4, SO_X, NO_X, and BC). Due to different scenarios, fugitive methane emissions assumptions, and representative concentration pathways, there is significant uncertainty present in the model inputs. At each time step, the model calculates (with some uncertainty) the atmospheric concentrations of individual constituents, and from that (with additional uncertainty) the individual radiative forcings. Since individual radiative forcings can be added linearly, the first system-level output metric is total radiative forcing. While small, an additional layer of uncertainty is added when using the radiative

forcing to calculate equivalent CO_2 concentrations. A much larger layer of uncertainty is added when using the radiative forcing to calculate temperature.

Temperature changes are well understood by the general public. While not as broadly understood, concentration metrics offer the ability to "draw lines in the sand" used by policy makers to argue for emissions targets such as "a doubling in greenhouse gas concentrations since pre-industrial".

Here we use four climate metrics. **Radiative forcing (W/m^2)** is given as a change relative to preindustrial conditions in the year 1765 and includes all constituents in the model. **Temperature increase (°C)** is derived directly from the radiative forcing and given as a change relative to 1765. In contrast to radiative forcing and temperature increase, **equivalent CO_2 (CO_2eq, ppm)** is defined here as a function of the change in greenhouse gases only (CO_2 and CH_4 only, not NOx, SO_2, PM, N_2O, or halogenated gases)**.** Secondary chemistry (e.g., changes in halogenated gases as a function of methane concentrations) is not included. Referencing MAGICC6, in 2010 these values were 2.15 W/m^2 for radiative forcing, 0.8 °C for temperature increase, and 416 ppm for CO_2eq. Because emissions comparisons are also of interest in some applications, we also provide **carbon dioxide equivalent (CDE, million metric tons)** as a function of CO_2 and CH_4 emissions (100-year global warming potential of 21 [4]).

To find the USA contribution toward CO_2eq in 2010, we used MAGICC6 for global emissions data [3] and national databases for USA emissions data [5, 6]. Total CO_2 annual average concentrations were 389 ppm in 2010; they were 278 ppm preindustrial. The USA is responsible for 24-26% of the CO_2 concentrations and 9% of CH_4 concentrations, with CO_2 values varying as a function of uncertainty in CO_2 lifetime (50-200 years, [5]). Under this definition, the USA's contribution to CO_2eq is thus roughly 30 ppm.

Detailed emission results

We used U.S. Department of Energy (DOE) forecasts of emissions and generation as the baseline for our analysis (see *Methods - Calculation of baseline emissions* in the main text). From this baseline, we replaced all coal plants with either natural gas or zero-emission plants, starting in 2016. The following are EIA's descriptions of the three baseline cases we used:

- **Reference case:** baseline assumptions for economic growth (2.4 percent for 2012 - 2040), oil prices, and technology. Brent spot price rises to about $141.50 per barrel (2012) in 2040
- **Low Oil and Gas Resource:** Estimated ultimate recovery per shale gas, tight gas, and tight oil well is 50% lower than in the Reference case. All other resource assumptions will remain the same as in the Reference case
- **High Oil and Gas Resource:** Estimated ultimate recovery per shale gas, tight gas, and tight oil well is 50% higher and well spacing is 50% lower (or the number of wells left to be drilled is 100% higher) than in the reference case. In addition, tight oil resources are added to reflect new plays or the expansion of known tight oil plays and the estimated ultimate recovery for tight and shale wells is increased 1% per year to reflect additional technological improvement. Also includes kerogen development, tight oil resources in Alaska, and 50% higher undiscovered resources in lower 48 offshore and Alaska than the Reference case

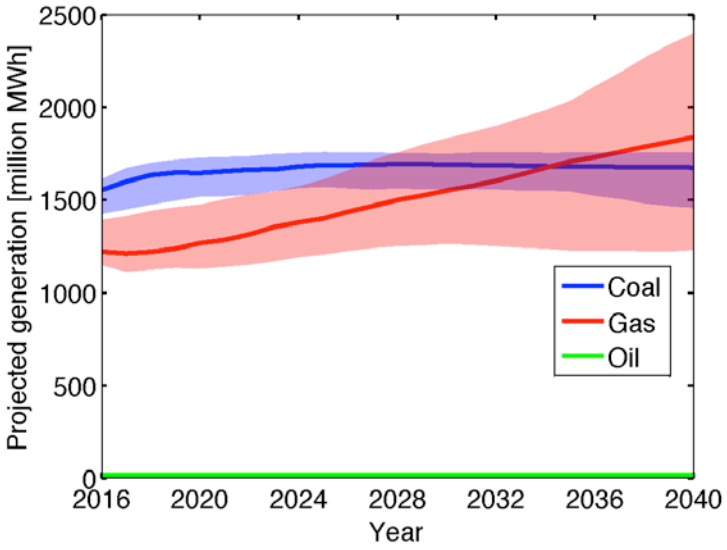

Figure B-2. EIA forecast of generation from coal, gas, and oil plants, 2016 – 2040. Solid lines are EIA Reference Case; ranges represent High Gas Resource Case and Low Gas Resource Case.

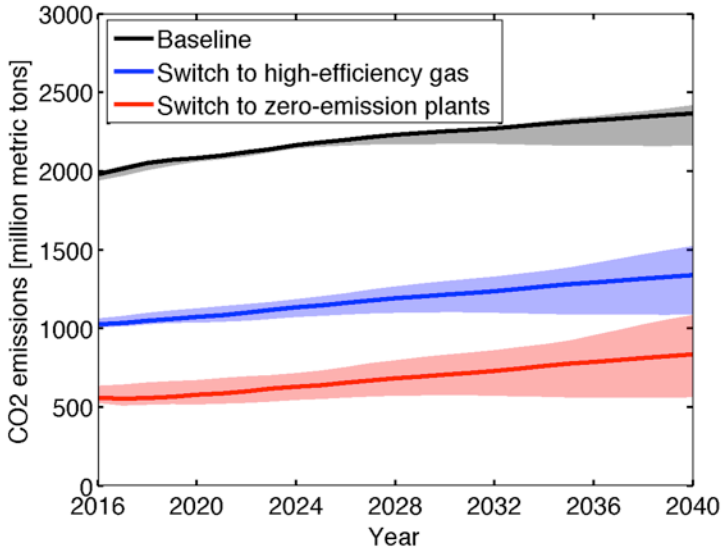

Figure B-3. CO_2 emissions. Solid line is EIA Reference Case; shaded area is range across EIA Reference Case, High Gas Resource Case, and Low Gas Resource Case.

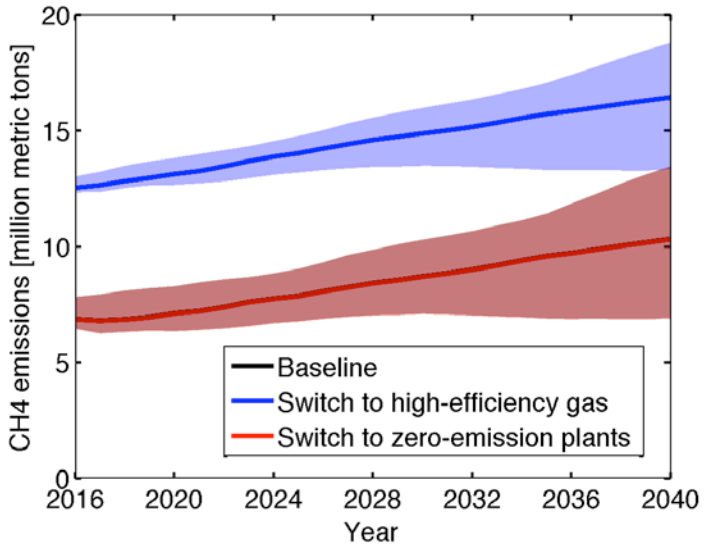

Figure B-4. CH_4 emissions. Solid line is EIA Reference Case; shaded area is range across EIA Reference Case, High Gas Resource Case, and Low Gas Resource Case. Note: Baseline and zero-emission cases are nearly identical.

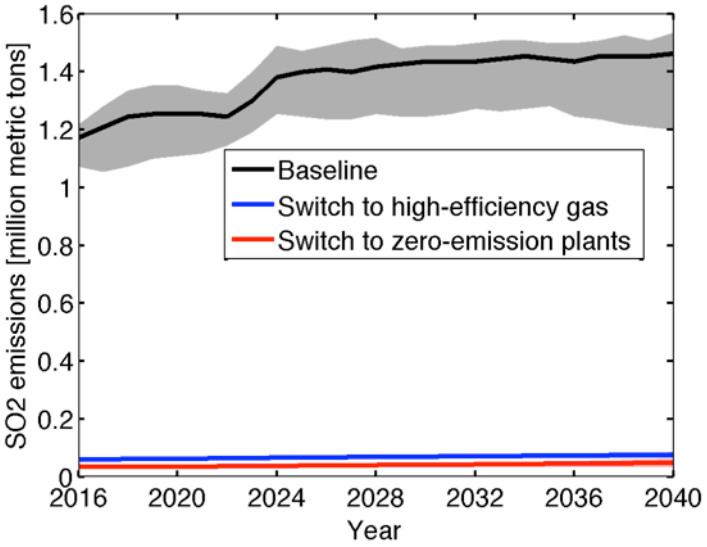

Figure B-5. SO_2 emissions. Solid line is EIA Reference Case; shaded area is range across EIA Reference Case, High Gas Resource Case, and Low Gas Resource Case.

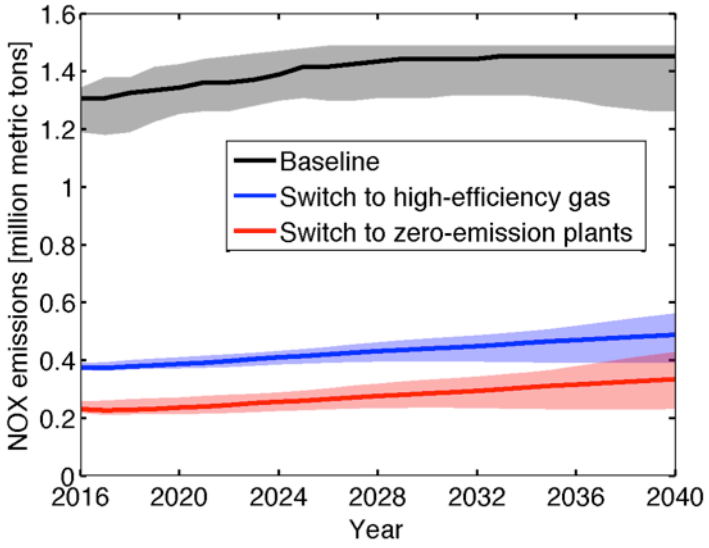

Figure B-6. NO_X emissions. Solid line is EIA Reference Case; shaded area is range across EIA Reference Case, High Gas Resource Case, and Low Gas Resource Case.

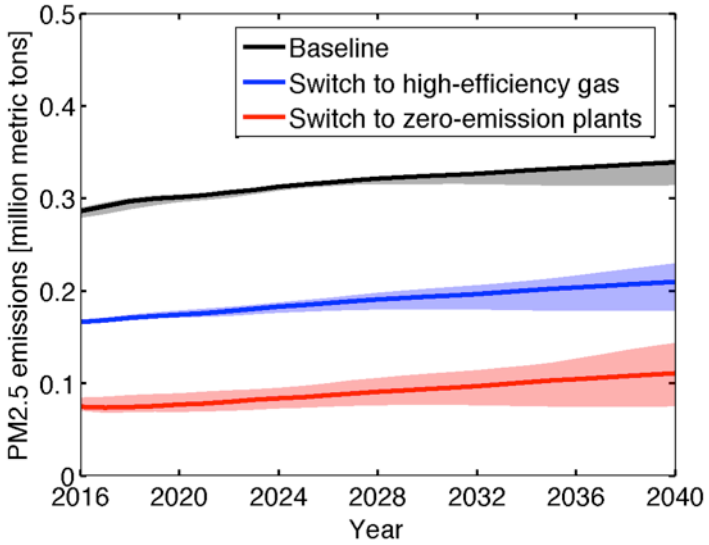

Figure B-7. $PM_{2.5}$ emissions. Solid line is EIA Reference Case; shaded area is range across EIA Reference Case, High Gas Resource Case, and Low Gas Resource Case.

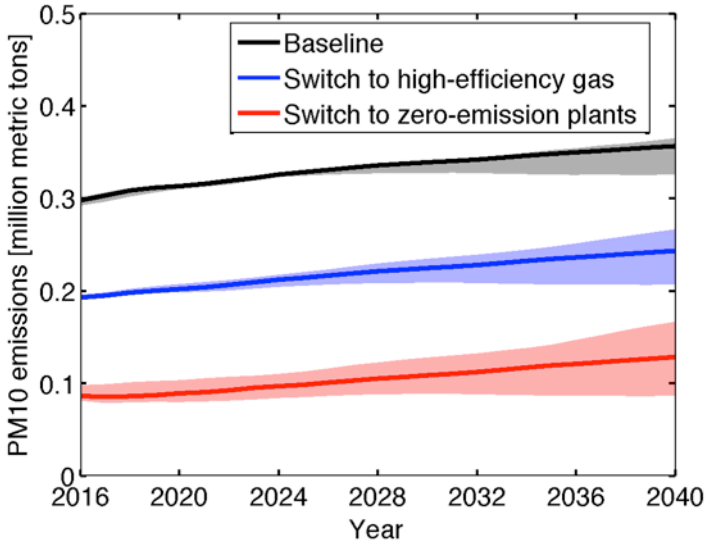

Figure B-8. PM_{10} emissions. Solid line is EIA Reference Case; shaded area is range across EIA Reference Case, High Gas Resource Case, and Low Gas Resource Case.

Global Warming Potential

We calculated the Global Warming Potential (GWP) of CO_2 and CH_4 emissions. GWP is defined as "the time-integrated radiative forcing due to a pulse emission of a given component, relative to a pulse emission of an equal mass of CO_2" [7]. Thus while GWP represents the total energy added to the climate system by a component relative to that added by CO_2, it does not provide information on radiative forcing or temperature changes. Fossil methane, including climate change feedbacks, has a GWP over 20 years (or GWP20) of 85 ± 25%, and a GWP100 of 30 ± 35%.

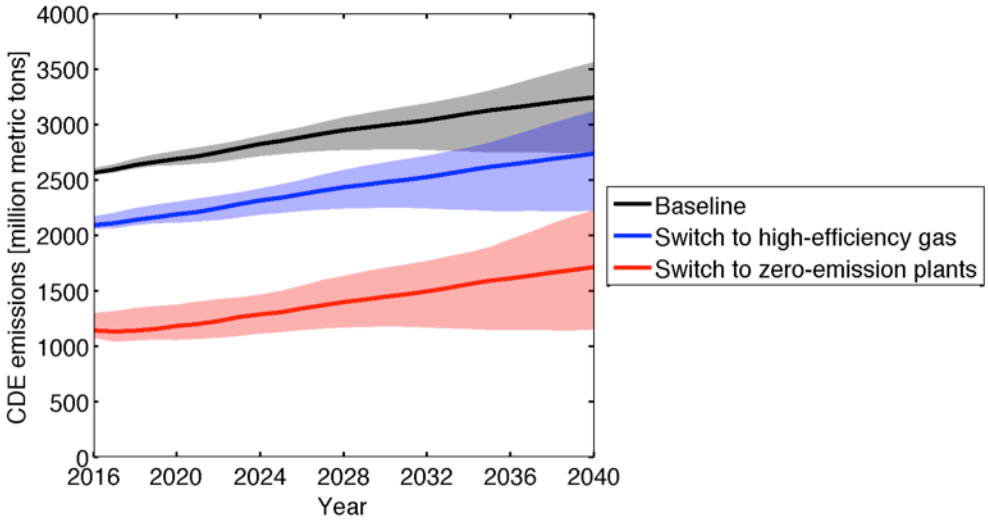

Figure B-9. Carbon dioxide equivalent emissions, CO_2 and CH_4 (20-year GWP of 85), 2016 - 2040. Solid line is EIA Reference Case; shaded area is range across EIA Reference Case, High Gas Resource Case, and Low Gas Resource Case. Assumed fugitive CH_4 rate of 3%.

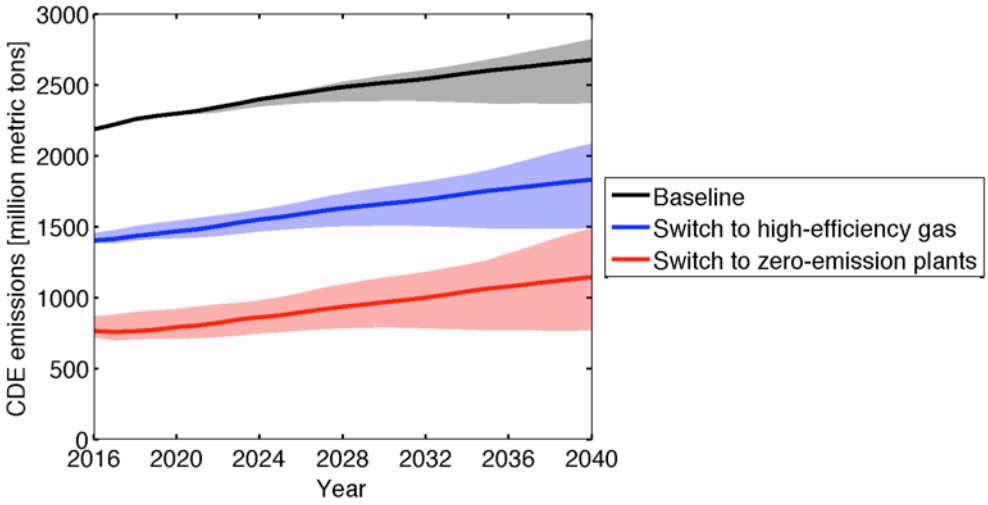

Figure B-10. Carbon dioxide equivalent emissions, CO_2 and CH_4 (100-year GWP of 30) 2016 - 2040. Solid line is EIA Reference Case; shaded area is range across EIA Reference Case, High Gas Resource Case, and Low Gas Resource Case. Assumed fugitive CH_4 rate of 3%.

Fugitive emissions

We analyzed the upstream fugitive emissions of CO_2, NO_x, SO_2, and CH_4 associated with the production and transportation of coal and natural gas (Table B-1). Fugitive emissions (sometimes used synonymously with leakage) can have different meanings in different contexts. Here we define fugitive emissions as the sum of intentional and unintentional releases of the modeled gases to the atmosphere. Because fugitive emissions are highly uncertain, we calculated both a low and high estimate. Fugitive emissions of NO_x and SO_2 for both coal and natural gas are taken from [8]. Upstream greenhouse gas (GHG) emissions from coal, in units of carbon dioxide equivalent mass (CDE), are the 5% and 95% confidence values reported by [9].

Upstream GHG emissions for natural gas plants come from two sources: electricity used in the fuel's transportation [8], and fugitive methane emissions from production and transportation. Of the two, fugitive methane dominates [8]. Because the amount of fugitive methane is highly uncertain, we parameterized the fugitive emission rate between 0 – 7%, a range that includes estimates from other researchers [10, 11]. Total annual CH_4 fugitive emissions were calculated by multiplying the fugitive emissions rate with the total gas consumption of all plants.

Other than potential CH_4 fugitive emissions from natural gas, all fugitive emissions are small when compared to combustion emissions. We therefore exclude all fugitive emissions except CH_4 fugitives from natural gas from our analysis.

Table B-1. Upstream fugitive emission factors

Pollutant	Emission rate (Low estimate, high estimate) [kg/MMBtu fuel produced] Coal	Gas
CDE	(1.055, 16.774)	(0.068, 0.068) (upstream electricity for transporting CH_4 only)
CH_4	0	(0, 1.347) (0% - 7% fugitive emissions rate)
NO_X	(0.014, 0.243)	(0.004, 0.243)
SO_2	(0.003, 0.013)	(0.003, 0.014)

Climate Model to 2100:

To model the complex chemistry associated with aerosols, SO_X, NO_X, BC, and OC, we needed to use a climate model. This section first describes the process used to model climate effects, and then provides the results. .

RCPs and their comparison to published data

The representative concentration pathways (RCPs) are new projections of future emissions to 2100 for the Intergovernmental Panel on Climate Change's fifth assessment report [12]. The four scenarios (RCP2.6, RCP4.5, RCP6.0, and RCP8.5) represent the range of global radiative forcing estimates by 2100, as low as 2.5 W/m^2 to between 8 and 9 W/m^2 and higher [13, 14]. While the RCPs provide values for land use, dust, and nitrate aerosol forcing, these are not included in the radiative forcing estimates [14].

The RCP authors caution that users must be careful to avoid over-interpreting the data. The RCPs were developed by four independent modeling groups [15 – 18]. While integrated assessment

models were used (IMAGE, MiniCAM, AIM, and MESSAGE)[2], the scenarios were created without consideration for changes in policy, technology, land-use, or climate. Thus, differences between the scenarios should be attributed in part to differences between models and to scenario assumptions (scientific, economic, and technological). Additionally, the authors caution that users should not attempt to parse out individual countries' contributions over time. This means we can examine only a snapshot in 2010 of the USA electric power fleet. Thus, we must instantaneously change generators in 2010 to those required in each scenario. This is not a limitation for the global RCPs that do report the primary energy sources individually in future years. So our global models examine for each RCP changing all future power plants as well as existing ones.

Observed CO_2 emissions are larger than the RCP 8.5 values [19]. Figure B-11 and Figure B-12 compare the RCPs to published primary energy usage outlooks from BP [20] and ExxonMobil [21]. BP's predicted primary energy usage of coal is similar to RCP8.5, the scenario with the highest emissions and strongest radiative forcing. ExxonMobil's predicted primary energy usage of coal is intermediate between RCP6.0 and RCP8.5 until 2040; after that date ExxonMobil predicts substantial reductions in coal usage. The total primary energy usage modeled by ExxonMobil is similar to RCP6.0 through ~2025.

[2] Contact Information: RCP 2.6 (IMAGE): Detlef van Vuuren (detlef.vanvuuren@pbl.nl); RCP 4.5 (MiniCAM): Allison Thomson (Allison.Thomson@pnl.gov); RCP 6.0 (AIM): Toshihiko Masui (masui@nies.go.jp); RCP 8.5 (MESSAGE): Keywan Riahi (riahi@iiasa.ac.at); Data and VOC details: Jean-Francois Lamarque (lamar@ucar.edu)

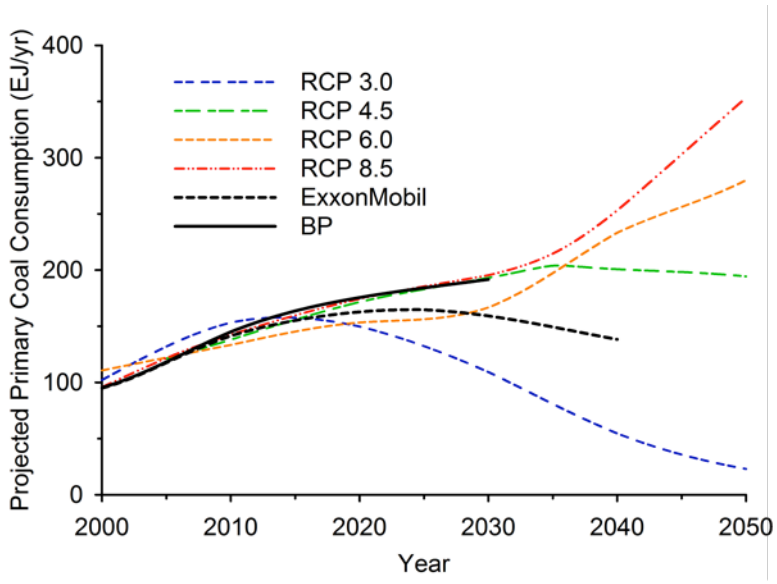

Figure B-11. Primary energy usage of coal, 2000-2040. BP's outlook matches that of RCP 8.5. ExxonMobil's outlook is in between RCP6.0 and RCP8.5 until 2025, at which time they predict substantial reductions in coal usage; its total primary energy usage is in line with RCP6.0.

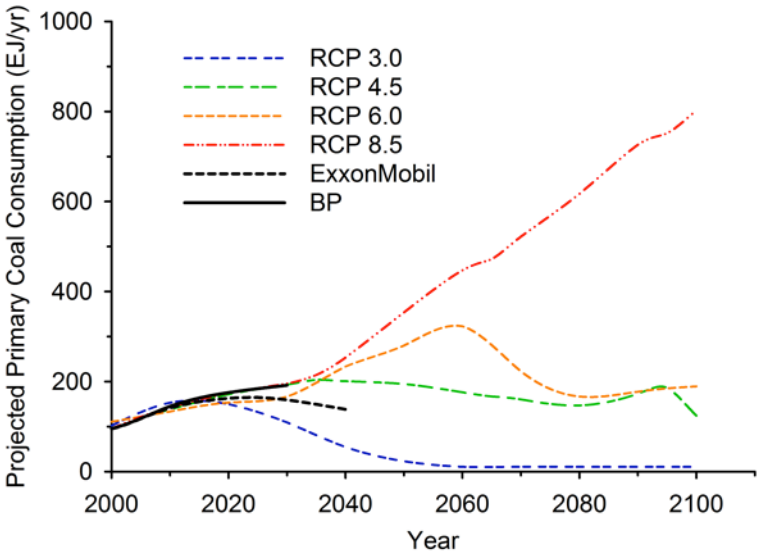

Figure B-12. Primary energy usage of coal, 2000-2100. BP's outlook matches that of RCP 8.5. ExxonMobil's outlook is between RCP6.0 and RCP8.5 until 2025, at which time they predict substantial reductions in coal usage; its total primary energy usage is in line with RCP6.0.

Climate Model Benchmarking

We modeled climate change effects with the publicly available MAGICC6 model [3]. MAGICC6 is a simple/reduced complexity climate model including an ocean, an atmosphere, a carbon cycle,

and indirect aerosol effects. MAGICC6 takes as inputs emissions scenarios (e.g., GtC, MtS, MtN, etc). The model outputs concentrations, radiative forcings, and temperatures. The MAGICC6 authors have converted the RCP scenarios to inputs for running in the model. To test our scenarios a) through c), we slightly modified the included RCP scenarios. Unfortunately, since the model is calibrated to run at higher emissions scenarios (e.g., RCP6.0 and RCP8.5), we were not able to run reductions from the lowest scenario, RCP2.6. Since the RCP2.6 case appears unreasonably optimistic compared to the trajectory we are now on, as well as to ExxonMobil's and BP's energy outlooks, we chose to examine the upper three RCPs (RCP4.5, RCP6.0, and RCP8.5).

Table B-2 lists other climate models used in the literature to examine the problem. MAGICC6 builds on several of these models, resulting in the most comprehensive model used thus far to examine this problem. Other models approach the problem differently by applying estimates of lifecycle emissions [22, 23] or by applying a Monte Carlo analysis of values published in the literature [10].

Table B-2. Climate models used in recent literature we cite.

Model	Type	Climate Feedback, λ	Ocean	Chemistry
Hayhoe et al. [24]	Energy-Balance Model	1.25 Wm^2/K (2.5°C degree rise for a doubling in CO_2)	Vertically-resolved upwelling-diffusion deep ocean	Gas cycle models
Myhrvold & Caldeira [25]	Energy-Balance Model	1.25 Wm^2/K	4 km thick, diffusive slab with a vertical thermal diffusivity 10^{-4} m^2/s	Basic
Wigley [26], Smith & Mizrahi [27], MAGICC6 [28]	Simple/reduced complexity climate model	Central value of 1.50 Wm^2/K; varies in model	Upwelling-diffusion-entrainment (UDE) ocean	Carbon cycle, indirect aerosol effects

Climate Model Validation

To validate our use of MAGICC6, we compared it to the closest published model used for a coal to natural gas switch, Wigley's Figure2.b. (Figure B-13). Scenario values are listed in Table B-3 and our temperature differences from business as usual is in Figure B-14. We find that we can replicate Wigley's CO_2 and CH_4 radiative forcings quite closely. While we can replicate the general trend of the SO_X closely, our increase in global temperature from 2040-2060 is not as pronounced as he finds (Figure B-14). It is likely that Wigley may have applied the SO_X reduction slightly differently than we did.

Table B-3. Model description used in Wigley's model and our choices to perform validation with MAGICC6.

Item	Wigley	This work
Baseline emissions scenario	standard "no-climate-policy"	RCP 8.5
Scenario	Replaces coal with natural gas as given in his Figure 1. For every 1EJ of coal replaced by gas, reduce coal GtC by 0.027GtC/EJ and increase gas GtC by 0.027GtC/EJ * 0.299 = 0.008073.	Same
Fugitive emissions	5%, or 66.6 $TgCH_4$/GtC of natural gas	Same
SO_X	Assume a value of 12 TgS/GtC for the present (2010) declining linearly to 2 TgS/GtC by 2060 and remaining at this level thereafter.	Same
BC	No change in input to model. BC's radiative forcing reduces the SOx radiative forcing by 30%.	Replace MAGICC6 output with Wigley assumption.

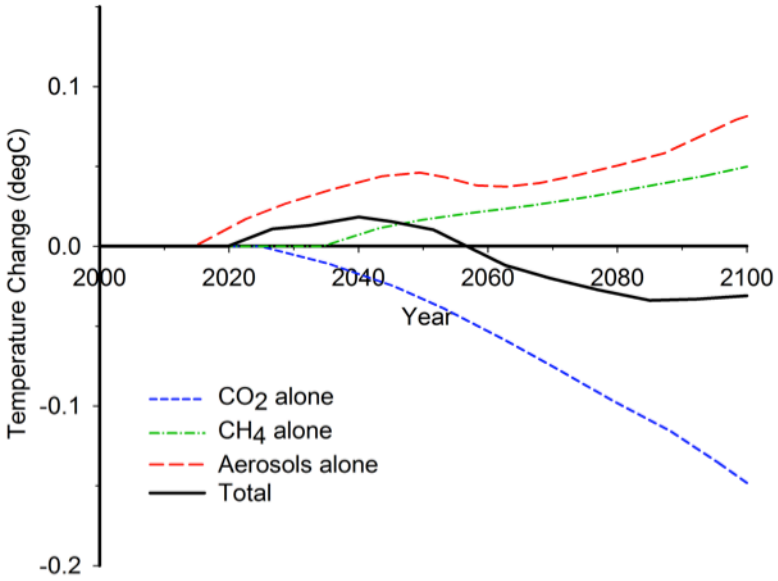

Figure B-13. Temperature changes from Wigley, Figure 2b (Adapted from [26]).

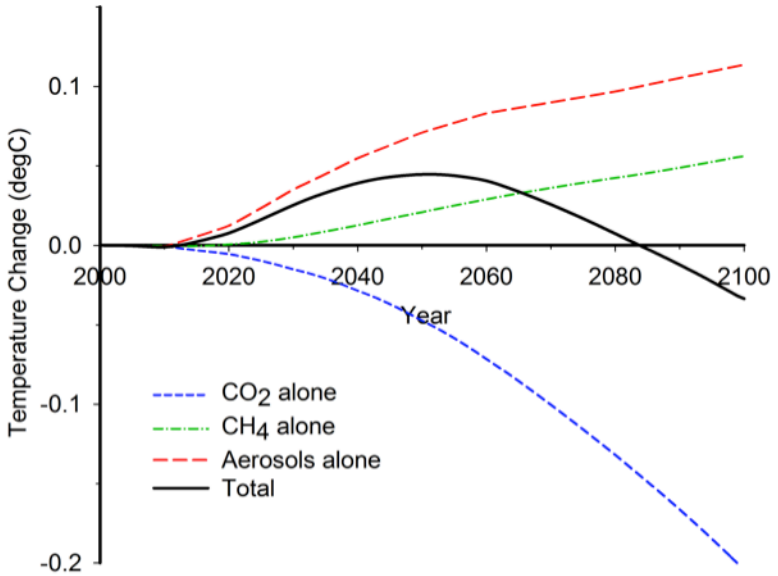

Figure B-14. Temperature changes recreating the Wigley estimates

Climate Results: Radiative forcing and temperature

Finally we examined the effects of a US switch as described in the main text in the MAGICC6 Model. For scenarios a) – c) and fugitive methane rates of 0% - 7%, we modeled changes from business as usual using MAGICC6's default emissions for representative concentration pathways (RCPs) 4.5, 6.0, and 8.5 [13, 22]. Since the MAGICC6 climate model can allocate total emissions by region, we allocated all changes to the OECD region and assumed no changes in other regions). For

each RCP, we assumed that, to first order that we could use the appropriate EIA Case Scenario: Low for RCP4.5, Reference for RCP 6.0, and High for RCP8.5. While the RCPs re not meant to be used this way, we believe this is an okay assumption. For 2000-2040, we used annual intervals of changes from business as usual as described in our main text; starting in 2040, we assumed the changes remained constant to 2100. We assumed all SO_2 could be considered SO_X. Additionally, we assumed NO_X is made of 90% NO and 10% NO_2 by mass [29]. Based on recent publications examining coal power plant particulate matter, we assumed that all particulate matter ($PM_{2.5}$ and PM_{10}) is 12% organic carbon, 4% black carbon, with the rest not relevant for the climate [30, 31]. Total emissions were not allowed to drop below zero.

In agreement with published literature [32 - 37], we find that climate benefits for a USA policy of switching from coal to natural gas are limited. Fuel switching increases temperature in the short term due to reduction in aerosols and increased fugitive methane emissions, and decreases temperatures by 2100 due to reduction in CO_2. The length of this "temperature delay" in 2100 is dependent on the amount of coal switched. Varying the methane fugitive emissions rate from 0-7% can alter changes from business as usual by as much as ±25%.

Figure B-15 shows the change in temperature from business as usual for the USA policy for scenarios a) -c). All of the coal to natural gas scenarios and RCPs are similar; scenario a) is best at reducing temperature concentrations, while scenario b) is least effective. The zero emissions scenario c) is roughly 2-3 times more effective at reducing temperature as the gas scenarios. While a USA policy reduces the nation's contribution to global temperatures in 2010 by, in some cases, over 33% as shown in the Main Text, the reduction values are small compared to global values. For reference, Figure B-16 shows the relation between radiative forcings and temperatures.

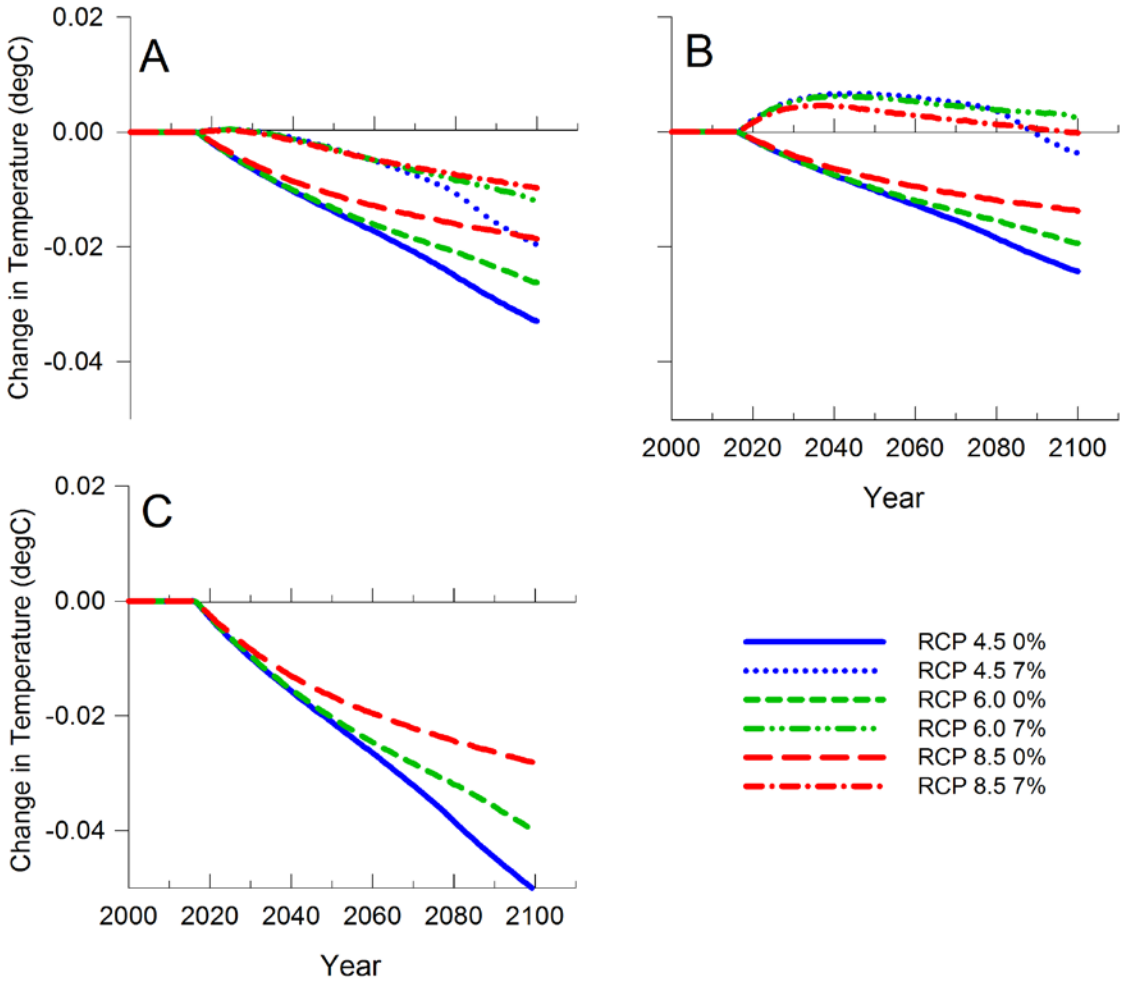

Figure B-15. Change in Temperature from Business as usual for the USA Policy for scenarios (A) High efficiency Gas, (B) Average Gas, (D) zero emissions. We note that this graph is meant to compare with the GTP value, and thus for our purposes includes changes from CO_2 and CH_4 only.

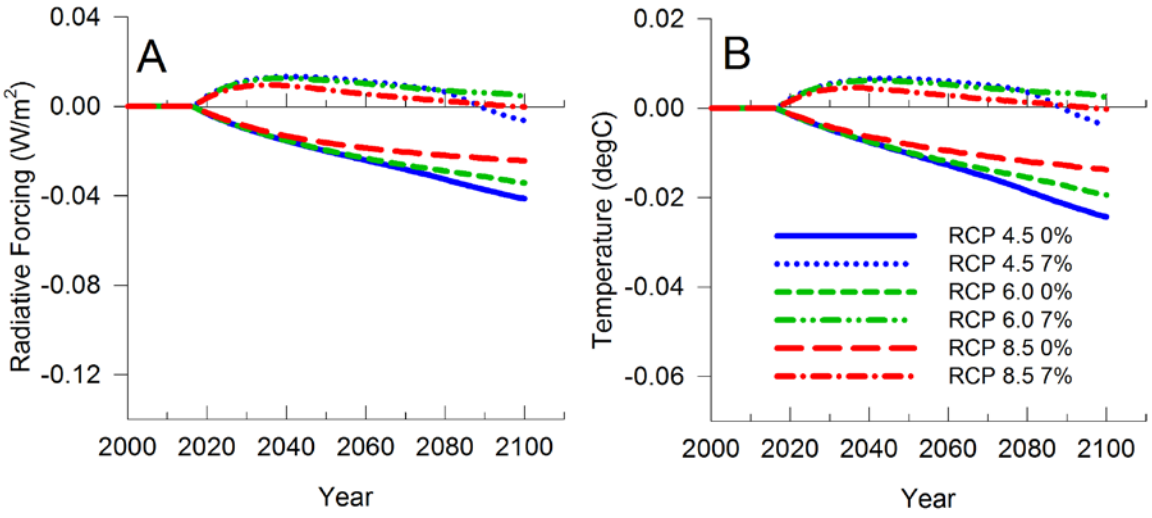

Figure B-16. Change from Business as usual for the USA Policy for Scenario b): Average Gas for (A) radiative forcings (W/m^2) and (B) temperature (°C)

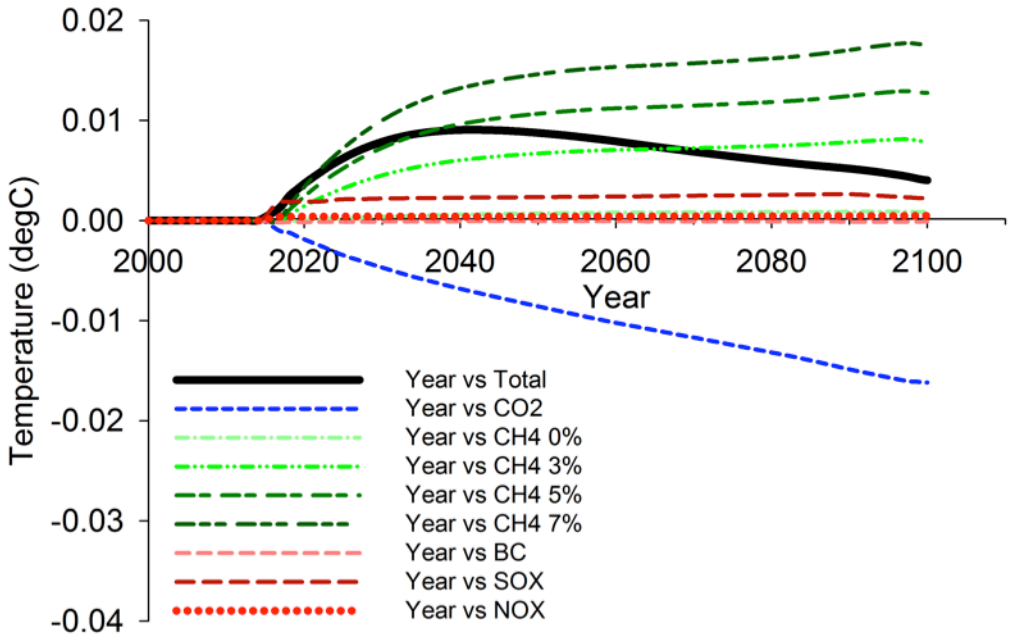

Figure B-17. Change from Business as usual for the USA Policy for Scenario b): Average Gas for RCP8.5 for temperature contribution (°C) by individual constituents. The total, shown as the solid black line, is for 3% fugitive methane emissions.

Figure B-17 includes the effect of aerosols and shows the temperature contribution by individual constituents for RCP8.5. While highly uncertain, the direct effect of aerosols in MAGICC6 is to cool the climate, so decreasing aerosols increases the temperature in the short term. Their lifetime is

short, so aerosol contributions decrease quickly. Reductions remain small compared to global values. We note that aerosol forcing has large uncertainties [38] that may be of the same size as that for methane leakage.

Previous literature assumes the base coal fleet emits a large amount of SO_2. Therefore, a shift from coal to gas would significantly reduce SO_2, offsetting both the climate forcing from the reduction in black carbon and some of the GHGs [26]. In our analysis, the baseline fleet in 2016 has been updated to reflect the MATS standard, and therefore already has low SO_2 emissions. Thus the avoided SO_2 emissions in scenarios a-d are no longer large enough to offset the changes from the reduction in black carbon. This effect means that for some scenarios, a coal to gas shift would result in an initially sharp decrease in radiative forcings followed by an increase as the longer-lived methane dominates.

We note that MAGICC6's chemistry model has many interesting secondary effects we have not reported with these data, e.g., the lifetime of halogenated gases decreases as methane concentrations increase. As part of their work examining a coal to natural gas shift, Smith and Mizrahi calculate the change in radiative forcing from business as usual for gases regulated under the Kyoto protocol [27]. Our analysis agrees with Smith and Mizrahi: depending on scenario and policy, we find the gases regulated under the Kyoto protocol result in an additional 20-30% reduction in radiative forcing in 2100. While this additional reduction suggests that a shift from coal to natural gas might be better for the climate than we suggest, the additional reduction is small compared to total reduction values and less than the model uncertainty.

Global replacement scenario

We next analyzed what would be the effect of switching all current and future coal power plants to natural gas. Here we assumed all global existing and future power plants are switched. The RCP

scenarios provide estimates of future primary energy use of coal. Using 2005 data, we estimated that 77% of the primary energy usage of coal is in the form of coal power plants [39]. While this percent is likely to change slightly from year to year, we assumed it was constant out to 2100. We then calculated the total electricity generation from the coal used for electric power. Finally, we assumed the coal plants generating this electricity were retired and replaced with natural gas or zero emission plants (Scenarios a)-c)). Note that we assumed that all coal plants and replacement generators in the global scenarios have the same heat rates and emission rates as those in the USA scenarios.

A global policy of switching all coal plants to natural gas would reduce total cumulative global GHG emissions to 2100 by 4% - 21% depending on the replacement scenario, assumed fugitive CH_4 emissions rate, and RCP. Scenario b with a 5% fugitive emissions rate and RCP 6 would reduce global GHG emissions by 9% (see Figure B-18). Switching to zero emission plants reduces emissions 26% assuming RCP 6.

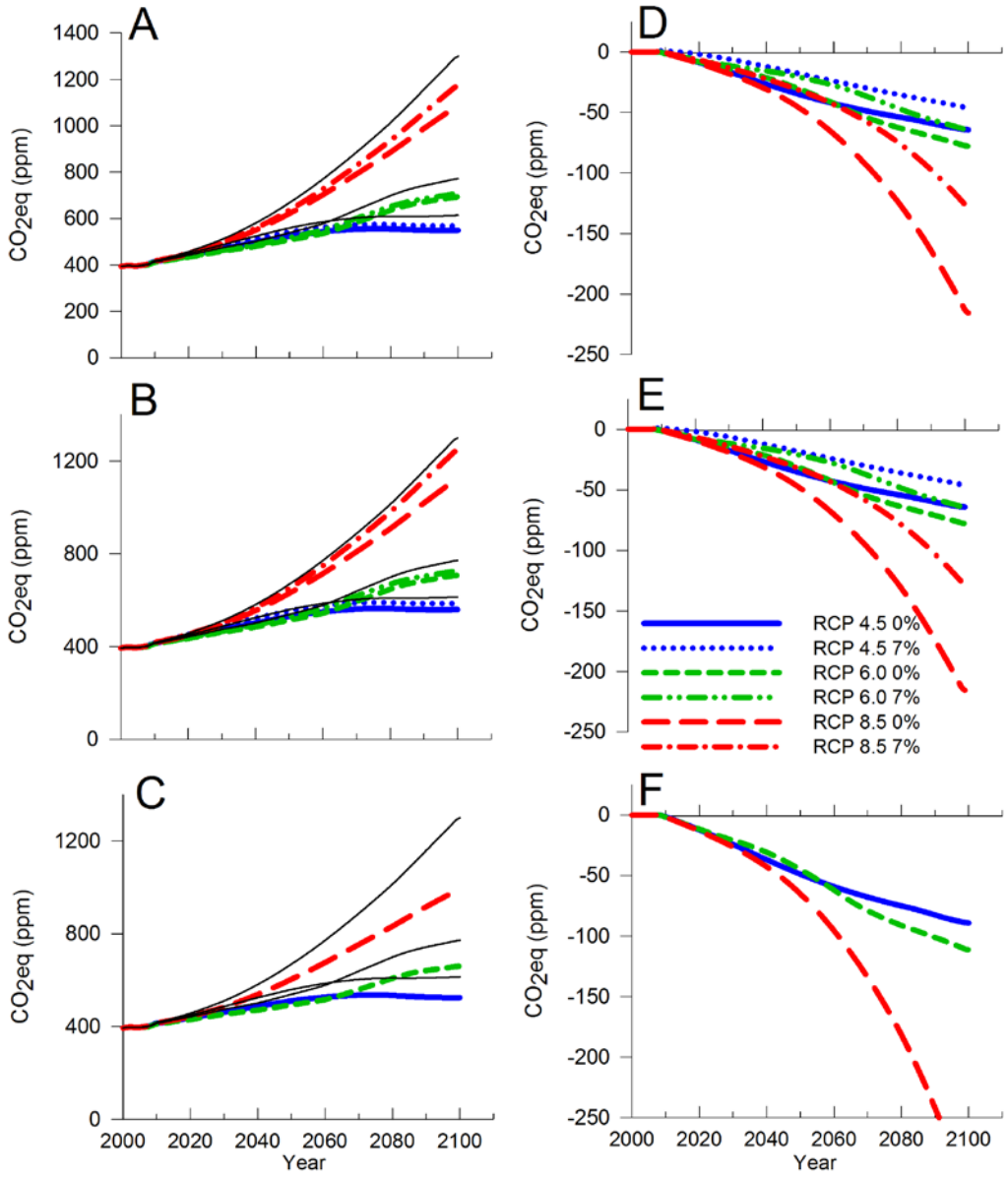

Figure B-18. Total CO_2eq (A-C) and Change in CO_2eq from Business as usual (D-F) for, from top to bottom, the Global Policy for Scenario a): High efficiency gas, Scenario b): Average, Scenario c): ZEG. Solid black lines indicate the business as usual scenario for 3% methane leakage.

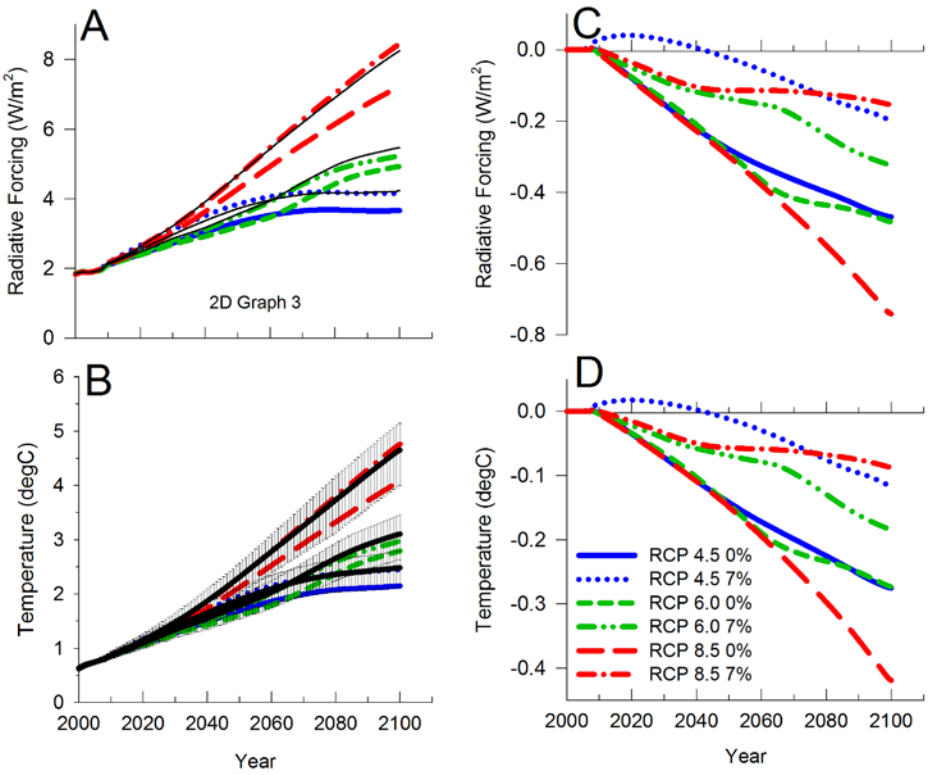

Figure B-19. Total (A-B) and change from Business as usual (C-D) for the Global Policy for Scenario b): Average for radiative forcings (A, C) and temperature (B, D). Solid black lines indicate the business as usual scenario for 3% methane leakage, and the error bars in B indicate the 66% confidence interval for a MAGICC6 multi-modal run where 171 Scenarios are run with all combinations of 19 AOGCM calibrations and 9 carbon cycle model calibrations.

Figure B-18 shows the total CO_2eq and change in CO_2eq from business as usual for the Global Policy for scenario a)-d). A global policy of switching from coal to natural gas could delay CO_2eq in 2100 by 5-25 years. All of the coal to natural gas scenarios are very similar; it appears that scenario a) is best at reducing CO_2eq concentrations, while scenario c) is the worst. Scenario d) is roughly 2-3 times as effective at reducing CO_2eq. Results vary with RCPs due to assumptions about future coal usage; since RCP8.5 assumes a large number of new coal power plants will be added to the fleet, it shows the largest decrease in concentrations.

Figure B-19 includes the effect of aerosols, and shows the radiative forcing and temperature for scenario b). The direct effect of aerosols is to cool the climate, so decreasing aerosols increases the

temperature in the short term. Their lifetime is short, so this effect quickly disappears. Reductions remain small compared to global values and model uncertainty.

References

[1] U.S. Department of Energy. *Annual Energy Outlook 2014 Early Release*; Energy Information Administration: Washington, DC, **2013**. http://www.eia.gov/forecasts/aeo/er/index.cfm (accessed Jan 8, 2014).

[2] Muller, N.Z.; Mendelsohn, R. Measuring the damages of air pollution in the United States. *Journal of Environmental Economics and Management*. 2007, *54*(1), 1-14.

[3] Meinshausen, M.; Raper, S.C.B.; Wigley, T.M.L. Emulating coupled atmosphere-ocean and carbon cycle models with a simpler model, MAGICC6–Part 1: Model description and calibration. *Atmospheric Chemistry and Physics*. **2011**, *11*(4), 1417-1456.

[4] Myhre, G.; Shindell, D.; Breon, F.-M.; Collins, W.; Fuglestvedt, J.; Huang, J.; Koch, D.; Lamarque, J.-F.; Lee, D.; Mendoza, B.; Nakajima, T.; Robock, A.; Stephens, G.; Takemura, T.; Zhang, H.. Anthropogenic and Natural Radiative Forcing. In: Climate Change 2013: The Physical Science Basis. Contribution of Working Group I to the Fifth Assessment Report of the Intergovernmental Panel on Climate Change [Stocker, T.F., D. Qin, G.-K. Plattner, M. Tignor, S.K. Allen, J.Boshung, A. Nauels, Y. Xia, V. Bex, and P.M. Midgley (eds.)]. Cambridge University Press, Cambridge, United Kingdom and New York, NY, USA, **2013.**

[5] U.S. EPA. *Inventory of U.S. Greenhouse Gas Emissions and Sinks: 1990-2010*; EPA-430-R-12-001; Washington, DC., **2012**.

[6] Boden, T.A.; Marland, G.; Andres, R.J. *Global Regional and National Fossil-Fuel CO2 Emissions*; Oak Ridge National Laboratory Publication: Oak Ridge, TN, **2013**.

[7] Myhre, G.; Shindell, D.; Breon, F.-M.; Collins, W.; Fuglestvedt, J.; Huang, J.; Koch, D.; Lamarque, J.-F.; Lee, D.; Mendoza, B.; Nakajima, T.; Robock, A.; Stephens, G.; Takemura, T.; Zhang, H.. Anthropogenic and Natural Radiative Forcing. In: Climate Change 2013: The Physical Science Basis. Contribution of Working Group I to the Fifth Assessment Report of the Intergovernmental Panel on Climate Change [Stocker, T.F., D. Qin, G.-K. Plattner, M. Tignor, S.K. Allen, J.Boshung, A. Nauels, Y. Xia, V. Bex, and P.M. Midgley (eds.)]. Cambridge University Press, Cambridge, United Kingdom and New York, NY, USA, **2013.**

[8] Jaramillo, P.; Griffin, W.M.; Matthews, H.S. Comparative life-cycle air emissions of coal, domestic natural gas, LNG, and SNG for electricity generation. *Environ. Sci. Technol.* **2007**, *41*(17), 6290-6296.

[9] Venkatesh, A.; Jaramillo, P.; Griffin, W. M.; Matthews, H. S. Uncertainty in life cycle greenhouse gas emissions from United States coal. *Energy & Fuels*. **2012**, *26*(8), 4917-4923.

[10] Weber, C.L.; Clavin, C. Life cycle carbon footprint of shale gas: Review of evidence and implications. *Environ. Sci. Technol.* **2012**, *46*(11), 5688-5695.

[11] Allen, D.T.; Torres, V.M.; Thomas, J.; Sullivan, D.W.; Harrison, M.; Hendler, A.; Herndon, S.; Kolb, C.; Fraser, M.; Hill, A.D.; Lamb, B.K.; Miskimins, J.; Sawyer, R.F.; Seinfeld, J.H. Measurements of methane emissions at natural gas production sites in the United States. *Proceedings of the National Academy of Sciences*. **2013**, *110*(44), 17768-17773.

[12] Van Vuuren, D.P.; Edmonds, J.A.; Kainuma, M.; Riahi, K.; Weyant, J. A special issue on the RCPs. *Climatic Change*. **2011**, *109*(1), 1-4.

[13] Meinshausen, M.; Smith, S.J.; Calvin, K.; Daniel, J.S.; Kainuma, M.L.T.; Lamarque, J.F.; Matsumoto, K.; Montzka, S.A.; Raper, S.C.B.; Riahi, K.; Thomson, A.; Velders, G.J.M.; van Vuuren, D.P.P. The RCP greenhouse gas concentrations and their extensions from 1765 to 2300. *Climatic Change*. **2011**, *109*(1-2), 213-241.

[14] Van Vuuren, D.P.; Edmonds, J.; Kainuma, M.; Riahi, K.; Thomson, A.; Hibbard, K.; Hurtt, G.; Kram, T.; Krey, V.; Lamarque, J.; Masui, T.; Meinshausen, M.; Nakicenovic, N.; Smith, S.J.; Rose, S.K. The representative concentration pathways: an overview. *Climatic Change*. **2011**, *109*(1-2), 5-31.

[15] Van Vuuren, D. P.; Stehfest, E.; den Elzen, M. G.; Kram, T.; van Vliet, J.; Deetman, S.; Isaac, M.; Goldewijk, K.K.; Hof, A.; Beltran, A.M.; Oostenrijk, R.; Ruijven, B. (2011). RCP2. 6: exploring the possibility to keep global mean temperature increase below 2 C. *Climatic Change*. **2011**, *109*(1-2), 95-116.

[16] Thomson, A.M.; Calvin, K.V.; Smith, S.J.; Kyle, G.P.; Volke, A.; Patel, P.; Delgado-Arias, S.; Bond-Lamberty, B.; Wise, M.A.; Clarke, L.E.; Edomonds, J.A. RCP4. 5: a pathway for stabilization of radiative forcing by 2100. *Climatic Change*. **2011**, *109*(1-2), 77-94.

[17] Masui, T.; Matsumoto, K.; Hijioka, Y.; Kinoshita, T.; Nozawa, T.; Ishiwatari, S.; Kato, E.; Shukla, P.R.; Yamagata, Y.; Kainuma, M. An emission pathway for stabilization at 6 Wm− 2 radiative forcing. *Climatic Change*. **2011**, *109*(1-2), 59-76.

[18] Riahi, K.; Rao, S.; Krey, V.; Cho, C.; Chirkov, V.; Fischer, G.; Kindermann, G.; Nakicenovic, N.; Rafaj, P. RCP 8.5—A scenario of comparatively high greenhouse gas emissions. *Climatic Change*. **2011**, *109*(1-2), 33-57.

[19] Sanford, T.; Frumhoff, P.C.; Luers, A.; Gulledge, J. The climate policy narrative for a dangerously warming world. *Nature Climate Change*. **2014**, *4*(1), 164–166.

[20] BP. *BP Energy Outlook 2030*; BP Publication, London, U.K., **2013**. http://www.bp.com/en/global/corporate/about-bp/statistical-review-of-world-energy-2013/energy-outlook-2030.html (accessed Jan 9, 2014).

[21] ExxonMobil. *The Outlook for Energy: A View to 2040*; ExxonMobil Publication, Irvin, TX, **2013**.

[22] Venkatesh, A.; Jaramillo, P.; Griffin, W.M.; Matthews, H.S. Implications of Near-Term Coal Power Plant Retirement for SO2 and NOX and Life Cycle GHG Emissions. *Environ. Sci. Technol.* **2012**, *46*(18), 9838-9845.

[23] Jaramillo, P.; Griffin, W.M.; Matthews, H.S. Comparative life-cycle air emissions of coal, domestic natural gas, LNG, and SNG for electricity generation. *Environ. Sci. Technol.* **2007**, *41*(17), 6290-6296.

[24] Hayhoe, K.; Kheshgi, H.S.; Jain, A.K.; Wuebbles, D.J. Substitution of natural gas for coal: climatic effects of utility sector emissions. *Climatic Change*. **2002**, *54*(1-2), 107-139.

[25] Myhrvold, N.P.; Caldeira, K. Greenhouse gases, climate change and the transition from coal to low-carbon electricity. *Environmental Research Letters*. **2012**, *7*(1), 014019.

[26] Wigley, T. M. Coal to gas: the influence of methane leakage. *Climatic change*. **2011**, *108*(3), 601-608.

[27] Smith, S. J.; Mizrahi, A. Near-term climate mitigation by short-lived forcers. *Proceedings of the National Academy of Sciences*. **2013**, *110*(35), 14202-14206.

[28] http://wiki.magicc.org/index.php?title=Model_Description#eq_A45

[29] Hanrahan, P. L. The plume volume molar ratio method for determining NO2/NOx ratios in modeling—Part I: Methodology. *Journal of the Air & Waste Management Association*. **1999**, 49(11), 1324-1331.

[30] Wang, X.; Williams, B. J.; Tang, Y.; Huang, Y.; Kong, L.; Yang, X.; Biswas, P. Characterization of organic aerosol produced during pulverized coal combustion in a drop tube furnace. *Atmospheric Chemistry & Physics*. **2013**, *13*(21).

[31] Goodarzi, F. Characteristics and composition of fly ash from Canadian coal-fired power plants. *Fuel.* **2006,** *85*(10), 1418-1427.

[32] Hayhoe, K.; Kheshgi, H.S.; Jain, A.K.; Wuebbles, D.J. Substitution of natural gas for coal: climatic effects of utility sector emissions. *Climatic Change.* **2002**, *54*(1-2), 107-139.

[33] Jaramillo, P.; Griffin, W.M.; Matthews, H.S. Comparative life-cycle air emissions of coal, domestic natural gas, LNG, and SNG for electricity generation. *Environ. Sci. Technol.* **2007**, *41*(17), 6290-6296.

[34] Wigley, T. M. Coal to gas: the influence of methane leakage. *Climatic change.* **2011**, *108*(3), 601-608.

[35] Venkatesh, A.; Jaramillo, P.; Griffin, W.M.; Matthews, H.S. Implications of Near-Term Coal Power Plant Retirement for SO2 and NOX and Life Cycle GHG Emissions. *Environ. Sci. Technol.* **2012**, *46*(18), 9838-9845.

[36] Myhrvold, N.P.; Caldeira, K. Greenhouse gases, climate change and the transition from coal to low-carbon electricity. *Environmental Research Letters.* **2012**, *7*(1), 014019.

[37] Weber, C.L.; Clavin, C. Life cycle carbon footprint of shale gas: Review of evidence and implications. *Environ. Sci. Technol.* **2012**, *46*(11), 5688-5695.

[38] Bond, T. C.; Doherty, S. J.; Fahey, D. W.; Forster, P. M.; Berntsen, T.; DeAngelo, B. J.; Flanner, M. G.; Ghan, S.; Kärcher, B.; Koch, D.; Kinne, S.; Kondo, Y.; Quinn, P. K.; Sarofim, M. C.; Schultz, M. G.; Schulz, M.; Venkataraman, C.; Zhang, H.; Zhang, S.; Bellouin, N.; Guttikunda, S. K.; Hopke, P. K.; Jacobson, M. Z.; Kaiser, J. W.; Klimont, Z.; Lohmann, U.; Schwarz, J. P.; Shindell, D.; Storelvmo, T.; Warren, S. G.; Zender, C. S. Bounding the role of black carbon in the climate system: A scientific assessment. *J. Geophys. Res. Atmos.* **2013**, 118 (11), 2169-8996.

[39] Cullen, J.M.; Allwood, J.M. The efficient use of energy: Tracing the global flow of energy from fuel to service. *Energy Policy.* **2010**, *38*(1), 75-81.

Chapter 5: ROBUST RESOURCE ADEQUACY PLANNING IN THE FACE OF COAL RETIREMENTS

Abstract

Over the next decade, many U.S. coal-fired power plants are expected to retire, posing a challenge to system planners. We investigate the resource adequacy requirements of the PJM Interconnection, and how procuring less capacity may affect reliability. We find that PJM's 2010 reserve margin of 20.5% was sufficient to achieve the stated reliability standard of one loss of load event per ten years with 90% confidence. PJM could reduce reserve margins to 13% and still achieve levels of reliability accepted by other U.S. and international power systems with 90% confidence. Reducing reserve margins from 20.5% to 13% would reduce PJM's capacity procurement by 11 GW, the same amount of coal capacity that PJM has identified as at high risk of retirement. We find that the risk posed by supply shortages is primarily due to very rare, but severe events. System operators should work to ensure that the system is robust to these extreme events.

5.1 Introduction

Over the next decade, significant coal plant retirements are expected in the United States. The Energy Information Agency forecasts that 40 GW of coal capacity will retire between 2014 – 2020 [1]. These retirements are due to a combination of factors. Many coal plants are near the end of their expected lifespan. Many small and outdated coal plants are finding it cost prohibitive to make the retrofits necessary to comply with emission regulations. Low natural gas prices have put downward pressure on revenues from wholesale electricity prices.

These retirements pose a new challenge to system operators, who are mandated to meet resource adequacy requirements [2]. To meet these requirements, systems procure generation capacity that is rarely used but is needed in extreme circumstances. This capacity, typically natural gas combustion turbines, has low upfront capital costs but high operating costs. In the traditional regulated utility model, these generators are compensated through rate-of-return ratemaking, even if they produce no power. The restructuring of 20 U.S. states in the late 1990s and early 2000s led to the industry to recognize the so-called "missing money problem", whereby market designs would not support sufficient generation investment [3]. Today, most restructured markets use capacity markets to compensate generators for the capacity they provide.

In both traditional regulated utilities and systems with capacity markets, the system operator centrally models the amount of capacity needed to achieve a given resource adequacy standard. These models consider the reliability of existing generators and forecasts of load. Both generator outages and load forecasts are highly uncertain, creating the risk that inaccurate modeling may lead to an over- or under-procurement of capacity. Over-procuring capacity will increase costs for ratepayers; under-procuring capacity will create outage risks above reliability targets.

The traditional metric of resource adequacy is the number of loss of load events (LOLE) per ten years. Most U.S. systems, including the PJM Interconnection, procure enough capacity to meet a LOLE standard of one expected event per ten years, or 0.1 events per year (0.1 LOLE standard) [4]. The 0.1 LOLE standard dates back to the 1950s, although its origins are unknown [2]. Here we follow the standard definition of an outage "event" as an outage lasting one or more consecutive hours. The LOLE metric is problematic, in that it does not consider either the duration of an outage, or magnitude of load that is shed during an outage.

Due to the limitations of the LOLE metric, some systems have adopted other standards. The Southwest Power Pool (SPP) uses the metric of 24 expected loss of load hours (LOLH) per ten years, or 2.4 hours per year (2.4 LOLH standard) [2]. The Scandinavian system uses the metric of expected unserved energy (UE) totaling 0.001% of total load served (0.001% UE standard). Australia's National Energy Market (NEM) and South West Interconnected System (SWIS) have adopted a 0.002% UE standard [5]. The North American Electric Reliability Corporation has recommended system operators adopt UE standards, as they explicitly consider the magnitude of outages [6]. All three metrics consider only the risk of generator outages, and exclude other risks such as transmission or distributions outages.

Resource planners base their capacity procurement decisions on the expected value of the metric used (0.1 LOLE, 2.4 LOLH, 0.001% UE). By considering only the expected value, resource planners imply that they are risk neutral to supply shortages. However, evidence suggests system operators are highly risk averse to supply shortages, as these shortages reflect poorly on the system operator, draw unwanted public attention, and can cause a host of grid management problems such as network collapse, leading to cascading failures [7].

Although a significant body of literature exists on the electric system reliability, resource adequacy risks have received less attention. As part of a study into electricity reliability more broadly, Hines et. al. find that supply shortages over the period 1984 – 2006 were responsible only for 2.3% of U.S. outage events [8]. The methods used by system planners today are very similar to those outlined by Billinton in the 1970s [9]. More recently, system planners have begun to analyze the economically optimal reserve margin, or the reserve margin that minimizes total system costs and outage costs [2, 5].

Here we analyze the resource adequacy requirements of the PJM Interconnection, and how future retirements could affect reliability. PJM anticipates 11 GW of coal capacity, or ~7% of total capacity, is "at high risk" of retirement [10]. Since 2007, PJM has procured capacity through its centralized capacity market. Capacity market billings were $8 billion in both the 2009/2010 and 2010/2011 auctions. In 2010, 2010 capacity costs were roughly 18% of total 2010 billings [11].

PJM uses a forecasting model to calculate the capacity needed to meet the 0.1 LOLE standard [12]. The robustness of this model is important, as it sets the amount of capacity PJM procures, and therefore costs on the capacity and energy markets. However, it is difficult to verify the model's accuracy due to the rarity of supply shortages in PJM.

We develop a robust statistical model of resource adequacy in PJM for the year 2010. The model consists of a probabilistic forecast of hourly load and a probabilistic forecast of generator outages. The load model explicitly considers three major drivers of uncertainty: uncertain load growth, natural temperature variability, and uncertainty in the underlying model/process. The load model uses five years of load data and sixty years of temperature data from Pittsburgh International Airport and Reagan National Airport. We combine the load and outage models into a probabilistic forecast of supply shortages.

We analyze the sensitivity of LOLE, LOLH, and UE to PJM's reserve margin, measured in terms of installed capacity. In 2010, PJM calculated a 15.5% reserve margin was needed to achieve the 0.1 LOLE standard. PJM procured more capacity than needed, making the realized reserve margin 20.5%. We vary PJM's reserve margin from 10% - 25% to see how LOLE, LOLH, and UE change.

We find that PJM's 15.5% reserve margin target met the 0.1 LOLE standard. By procuring additional capacity such that the actual reserve margin was 20.5%, PJM's revealed risk preference was to meet the 0.1 LOLE standard with 90% confidence.

PJM could reduce reserve margins to 13% or 14% by switching to the 2.4 LOLH or 0.001% UE standard, while maintaining current risk preferences. This represents a 9 – 11 GW reduction in capacity from a 20.5% reserve margin. We therefore conclude that PJM could significantly reduce reserve margins and still maintain reliability standards commonly used by other systems and current risk preferences. More specifically, the 11 GW of coal capacity identified by PJM as "at high risk" of retirement could retire. Maintaining a reserve margin of 13% or 14% would also minimize total system costs.

However, the risk of a supply shortage rises if the potential for correlated outages among generators is considered. We show that the risk of a natural gas supply disruption to PJM's natural gas combustion turbines could increase outage risk, and cause PJM to underestimate this risk.

We also find that the distribution of outage size is 'fat tailed', and the largest 10% of outages account for half of total load shed. Therefore, system operators should recognize that supply shortages are more rare, but more disruptive than implied by reliability metrics.

5.2 Methods

We develop a probabilistic forecast of supply shortages in PJM for 2010. This forecast consists of two separate analyses: a probabilistic simulation of hourly load, and a probabilistic simulation of capacity available at each hour. These analyses are described in detail below. We then use Monte Carlo analysis to find the probability that load exceeds supply for each hour of the year. We analyze three reliability metrics: LOLE, LOLH, and UE, and their sensitivity to PJM's reserve margin. We perform several sensitivity analyses, and compare the results of our simulation to PJM's modeling of capacity needs.

5.2.1 Load forecast

We use historic load and temperature data to forecast load in PJM. Load forecasts have three sources of uncertainty: uncertainty in load growth, natural temperature variability, and uncertainty in the underlying model/process. We consider each separately to robustly forecast load.

A large literature exists on forecasting load. Techniques commonly used include regression analysis, time-series analysis, and neural networks [13 – 15]. The model used by PJM to set reserve margin targets is a probabilistic model derived from Billinton [4, 9]. The model is not regression based, but uses heuristics that PJM has developed over time. PJM uses a separate regression model to forecast long-term load growth [13].

We use regression analysis to forecast hourly load in PJM. The regression model shares many features in common with the regression model PJM uses to forecast long-term load growth [13]. Regression analysis is useful for estimating the expected value of load at each time period. However, our focus is extreme events, i.e. high-load hours in which outages are more likely. To account for these extreme events, we bootstrap the model's residuals to simulate uncertainty in load at each time period.

We forecast hourly load in 2010 using hourly data from the previous five years. Using five years worth of data results in higher accuracy than if 10 or 15 years of data were considered. This is because the relationship between temperature and load has changed in PJM over time, with loads becoming increasingly sensitive to high temperatures. Using data more than five years old causes the model to under-forecast load at high temperatures. For more details, see Appendix D.

Hourly load data is from PJM [16]. Hourly temperature and associated weather data is from the National Oceanic and Atmospheric Association (NOAA) for the Reagan National Airport and Pittsburgh International Airport weather stations [17]. These weather stations were chosen as they have reliable temperature data available dating back to the 1940s, which is used to forecast 2010 temperatures. Data on the minutes of daylight for each day is from the US Naval Observatory [18] for Washington DC.

Since its inception, the PJM territory has undergone several expansions (Table 5-1) [16]. To account for these expansions, we forecast load separately for "PJM Classic" (the PJM region prior to any expansions) and each expansion zone. We then combine the forecasts into an overall PJM load forecast.

Table 5-1. PJM Expansions, 1993 – 2010 [16]

Expansion	Date
Rockland Energy	March 2002
Allegheny Energy	April 2002
Exelon – Commonwealth Edison	May 2004
AEP	October 2004
Dayton Power & Light	October 2004
Duquesne Light Co	January 2005
Dominion Virginia	May 2005

For each zone, the analysis has the following seven steps:

Step 1: Regress long-term trend

We first identify and remove the five year, long-term trend in load growth. By removing the long-term trend, we are able to explicitly incorporate PJM's forecast of future load growth (step 5). To remove the long-term trend, we use a non-parametric, additive model and regress load against the hour index (5–1). The hour index starts at 1 for the first hour of 2005, and ends at the last hour of 2009. Using an additive model allows us to account for nonlinearities in load growth, and regressing the logarithm of load allows us to account for higher variability at high-load hours. The model's residuals, X, are stationary. We use these residuals in step 2. Figure 5-1 shows the long-term trend of "PJM Classic", the original PJM footprint, and the model's stationary residuals.

$$\log(load) = hourIndex + X \tag{5–1}$$

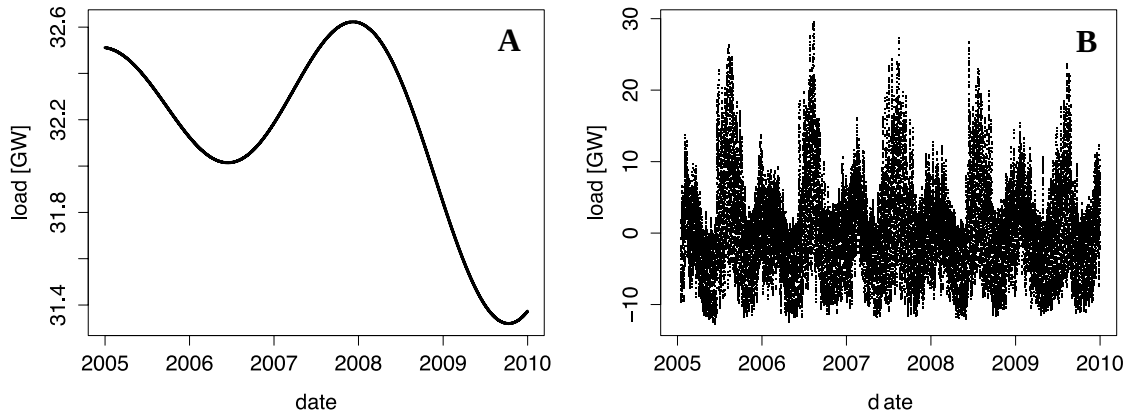

Figure 5-1. (A) Fitted long-term trend and (B) stationary hourly residuals, *X*, for PJM Classic.

Step 2: Regress stationary time series

The second step is to regress *X*, the stationary residuals from step 1, on several explanatory variables, including calendar events, temperature, and length of daylight hours (5–2). For hour of the day and length of daylight hours, we include interaction terms with the month of the year to account for changes in electric load patterns throughout the year. Table D-1 lists all explanatory variables. We use model's residuals, *Y*, to account for uncertainty in the underlying model/process (see step 7).

$$X = weekday + hour * month + holidays + Tadj, avg_D + daylightHours * month + Y \quad (5–2)$$

We use hourly weather data to calculate the $Tadj, avg_D$, the average daily temperature adjusted for wind chill index (WCI) and temperature humidity index (THI) (Equations (5–3) to (5–6)). For each region, we use data for either Reagan National Airport (DCA) or Pittsburgh International Airport (PIT) [17], depending on which is closest (Table 5-2).

Because the relationship between temperature and load is highly nonlinear (Figure 5-2), we used a nonlinear, additive term to account for temperature in the regression. We found that using a non-linear model of temperature was more accurate than using linear relationships (see Appendix D). The remaining regression terms are linear.

Table 5-2. Weather station used for each zone's regression

Region	Weather station used
PJM Classic	DCA
Rockland Energy	DCA
Allegheny Energy	DCA
Exelon – Commonwealth Edison	PIT
AEP	PIT
Dayton Power & Light	PIT
Duquesne Light Co	PIT
Dominion Virginia	DCA

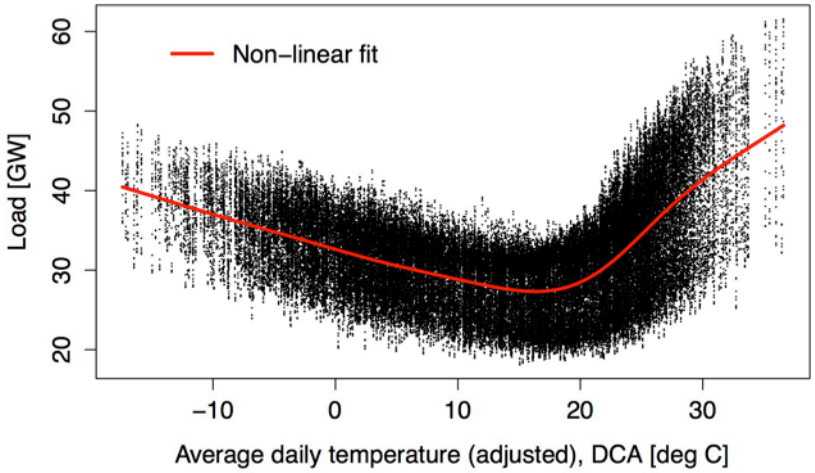

Figure 5-2. Relationship between hourly load in PJM Classic and adjusted average daily temperature at Reagan National Airport (DCA), 2005 - 2009. Because the relationship is highly nonlinear, we use a non-linear, additive model to account for temperature dependence.

Table 5-3: Temperature calculations

$$THI_h = c_1 + c_2T_h + c_3R_h + c_4T_hR_h + c_5T_h^2 + c_6R_h^2 + c_7T_h^2R_h + c_8T_hR_h^2 + c_9T_h^2R_h^2 \quad (5\text{–}3)$$

c_1 = -42.379
c_2 = 2.04091523
c_3 = 10.14333127
c_4 = -0.22475541
c_5 = -6.83783×10^{-3}
c_6 = -5.481717×10^{-2}
c_7 = 1.22874×10^{-3}
c_8 = 8.5282×10^{-4}
c_9 = -1.99×10^{-6}

$$WCI_h = 35.74 + 0.6215T_h - 35.75V_h^{0.16} + 0.4275TV_h^{0.16} \quad (5\text{–}4)$$

$$Tadj_h = \begin{cases} THI_h, & \text{if } T_h \geq 80\ ^oF \text{ and } R_h \geq 40\% \\ WCI_h, & \text{if } T_h \leq 50\ ^oF \text{ and } V_h \geq 3 \text{ mph} \\ T_h, & \text{otherwise} \end{cases} \quad (5\text{–}5)$$

$$Tadj,avg_D = mean(Tadj_h), \quad \forall h \in D \quad (5\text{–}6)$$

h = hour of the day
D = day of the year
T_h = hourly temperature [^{o}F]
R_h = hourly relative humidity [percentage value between 0 and 100]
V_h = hourly wind speed [mph]
THI_h = temperature humidity index [^{o}F]
WCI_h = wind chill index [^{o}F]
$Tadj_h$ = hourly adjusted temperature
$Tadj,avg_D$ = daily average adjusted temperature [^{o}F]

WCI index equation from [19]; THI index equation based on [20].
Although conversion equations are in English units, the remainder of our analysis uses Celsius.

Step 3: Bootstrap residuals of the stationary model

To account for uncertainty in the underlying process/model, we bootstrap the residuals of the stationary time series model, *Y*, (5–2). We bootstrap residuals by month, in 24-hour blocks. Bootstrapping by month allows us to account for heteroskedasticity in the residuals (Figure D-9);

using 24-hour blocks allows us to account for time dependence in the residuals (Figure D-10). The resulting bootstrapped residuals are used in Step 7.

Step 4: Forecast temperatures

Because the next year's temperatures are uncertain, we develop temperature forecasts for 2010 based on historic NOAA weather data dating back to 1949 for DCA and PIT airports [17] (years 1966 – 1972 were excluded due to missing data). We use hourly temperature, relative humidity, and wind speed data to calculate the average adjusted daily temperature ($Tadj,avg_D$) for DCA and PIT each day (Equations (5–3) to (5–6)). We bootstrap days from this 60 year dataset, by month, in 10-day blocks. Bootstrapping by month allows us to account for the seasonal variations in temperature; using 10-day blocks allows us to account for time dependence in weather patterns that can last for several days (Figure D-8). Using 60 years of temperature data allows us to robustly account for extreme temperatures that may occur. We do not observe a secular trend in the NOAA temperature data. By using historic data, we do not account for the possibility of future climate-induced changes in temperature levels or volatility.

Step 5: Forecast the stationary time series

Once we have a model of the underlying stationary process (step 2), we use the model to predict the next year's stationary time series. This stationary time series excludes the effects of load growth. In this prediction, we use the temperature forecast developed in step 4.

Step 6: Forecast load growth

Our forecast of growth in average load is based on PJM's 2009 forecast for 2010 load growth. We adjust the forecast to account for the historic accuracy of the Energy Information Agency's (EIA) load forecasts in the Annual Energy Outlook; insufficient data on PJM forecast accuracy is publically available. Between 1999 – 2008, EIA load growth forecasts had an average bias of -0.3% and standard deviation of 1.9% [21]. We assume forecast errors are normally distributed, and

develop a distribution of possible load growth rates (Figure 5-3). We then sample growth rates from the resulting distribution. We assume load growth is linear throughout the year.

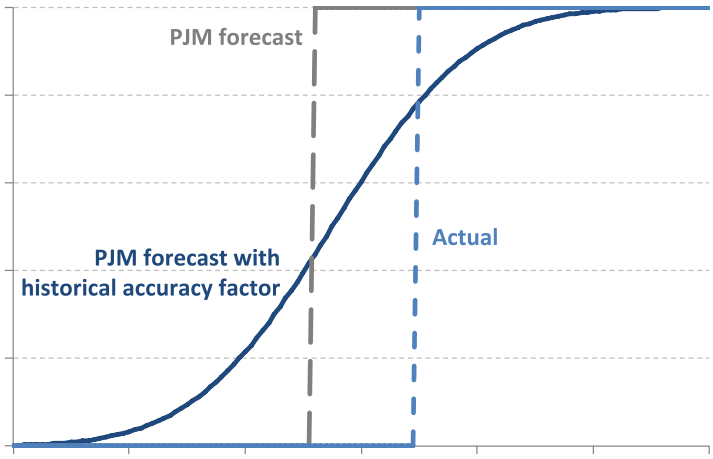

Figure 5-3. PJM's 2010 load growth forecast, with and without the historical accuracy factor, and actual load growth that occurred.

Step 7: Forecast hourly load

Finally, we sum the three components of our load forecast model: forecast load growth (step 6), the forecast stationary time series (step 5), and the residuals of the stationary time series regression (step 3). This allows us to separately account for the three sources of uncertainty: uncertain load growth, natural temperature variability, and uncertainty in the underlying model/process. As all three components are probabilistic, we repeat the process many times to measure the uncertainty associated with each. The result is a probabilistic hourly forecast of load.

Once we have developed probabilistic hourly load forecasts for each zone, we sum these forecasts to find the total load forecast for PJM. We repeat the entire process 5,000 times to develop a probabilistic forecast of hourly PJM load in 2010.

5.2.2 Supply forecast

We next forecast the total capacity available at each hour. Total available capacity is the summed capacity of all online dispatchable plants, demand response, import capacity, and firm wind capacity. We use data from the 2010 PJM Form EIA-411 to identify each dispatchable plant's summer and winter capacity, as cleared in the capacity auction [22]. We therefore assume the system operator has perfect information as to what generators will be available for the forecast year. We simulate the online status of each PJM generator, taking into consideration forced outages, planned outages, and maintenance outages. We simulate total capacity available for each of the 8760 hours of the year, and repeat the simulation 5,000 times to get a distribution of capacity available at each hour. We do not model other supply-side actions PJM can take to mitigate outage risks, such as voltage reductions.

We first schedule planned outages and maintenance outages for all plants. These outages are scheduled such that the likelihood of a supply shortage is minimized. As such, the majority of outages are scheduled during the spring and fall. NERC's Generating Availability Data System (GADS) provides data on the average number of planned outage hours and maintenance outage hours for plants, aggregated by plant type and size [23]. We find that these outages can be scheduled with minimal effect on LOLE. More details on planned and maintenance outages can be found in Appendix D.

We next model forced outages. Forced outages are caused by unforeseen technical problems, occur randomly throughout the year, and have an uncertain duration. We model plant forced outages as a two-stage discrete Markov chain [9]. Figure 5-4 illustrates this process. At each time period t, if the plant is online there is probability $P_{1,1}$ that it remains on at period t+1 and probability $P_{1,0}$ that is fails. If the plant is offline, it remains off with probability $P_{0,0}$ and is repaired with

probability $P_{0,1}$. Accounting for the duration of outages increases the uncertainty of how much capacity is available at each hour. We simulate each plant's forced outages over one year (8760 hours), then sum the total online capacity of all PJM plants.

GADS provides data on the mean number of forced outages, and PJM provides data on plant equivalent demand forced outage rates (EFORd) [24]. We use these data to calculate the transition probabilities with equations (5–7) through (5–11). EFORd is defined as "the probability that a generating unit will fail, either partially or totally, to perform when it is needed to operate" [11]. All data are aggregated by plant type and size.

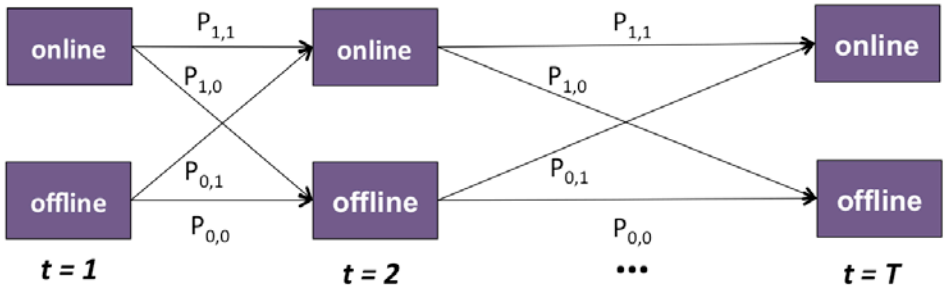

Figure 5-4. Forced outages 2-stage discrete Markov process

Table 5-4. Forced outage equations

$$MOD = \frac{EFORd * 8760}{NFO} \quad (5–7)$$

$$P_{0,1} = \frac{1}{MOD} \quad (5–8)$$

$$P_{0,0} = 1 - P_{0,1} \quad (5–9)$$

$$P_{1,0} = \frac{NFO}{8760} \quad (5–10)$$

$$P_{1,1} = 1 - P_{1,0} \quad (5–11)$$

MOD = mean outage duration
NFO = Annual number of forced outages
$EFORd$ = Equivalent forced outage rate

We assume that each plant's transition probabilities are constant throughout the year. We also assume the duration of outages is uniformly distributed.

We estimate the available DR capacity and net import capacity based on the results of the capacity auctions [25] (Table 5-5). Each auction covers the period of June 1 of the first year to May 31 of the second year. We derate DR capacity by 5%, as is PJM's practice to account for DR that does not respond to PJM requests [26]. Firm wind capacity is assumed by PJM to be 13% of nameplate capacity [25]; for both 2009 and 2010, firm wind capacity was 40 MW.

Table 5-5. DR capacity and net import capacity, by capacity auction [25]

Capacity auction	DR capacity (MW)	Net import capacity (MW)
2009/2010	7,290	+320
2010/2011	9,050	-400

5.2.3 Outage forecast

We assume an outage occurs when total load exceeds total available capacity. Using the procedures outlined above, we develop yearly forecasts of hourly load and available capacity. We then subtract the hourly load forecast from the hourly forecast of available capacity to identify if an outage has occurred (5–12). We append 10 of these yearly forecasts together, and then calculate UE and LOLH with equations (5–13) and (5–14). LOLE is calculated in a similar manner as LOLH, but all consecutive outage hours are counted as one outage event. We repeat the process 10,000 times to develop distributions of LOLE, UE, and LOLH. We repeat the entire process, varying the amount of installed capacity in order to see how reliability metrics change versus reserve margin. To vary capacity, we add or subtract a constant amount from each hour's available capacity.

Table 5-6. Outage equations

$$Outage_h = \begin{cases} 1 : \sum AvailableCapacity_h < Load_h \\ 0 : \sum AvailableCapacity_h > Load_h \end{cases} \quad \forall h \in H \qquad (5\text{–}12)$$

$$LOLH = \sum_h Outage_h \quad \forall h \in H \qquad (5\text{–}13)$$

$$EUE = \sum_h (Load_h - AvailableCapacity_h) \quad \forall h \in Outage_h = 1 \qquad (5\text{–}14)$$

H = set of 8760 annual hours

$AvailableCapacity_h$ = summed capacity of all online PJM generators, DR, net imports, and reliable wind power at hour h

$Load_h$ = total PJM load at hour h

$Outage_h$ = binary variable indicating if an outage occurred at hour h

In our modeling, we do not consider the effect of transmission constraints on resource adequacy. In the 2009/2010 auction, PJM found inflows were constrained to the Eastern Mid-Atlantic Area Council (EMAAC) and southwestern MAAC. Additional capacity was procured in these regions, resulting in higher capacity prices in these regions [27]. In the 2010/2011 auction, PJM found no transmission constraints, and capacity prices were equal throughout the interconnection. We also ignore any operating or synchronous reserve requirements.

PJM's Base Residual Auction is held in May, three years prior to the delivery year. By conducting the auction three years in advance, PJM seeks to reduce uncertainty for market participants. Each year after the Base Residual Auction, PJM conducts Incremental Auctions to account for changes in market conditions. Our analysis simulates the last Incremental Auction, one year in advance of the delivery date. As such, we use data from 2009 and earlier to develop the 2010 forecast. In principle, our methods could be used to simulate the Base Residual Auction, but would

need to be adjusted to account for the increased uncertainty in available capacity and load three years in advance.

5.2.4 Economically optimal reserve margin

An alternative to basing capacity decisions on reliability mandates is to instead base decisions on minimizing total system costs. The 'economically optimal reserve margin' is the reserve margin that minimizes total system costs, including costs on the capacity market, energy market, supply shortage costs, and outage costs. We estimate the total system costs in PJM for reserve margins of 10% to 20%. This analysis is described in detail in Appendix C.

5.2.5 Correlated outages

We test how LOLE, LOLH, and UE would vary if all 30 GW of PJM natural gas combustion turbines (NGCTs) were subject to the risk of a natural gas supply disruption. We model the hourly risk of a fuel supply shortage as $P_{FS.}$ We then evaluate each hour if a supply shortage occurs (5–15). We assume the risk of a supply shortage is uniform throughout the year. If a supply shortage occurs, the probability of each individual NGCT failing is $P_{outage,FS}$ (5–16); if no supply shortage occurs, we adjust the probability of an independent failure occuring such that the overall risk of failure is equal to the case in which all outages are independent (5–10). We therefore do not change the probability of an outage occurring. Rather, we adjust the fraction of outages due to a supply shortage versus an independent failure.

Because data on the frequency and severity of correlated outages is not publically available, we test the sensitivity to each parameter. First, we vary the hourly probability of a supply shortage from 0.023% to 0.002% (twice per year to once every 5.5 years), assuming that all NGCTs fail if a shortage occurs ($P_{outage,FS} = 1$). In the second test, we vary fraction of generators forced offline by a

supply shortage from 0% to 100%, assuming that shortage occur on average once per year (P_{FS} = 0.011%).

Table 5-7. Correlated outage equations

$$fuelShortage_h = \begin{matrix} 1 : rand() \le P_{FS} \\ 0 : rand() > P_{FS} \end{matrix} \quad \forall h \in H \qquad (5\text{–}15)$$

$$P_{1,0,h}' = \begin{matrix} P_{outage,FS} : fuelShortage_h = 1 \\ P_{1,0} - P_{outage,FS} * P_{FS} : fuelShortage_h = 0 \end{matrix} \quad \forall h \in H \qquad (5\text{–}16)$$

$$P_{1,1}' = 1 - P_{1,0}' \qquad (5\text{–}17)$$

H = set of 8760 annual hours

P_{FS} = Probability of a fuel shortage

$fuelShortage_h$ = binary variable indicating if there is a fuel shortage at hour h

$P_{outage,FS}$ = Probability that a generator goes offline if a fuel shortage occurs

5.3 Results

Table 5-8 shows accuracy statistics of the load model, both in the training data for 2005-2009 and test data when predicting 2010 load. The test error is the model's prediction error when given actual 2010 temperatures and load growth; it therefore ignores uncertainty in temperature and load growth. Normalized root-mean-square error (NRMSE) controls for the size of the PJM region (5–18). Table D-1 shows detailed regression results for the PJM Classic regression. Figure 5-5 shows training and test residuals distributions. Because the distributions are similar, resampling from the training residuals should reasonably account for model uncertainty (see Methods - Step 3).

$$NRMSE = \frac{RMSE}{load_{\max} - load_{\min}} \qquad (5\text{–}18)$$

Table 5-8. Accuracy statistics of the load forecast model, both training error (1993 – 2009) and test prediction error (2010).

	Training, 1993 - 2009		Test, 2010	
PJM Region	**RMSE [MW]**	**NRMSE [%]**	**RMSE [MW]**	**NRMSE [%]**
PJM Classic	1690	4.0	1800	4.5
AEP	790	5.2	910	6.7
Allegheny Energy	300	5.3	330	6.2
Dayton Power & Light	130	4.7	140	6.1
Dominion Virginia	640	3.3	760	5.8
Duquesne Light Co	80	4.1	90	5.2
Exelon – Commonwealth Edison	930	5.6	1000	6.9
Rockland Energy	20	4.2	20	5.1
PJM total	3510	3.5	3840	4.3

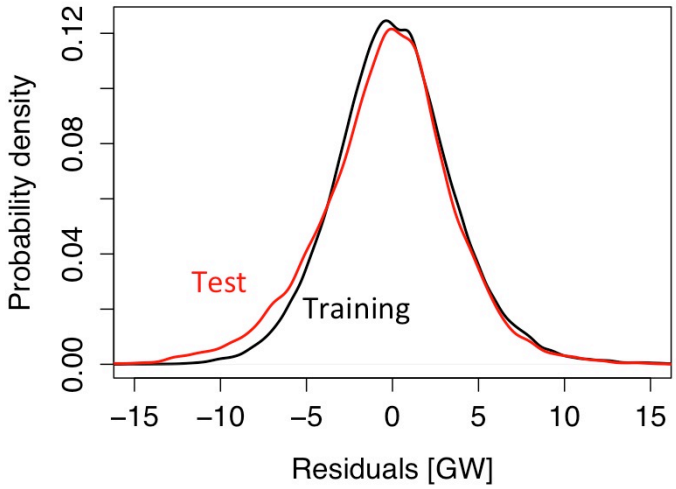

Figure 5-5. Distribution of training residuals and test residuals for PJM total.

The model's accuracy could certainly be improved further. Including weather data from more points within PJM would likely have the greatest effect on model accuracy. Our model uses weather data from Reagan National and Pittsburgh International Airports; PJM's long-term load forecasting model uses temperature data from 24 airports [13]. However, the availability of reliable weather data dating to 1945 is spotty.

5.3.1 The effect of temperature and load growth uncertainty

Our probabilistic forecast of 2010 load considers uncertainty in temperature, load growth, and model error. Figure 5-6 illustrates the model's accuracy when these uncertain factors are considered. Although the actual load is within the forecast's 95% confidence bounds, the forecast is biased to somewhat under-predict the probability of high loads. This is because 2010 was a historically warm year compared to the past 60 years (Figure 5-7). Using actual 2010 temperatures and load growth instead of probabilistic forecasts removes the model's bias to underpredict the probability of high loads (Figure 5-6).

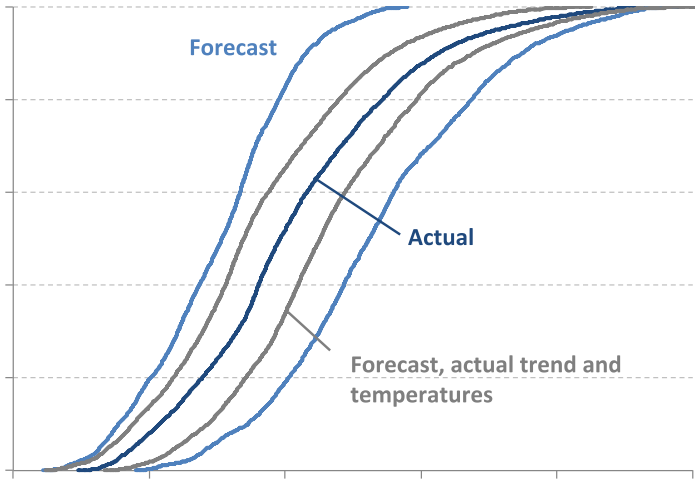

Figure 5-6. Accuracy of load model. Cumulative probability of actual 2010 hourly load, and forecasts' 95% confidence intervals.

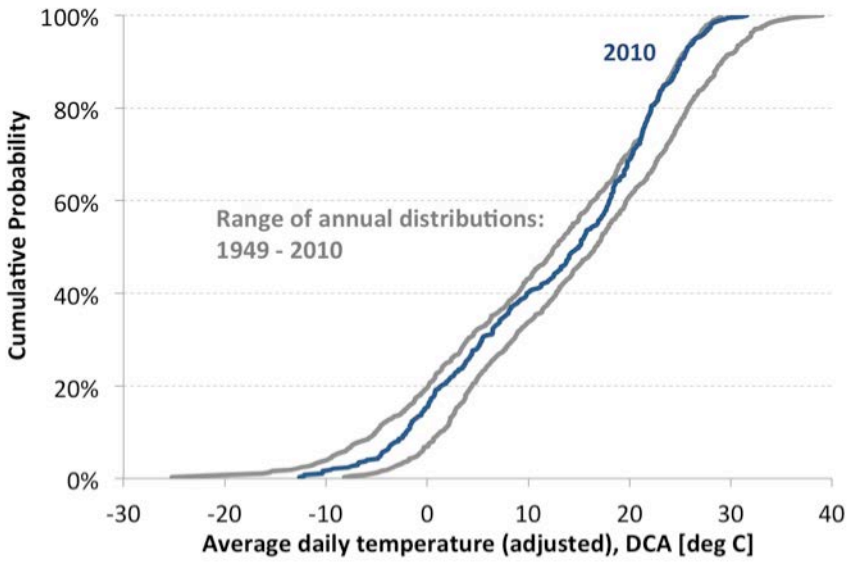

Figure 5-7. 2010 temperature distributions, and historic range of values 1949 – 2010. 2010 had an unusually high number of days with average adjusted temperatures of 20 °C – 30 °C.

5.3.2 Reliability metrics

Figure 5-8 shows simulated 2010 LOLE for reserve margins of 10% to 25%. The expected value of our 2010 simulation closely matches that of PJM's 2013 simulation (data on PJM's 2010 simulation is not available, but the results of the simulation have changed very little over time [26]). In 2010, PJM found a 15.5% reserve margin was necessary to meet the 0.1 LOLE standard [26]; we find a 15.5% reserve margin would have resulted in an LOLE of 0.09 events per year. Our simulation's 90% confidence interval ranges from zero to three events per ten years at 15.5% reserve margin.

The actual 2010 reserve margin was 20.5% (164 GW), as PJM procured more capacity than was needed on the capacity market [27][3]. We find that a 20.5% reserve margin corresponds to an expected LOLE of 0.02 events per year, and achieves the 0.1 LOLE standard with 90% confidence. Therefore, PJM's revealed risk preference in 2010 was to meet the 0.1 LOLE standard with 90% confidence.

[3] Generation offered + fixed resource requirement (FRR) commitments – generation offered but not accepted

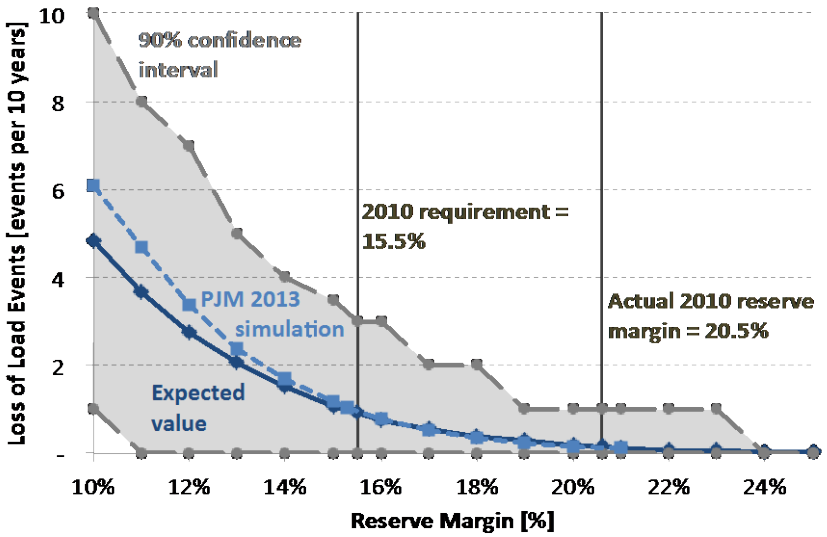

Figure 5-8. 2010 LOLE versus reserve margin. Also shown are results from PJM's 2013 resource adequacy modeling (recreated from [26]).

Figure 5-9 shows simulated 2010 unserved energy versus reserve margin. At a 15.5% reserve margin, the expected UE is 1.5 GWh per year, or 0.0002% of actual 2010 load. The 90% confidence interval ranges from 0 GWh per year to 7.5 GWh per year (0.0000% - 0.0011% of load unserved, respectively). UE becomes increasingly uncertain at lower reserve margins. Expected LOLH is 4, with a 90% confidence range of 0 to 16.

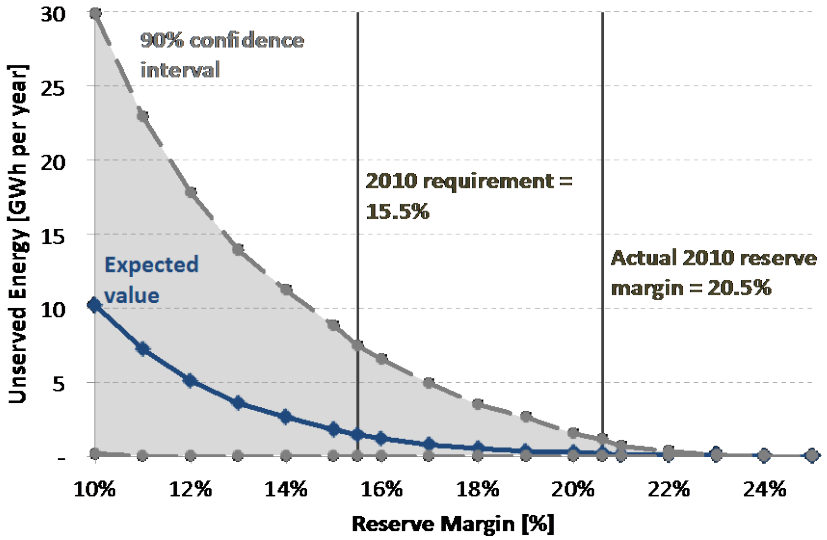

Figure 5-9. 2010 unserved energy versus reserve margin.

5.3.3 Optimal reserve margin and the effects of risk aversion

We find that PJM's target 2010 reserve margin of 15.5% was sufficient to meet the 0.1 LOLE standard. Switching to either the 2.4 LOLH standard or the 0.001% UE standard could reduce reserve margins to 10% or 11% (Table 5-9). By procuring additional capacity such that the realized reserve margin was 20.5%, PJM's implied risk preference is to meet the 0.1 LOLE standard with 90% confidence. PJM could meet the 2.4 LOLH standard and 0.001% UE standard with 90% confidence at reserve margins of 13% and 14%, respectively. Requiring that the reliability metric be met with 95% or 99% confidence would further increase reserve margin requirements.

Table 5-9. Sensitivity of the target reserve margin and installed capacity to different reliability metrics and risk tolerances. PJM's target 2010 reserve margin was 15.5% (158 GW), and actual 2010 reserve margin was 20.5% (165 GW).

	Optimal reserve margin [%] (installed capacity [GW])			
Metric	**Risk Neutral**	**90% Confidence**	**95% Confidence**	**99% Confidence**
0.1 LOLE	15.5% (158)	20.5% (165)	23% (168)	>25% (>170)
2.4 LOLH	10% (151)	13% (154)	14% (156)	16% (159)
0.001% UE	11% (152)	14% (156)	16% (159)	18% (161)

5.3.4 Distribution of outage size

We find that there is extreme variation in the magnitude of outages. As shown in Figure 5-10, the distribution of unserved energy resulting from an outage is extremely fat tailed. At a 15.5% reserve margin, the mean outage is 15 GWh, but outages range from 0 GWh to 126 GWh (Table 5-10). The top 10% largest outages account for half of total unserved energy, and the top 1% of outages account for 10% of total unserved energy. The risk of a very large outage becomes more pronounced at lower reserve margins.

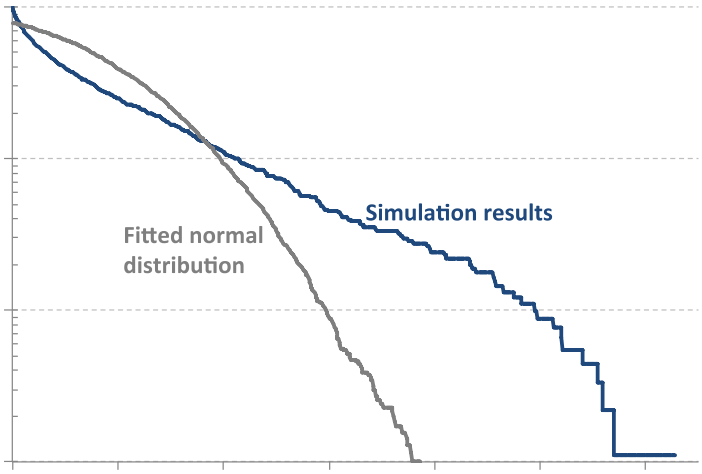

Figure 5-10. Distribution of the size of simulated outages, in terms of unserved energy, versus a fitted normal distribution. Assumed reserve margin is 15.5%.

Table 5-10. Outage summary statistics, 15.5% reserve margin

	Expected value	90% Confidence Interval	Maximum
Outage duration [hours]	4	1 - 9	11
Largest magnitude [GW]	4	0 - 11	18
Total load shed [GWh]	15	0 - 58	126

5.3.5 Model form uncertainty

Load in PJM is highly sensitive to temperature, and accurately modeling this relationship is important for accurately calculating LOLE. We used a nonparametric, additive model to account for the relationship between load and temperature. We also tested a linear model to account for the relationship. The linear model divided days into heating degree days (HDD) and cooling degree days (CDD). Details can be found in Appendix D. We find that the linear model significantly over-predicts load at high temperature hours, which increases the modeled probability of outages relative to the nonparametric, additive model (Figure 5-11).

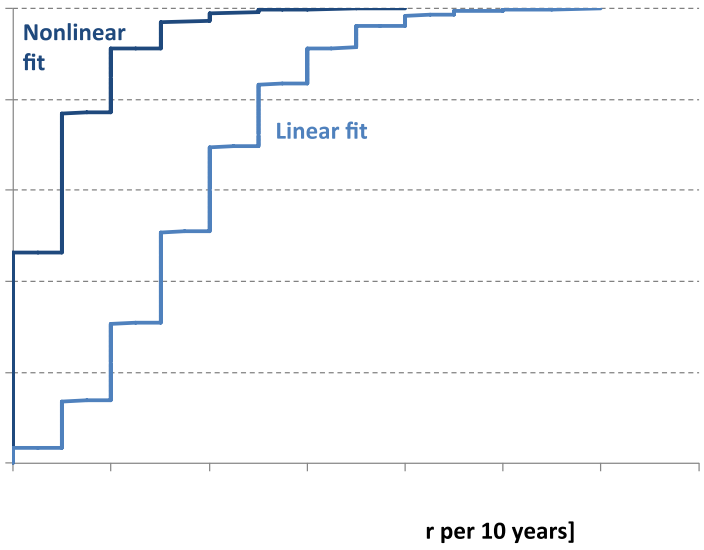

Figure 5-11. Comparison of LOLE estimates for non-parametric and linear temperature models at 15.5% reserve margin. The linear model overestimates load at high temperature hours, and therefore overestimates the probability of an outage occurring.

We also analyze the sensitivity of the model's parameters to 'leave-one-out' testing (Figure 5-12). The base model uses data from 2005 – 2009 to estimate model parameters. Estimating model parameters from only four years worth of data, leaving one of the years out, would change model parameters and therefore estimates of LOLE, LOLH, and UE. The baseline expected value of LOLE is 0.9 at a 15.5% reserve margin; 'leave-one-out' testing can vary the mean LOLE by +/- 30% (0.64 to 0.97).

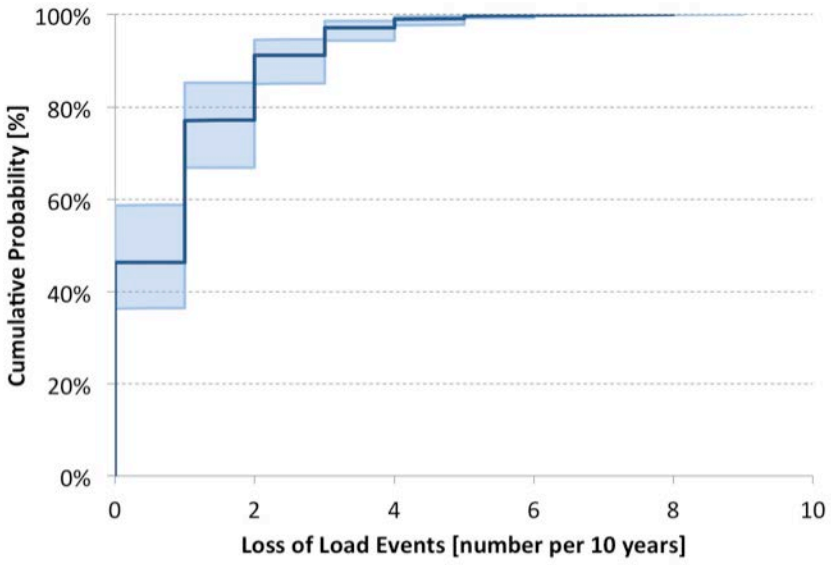

Figure 5-12. Sensitivity of LOLE to 'leave-one-out' parameter testing. The base model (solid line) estimates parameters with data from 2005 – 2009. The shaded area shows the range of results if one year's worth of data is left out when estimating the parameters. Evaluated at 15.5% reserve margin.

Finally, we test the sensitivity of results to a scenario in which EFORd varies with ambient temperature. We find that LOLE would increase if EFORd rose in summer months and fell in winter months. For more details, see Appendix D.

5.3.6 Correlated failures

We find that natural gas supply disruptions have the potential to significantly increase the risk of a supply shortage, assuming such outages force a large percentage of PJM's NGCTs offline at once. If a supply disruption that forces all 30 GW of NGCTs offline occurs on average once every five years, the expected UE more than doubles (Figure 5-13). If this supply disruption were to occur on average once per year, it would raise expected UE by more than 10 times. However, supply disruptions pose a significant risk only if they force more than 50% of NGCTs offline at once (Figure D-12). Supply disruptions can significantly increase the maximum size of supply shortages (Figure D-13). We assume supply disruptions can occur at any time throughout the year; limiting supply disruptions to winter months would change the associated risk of supply shortages.

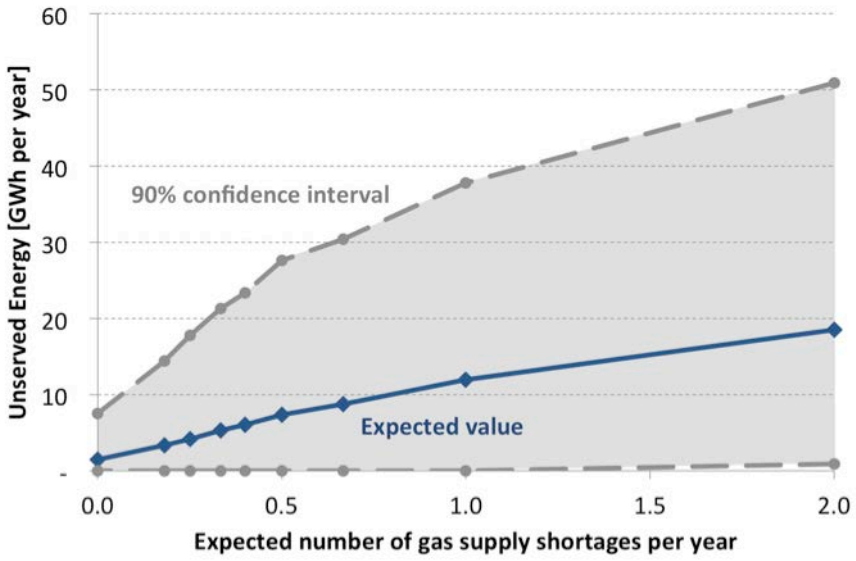

Figure 5-13. Sensitivity of unserved energy to natural gas supply shortages that force all PJM NGCTs offline. Evaluated at 15.5% IRM.

5.4 Discussion

Using our probabilistic regression method, we find the 2010 reserve margin target of 15.5% was sufficient to meet the mandated 0.1 LOLE standard. PJM procured 7 GW more capacity than needed to meet the 15.5% target, making the realized reserve margin 20.5%. By procuring more capacity than needed, PJM's revealed 2010 risk preference was to meet the 0.1 LOLE standard with 90% confidence. This risk aversion is due to PJM's policy to procure more capacity than needed if the capacity can be procured at a cost less than the net cost of new entry of a natural gas combustion turbine (~$270/MW-day) [27, 28].

Switching from the 0.1 LOLE standard to either the 2.4 LOLH or 0.001% UE standard would have reduced PJM's 20.5% reserve margin in 2010. A 14% reserve margin would have been sufficient to meet the 0.001% UE standard with 90% confidence. A 13% reserve margin would have been sufficient to meet the 2.4 LOLH standard with 90% confidence. This represents a 9 GW – 11 GW reduction in capacity procurement, while still maintaining levels of reliability accepted by

other systems. If PJM were to switch to either standard, the 11 GW of coal capacity "at high risk" of retirement could be retired without needing to be replaced.

In line with NERC, we recommend that PJM adopt a reliability metric based on unserved energy. The LOLE metric is flawed, in that it measures only the probability of an outage occurring and ignores both the severity and duration of outages. Our modeling shows that the severity and duration of outage events vary greatly (Table 5-10), undermining the usefulness of the LOLE metric. Because supply shortages could cause political fallout both regionally and for PJM management, we recommend that PJM work through their stakeholder process to identify both the appropriate UE target and the risk tolerance of PJM participants.

Basing capacity decisions on traditional reliability standards ignores the cost effectiveness of carrying excess capacity. Achieving a very high reliability standard may be possible, but extremely costly. Recently, system operators such as ERCOT have begun to incorporate the cost effectiveness metrics into their decision making process [30]. The 'economically optimal reserve margin' is the reserve margin that minimizes total system costs, including costs associated with outages.

As discussed extensively in the Appendix C, we find that the long run, economically optimal reserve margin in PJM is 13% - 15%. This is the same reserve margin needed to meet either the 2.4 LOLH standard or the 0.001% UE standard with 90% confidence. We therefore conclude that either standard would be economically efficient. However, maintaining PJM's realized 2010 reserve margin of 20.5% would result in annual system costs $600 million higher than economically optimal in the long run.

System operators should be aware that the risk posed by supply shortages is primarily due to extremely severe, but infrequent outages. Our simulations show that the largest 10% of supply shortages are responsible for 50% of unserved energy. Taking into account the possibility of

correlated generator outages further exacerbates this risk. The risk of very large outages increases at low reserve margins, suggesting that some risk aversion on part of PJM may be justified. System operators should work to ensure that their system is robust to large supply shortages, and that these shortages do not lead to cascading network failures.

PJM's resource adequacy modeling assumes that generator outages are independent. We find that correlated outages among plants due to natural gas supply shortages could increase outage risk, and cause PJM to underestimate this risk. Evidence suggests that correlated outages do occur with some regularity; winter storms on January 7, 2013 led to 19 GW of natural gas plants and 21 GW of other capacity simultaneously experiencing forced outages [29]. We recommend further research into the risks posed by correlated outages. If the risks posed by correlated outages are found to be significant, we recommend that PJM consider this risk when planning resource adequacy needs. If correlated outage risks are found to be significant, PJM may need to significantly increase reserve margins.

5.5 References

[1] U.S. Department of Energy. *Annual Energy Outlook 2014 Early Release*; Energy Information Administration: Washington, DC, **2013**. http://www.eia.gov/forecasts/aeo/er/index.cfm (accessed July 2014).

[2] Eastern Interconnection States' Planning Council (EISPC). The Economic Ramifications of Resource Adequacy White Paper. 2013. Prepared by Astrape Consulting for EISPC and the National of Regulatory Utility Commissioners (NARUC). http://www.naruc.org/grants/Documents/Economics%20of%20Resource%20Adequacy%20WhitePaper_Astrape_Final.pdf (accessed September 2014).

[3] Spees, K., Newell, S., Pfeifenberger, J. "Capacity Markets-Lessons Learned from the First Decade." *Economics of Energy & Environmental Policy* 2.2 (2013).

[4] PJM Interconnection. PJM Generation Adequacy Analysis: Technical Methods. Capacity Adequacy Planning Department. 2003. http://www.pjm.com/~/media/etools/oasis/references/whitepaper-sections-12.ashx (accessed September 2014).

[5] Pfeifenberger; J.; Spees, K.; Carden, K.; Wintermantel, N. (2013). Resource Adequacy Requirements: Reliability and Economic Implications. Prepared for the U.S. Federal Energy Regulatory Commission. https://www.ferc.gov/legal/staff-reports/2014/02-07-14-consultant-report.pdf (accessed September 2014).

[6] North American Electric Reliability Corporation. *Final Report on Methodologies and Metrics - September and December, 2010 with Approvals and Revisions*. 2010. http://www.nerc.com/comm/PC/Reliability%20Assessment%20Subcommittee%20RAS%20DL/GTRPMTF_Meth__Metrics_Report_final_w%20_PC_approvals_revisions_12%2008%2010.pdf (accessed July 2014).

[7] Joskow, P., & Tirole, J. (2007). Reliability and competitive electricity markets. *The Rand Journal of Economics*, *38*(1), 60-84.

[8] Hines, P., Apt, J., & Talukdar, S. (2009). Large blackouts in North America: Historical trends and policy implications. *Energy Policy*, *37*(12), 5249-5259.

[9] Billington R., Ringlee, R., Wood A. (1973). "Power-System Reliability Calculations". MIT Press, (1973)

[10] PJM Interconnection. *Coal Capacity at Risk of Retirement in PJM: Potential Impacts of the Finalized EPA Cross State Air Pollution Rule and Proposed National Emissions Standards for Hazardous Air Pollutants*; Norristown, PA, **2011**. http://pjm.com/~/media/documents/reports/20110826-coal-capacity-at-risk-for-retirement.ashx (accessed July, 2014).

[11] PJM Interconnection. 2010 State of the Market Report for PJM, Volume 2. Prepared by Monitoring Analytics, LLC. (2011). http://www.monitoringanalytics.com/reports/pjm_state_of_the_market/2010/2010-som-pjm-volume2.pdf (accessed September 2014).

[12] PJM Interconnection. PJM Generation Adequacy Analysis: Technical Methods. Capacity Adequacy Planning Department. 2003. http://www.pjm.com/~/media/etools/oasis/references/whitepaper-sections-12.ashx (accessed September 2014).

[13] PJM Interconnection. PJM Manual 19: Load Forecasting and Analysis, Revision 23. Prepared by Resource Adequacy Planning, 2013. http://www.pjm.com/~/media/documents/manuals/m19.ashx (accessed September 2014).

[14] Hagan, M. T., & Behr, S. M. (1987). The time series approach to short term load forecasting. *Power Systems, IEEE Transactions on*, *2*(3), 785-791.

[15] Hippert, H. S., Pedreira, C. E., & Souza, R. C. (2001). Neural networks for short-term load forecasting: A review and evaluation. *Power Systems, IEEE Transactions on*, *16*(1), 44-55.

[16] PJM Interconnection. Historical Metered Load Data. http://www.pjm.com/markets-and-operations/ops-analysis/historical-load-data.aspx (2014). Accessed June 2014.

[17] U.S. National Oceanic and Atmospheric Administration. National Climatic Data Center website. http://cdo.ncdc.noaa.gov/pls/plclimprod/poemain.accessrouter?datasetabbv=DS3505 (2014). Accessed June 2014.

[18] U.S. Naval Observatory. Duration of Daylight/Darkness Table for One Year. 2012. http://aa.usno.navy.mil/data/docs/Dur_OneYear.php. Accessed June 2014.

[19] U.S. National Oceanic and Atmospheric Administration. NWS Windchill Chart. http://www.nws.noaa.gov/os/windchill/index.shtml. 2013. Accessed August 2014.

[20] U.S. National Oceanic and Atmospheric Administration. NOAA's NWS Weather Service Heat Index. http://nws.noaa.gov/os/heat/index.shtml. 2014. Accessed August 2014.

[21] Based on Annual Energy Outlook reports from 1999 – 2008. U.S. Department of Energy. *Annual Energy Outlook*. Energy Information Administration: Washington, DC, 1999 – 2008. http://www.eia.gov/forecasts/aeo/archive.cfm. 2014. Accessed August 2014.

[22] PJM Interconnection. EIA 411 Report. http://www.pjm.com/documents/reports/eia-reports.aspx (2010). Accessed June 2014.

[23] North America Electric Reliability Corporation. Generator Availability Data System. http://www.nerc.com/pa/RAPA/gads/Pages/default.aspx (2014). Accessed August 2014.

[24] PJM Interconnection. PJM Monthly EFORd Data. 2014. http://www.pjm.com/markets-and-operations/energy/real-time/historical-bid-data/eford.aspx. Accessed June 2014.

[25] PJM Interconnection. 2012/2013 RPM Base Residual Auction Results. 2009. http://www.pjm.com/~/media/markets-ops/rpm/rpm-auction-info/2012-13-base-residual-auction-report-document-pdf.ashx. Accessed June 2014.

[26] PJM Interconnection. 2010 PJM Reserve Requirement Study. 2010. http://www.pjm.com/~/media/documents/reports/2010-pjm-reserve-requirement-study.ashx. Accessed July 2014.

[27] PJM Interconnection. 2010/2011 RPM Base Residual Auction Results. 2008. http://www.pjm.com/~/media/markets-ops/rpm/rpm-auction-info/20080201-2010-2011-bra-report.ashx. Accessed July 2014.

[28] Spees, K.; Newell, S. A.; Carlton, R.; Zhou, B.; Pfeifenberger, J. (2011). Cost of New Entry Estimates For Combustion Turbine and Combined-Cycle Plants in PJM. Prepared for the PJM Interconnection, L.L.C.

[29] PJM Interconnection. Analysis of Operational Events and Market Impacts During the January 2014 Cold Weather Events. 2014.

[30] Newell, S. A.; Spees, K.; Pfeifenberger, J.; Karkatsouli, I. (2014). Estimating the Economically Optimal Reserve Margin in ERCOT. Prepared for the Public Utility Commission of Texas.

C Appendix: The economically optimal reserve margin

Introduction

In the main text of this chapter, we investigate how adopting a different resource adequacy standard in PJM would change the reserve margin. We analyze three standards: the 0.1 LOLE standard, the 2.4 LOLH standard, and the 0.001% UE standard.

Recently, system operators and researchers have begun to consider basing capacity decisions on system cost, rather than mandated resource adequacy standards [1, 2]. The decision to procure a given level of capacity affects costs not only on the capacity market, but also energy market costs, ancillary service market costs, and outage costs. The 'economically optimal reserve margin' is the reserve margin that minimizes total system costs [1].

Here, we perform a simplified analysis to identify the level of capacity procurement that minimizes total system costs, both in the long run and short run. We use PJM generator data and load data from 2010 in this analysis. We consider costs from four sources: costs on the capacity market, energy market, outage costs, and reserve shortage costs. We assume plant forced outages are independent of one another. In 2010, PJM's reserve margin (installed capacity) was 20.5%. We quantify total system costs for reserve margins of 10% - 20%. These methods are similar to those used by other studies of the economically optimal reserve margin [1,2].

The consequences of reducing PJM's reserve margin depend greatly on the type of capacity that is no longer procured (retired). Procuring less capacity would force the retirement of plants with the highest capacity market bids. However, individual capacity market bids are not publically available, and therefore we cannot know which plants would retire. If baseload capacity retired, costs on the

energy market increase significantly. If peaking capacity retired, energy market costs would be unchanged.

As a first order approximation, we assume procuring less capacity would force the retirement of coal plants that are expensive to operate. PJM has identified 11 GW of coal capacity "at high risk" of retirement, and an additional 14 GW of coal capacity "at some risk" of retirement [3]. These plants are smaller than 400 MW and older than 40 years. However, it is possible that lower reserve margins might force other types of capacity to retire. We therefore bound our analysis with two scenarios: only baseload plants retire, and only peaking plants retire.

We estimate that PJM's long run, economically optimal reserve margin is 13% - 15%. System costs change by less than $100 million within this range, or less than 1% of the total $28 billion in estimated system costs. Because this range includes the targets needed to meet the 2.4 LOLH standard and 0.001% UE standard with 90% confidence (13% and 14%, respectively), we conclude that either of these standards could be considered efficient. However, maintaining PJM's realized 2010 reserve margin of 20.5% would increase annual system costs by $600 million in the long run.

In the short run, the economically optimal reserve margin is higher, at 15% to 18% or higher. This is because PJM currently has a large supply of relatively cheap capacity. The costs of procuring capacity on today's capacity market are therefore less than they are expected to be in the long run. PJM takes this fact into consideration when procuring capacity, which explains why PJM's 2010 reserve margin was 20.5%, 5% higher than needed to meet the 0.1 LOLE standard. This policy of over-procuring capacity manifests itself as risk aversion on the part of PJM system planners.

Our sensitivity analysis shows that system costs would significantly increase if baseload plants retired instead of the newest plants. Baseload retirements significantly increase costs on the energy

market. This suggests some additional incentives may be warranted to discourage the retirement of baseload plants. If peaking plants were to retire, the optimal reserve margin would be 13%.

Methods

We evaluate four types of system costs: costs on the capacity market, energy market, outage costs, and reserve shortage costs. Total system costs are approximated as the sum of these four cost categories. We exclude several other types of costs, including costs on regulation markets, emergency import costs, and demand response costs. Although these categories are small relative to the costs considered here [1], a more thorough analysis would consider these and other system costs.

Energy market costs

We quantify energy market costs with a simplified supply curve dispatch model. Energy market costs are calculated as the sum of generator fuel and variable operation and maintenance costs throughout the year. We assume generators are dispatched each hour in order of least cost. We do not capture constraints that can lead to out-of-merit-order dispatch, such as transmission constraints and generator ramping constraints.

We use 2010 hourly load data and generator capacity data from PJM [4, 5]. We derate each plant's capacity by the forced outage rate [6]. Delivered fuel cost data is from the Energy Information Agency [7] and Lazard [8]. Variable operation and maintenance costs are from Lazard [7]. Plant heat rates are from eGRID [9].

In the baseline scenario, the most expensive coal plants to operate are retired. For the sensitivity analysis, we retire plants with the lowest operating costs (baseload) and highest operating costs (peakers).

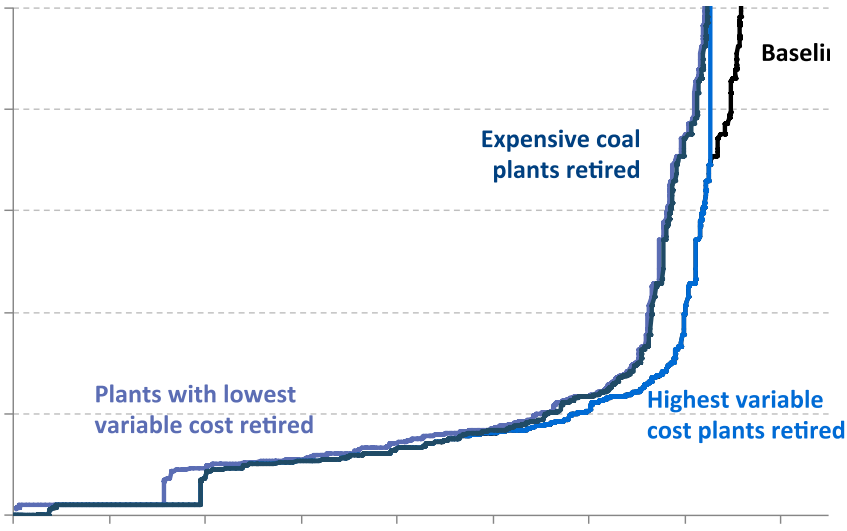

Figure C-1. Energy market supply curves for baseline 20.5% reserve margin, and 15.5% reserve margin with different types of capacity retired.

Capacity market costs

We estimate long run capacity costs as the total cost of building and operating a new natural gas combustion turbine (NGCT) plant, net expected revenues on the energy market. We approximate this quantity, known as the net cost of new entry (net CONE), as $100/kW-yr ($274/MW-day) based on findings of existing studies [10].

Short run capacity costs are derived from the 2010/2011 capacity market supply curve [11] (Figure C-2). The 2010/2011 market clearing price was $174/MW-day, corresponding to a market clearing quantity of 131 GW [12]. In addition to the quantity cleared on the capacity market, PJM resource adequacy planners took into account an additional 26 GW of capacity procured by load serving entities through bilateral, fixed resource requirement commitments [11], making the realized reserve margin 20.5%. We measure long-run and short-run capacity market costs for reserve margins of 10% to 20%, corresponding to market quantities of 151 GW – 164 GW.

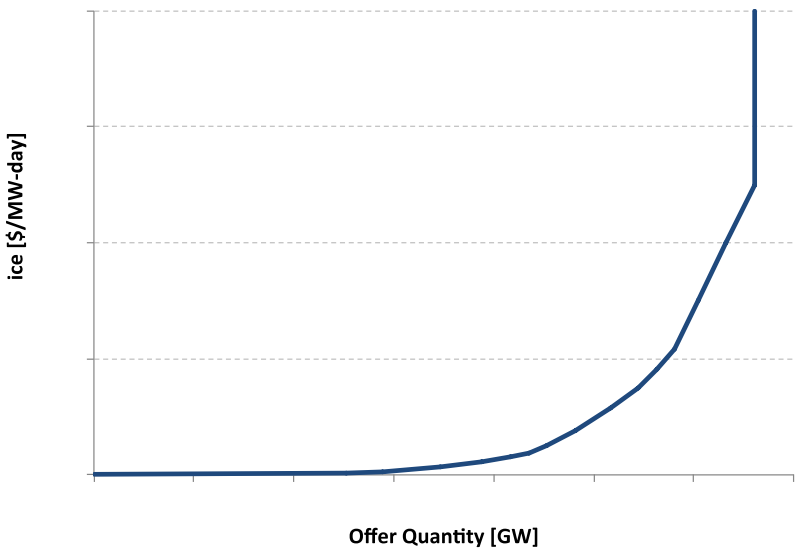

Figure C-2. 2010/2011 capacity market supply curve. Based on [10].

Cost of reserve shortages

We assume a reserve shortage occurs whenever hourly load is high enough to force PJM to draw from their day ahead schedule reserves (DASR) (C-1). Shortages are valued at PJM's current price cap of $2,700 / MWh [13]. Data on hourly 2010 DASR requirements is from PJM [14].

$$ReserveShortage_h = \min(0, Load_h - (TotalCapacity - ReserveRequirement_h)) \ \forall h \in H \qquad \text{(C-1)}$$

Cost of outages

The cost of an outage is the total unserved energy (UE), multiplied by the value of lost load (VoLL) of consumers. In the main text of this chapter, we simulate expected UE for various reserve margins, assuming plant outages are independent of one another. Here, we multiply these simulated values by an assumed VoLL to approximate the total cost of outages. By using the expected value of unserved energy, we assume PJM is risk-neutral to outage costs. We assume a VoLL of $15/kWh, based on the estimated costs of a one-hour interruption for medium/large commercial and industrial consumers [15].

Results and Discussion

Long run system costs

We find the long run, optimal economic reserve margin is 13% - 15%. Total system costs vary by less than $100 million per year within this range. As shown in Figure C-3, costs associated with outages and reserve shortages become more significant as reserve margins fall below 14%. Above 14%, capacity market costs increase significantly.

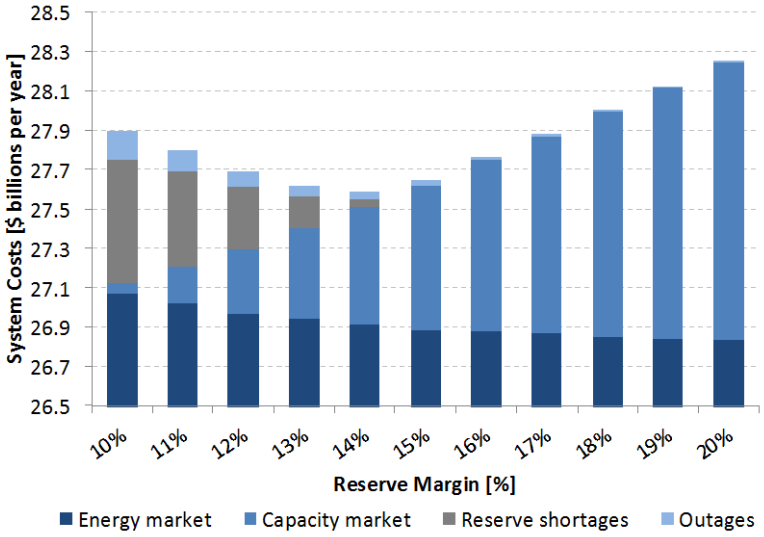

Figure C-3. Long run system costs. Capacity market costs above a $15B/yr baseline.

Short run system costs

The short run, the optimal economic reserve margin is 15% - 16%. As shown in Figure C-4, system costs are within $100 million for reserve margins of 15% - 18%. Below 15%, reserve shortage costs and outage costs become significant.

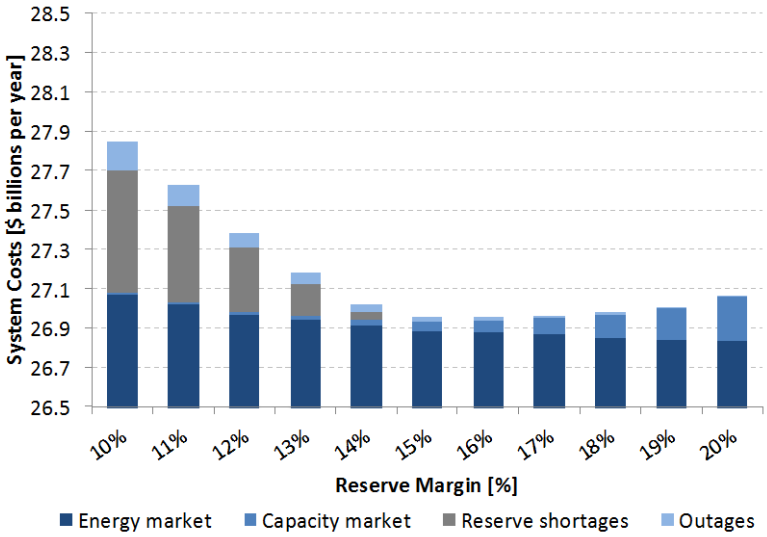

Figure C-4. Short run system costs. Capacity market costs above a $15B/yr baseline.

Sensitivity to type of capacity retired

System costs are very sensitive to the type of capacity that is retired when PJM procures less capacity. As shown in Figure C-5, if the retired capacity is baseload plants, total system costs increase significantly as reserve margins decrease. This suggests that incentives to discourage the retirement of baseload capacity may be warranted. If retired capacity is either expensive coal plants or peaker plants, system costs are minimized for reserve margins of 13% - 15%.

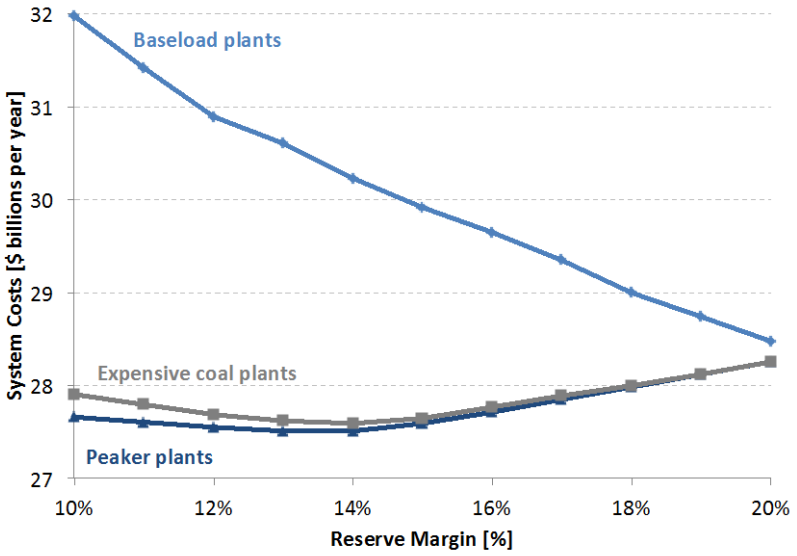

Figure C-5. Long run system costs, for different assumptions about what type of capacity is retired. Baseload plants are those with the lowest operating costs; peaker plants are those with the highest operating costs.

We find that outage costs are small in both the long run and short run, as the expected unserved energy is small. We therefore conclude that the economically optimal reserve margin is insensitive to VoLL, here assumed to be $15/kWh. More important is the shortage price cap, currently set at $2,700/MWh in PJM.

We find that the economically optimal reserve margin is 13% - 15% in the long run. As this range includes the reserve margins needed to meet the 2.4 LOLH standard and 0.001% UE standard with 90% confidence, we conclude that either of these standards could be considered efficient. However, maintaining PJM's realized 2010 reserve margin of 20.5% would result in annual system costs $600 million higher than economically optimal.

Our results are similar to those of other, similar, studies [1, 2]. The Brattle Group found that the economically optimal reserve margin in the ERCOT system is 10.2%, or lower than the reserve margin we find is optimal in PJM [1]. This is likely due to differences between the system such as generator makeup and fuel prices. Similar to our results, the Brattle study found that system costs

do not vary significantly for reserve margins of 8% - 14%. The study does note that there is more uncertainty in system costs at lower reserve margins.

Future work in this area should include an expanded treatment of uncertainty. In particular, we base outage costs on the expected unserved energy and therefore assume system operators are risk neutral to outage costs. In the main text of this chapter, we show that unserved energy is highly uncertain. Accounting for this uncertainty and system operator risk aversion may increase outage costs. We also base our estimates of fuel costs and generation mix on 2010 data; considering a wider range of scenarios would allow for more robust results.

References

[1] Newell, S. A.; Spees, K.; Pfeifenberger, J.; Karkatsouli, I. (2014). Estimating the Economically Optimal Reserve Margin in ERCOT. Prepared for the Public Utility Commission of Texas. http://brattle.com/system/publications/pdfs/000/004/978/original/Estimating_the_Economically_Optimal_Reserve_Margin_in_ERCOT_Revised.pdf?1395159117 (accessed September 2014)

[2] Pfeifenberger; J.; Spees, K.; Carden, K.; Wintermantel, N. (2013). Resource Adequacy Requirements: Reliability and Economic Implications. Prepared for the U.S. Federal Energy Regulatory Commission. https://www.ferc.gov/legal/staff-reports/2014/02-07-14-consultant-report.pdf (accessed September 2014).

[3] PJM Interconnection. *Coal Capacity at Risk of Retirement in PJM: Potential Impacts of the Finalized EPA Cross State Air Pollution Rule and Proposed National Emissions Standards for Hazardous Air Pollutants*; Norristown, PA, **2011**. http://pjm.com/~/media/documents/reports/20110826-coal-capacity-at-risk-for-retirement.ashx (accessed July 2014).

[4] PJM Interconnection. Historical Metered Load Data. http://www.pjm.com/markets-and-operations/ops-analysis/historical-load-data.aspx (2014). Accessed June 2014.

[5] PJM Interconnection. EIA 411 Report. http://www.pjm.com/documents/reports/eia-reports.aspx (2010). Accessed June 2014.

[6] PJM Interconnection. 2010 State of the Market Report for PJM, Volume 2. Prepared by Monitoring Analytics, LLC. (2011). http://www.monitoringanalytics.com/reports/pjm_state_of_the_market/2010/2010-som-pjm-volume2.pdf (accessed September 2014).

[7] U.S. Department of Energy, Energy Information Agency. Electricity Data Browser. http://www.eia.gov/electricity/data/browser/ (2014). Accessed August 2014.

[8] Lazard. (2010). Levelized Cost of Energy Analysis – Version 4.0. http://webapp.psc.state.md.us/Intranet/casenum/NewIndex3_VOpenFile.cfm?filepath=C:%5CCasenum%5C9200-9299%5C9214%5CItem_119%5C%5CSierra%20Club%20and%20CCAN_Case%209214_Supplemental%20Exhibits%20to%20Comments%5CLAZARD%20LCOE%206-12-10.pdf (accessed September 2014).

[9] U.S. Environmental Protection Agency. eGRID2012 Version 1.0. http://www.epa.gov/cleanenergy/energy-resources/egrid/index.html (accessed Aug, 2014).

[10] Spees, K.; Newell, S. A.; Carlton, R.; Zhou, B.; Pfeifenberger, J. (2011). Cost of New Entry Estimates For Combustion Turbine and Combined-Cycle Plants in PJM. Prepared for the PJM Interconnection, L.L.C.

[11] Pfeifenberger, J.; Newell, S. A.; Spees, K.; Hajos, A.; Madjarov, K. (2011). Second Performance Assessment of PJM's Reliability Pricing Model. Prepared for the PJM Interconnection, L.L.C. http://www.pjm.com/~/media/committees-groups/committees/mrc/20110818/20110826-brattle-report-second-performance-assessment-of-pjm-reliability-pricing-model.ashx (accessed September 2014).

[12] PJM Interconnection. 2010/2011 RPM Base Residual Auction Results. 2008. http://www.pjm.com/~/media/markets-ops/rpm/rpm-auction-info/20080201-2010-2011-bra-report.ashx. (accessed July 28, 2014).

[13] PJM Interconnection. Scarcity Pricing. http://www.pjm.com/~/media/about-pjm/newsroom/fact-sheets/shortage-pricing-fact-sheet.ashx (2014). (accessed August 2014).

[14] PJM Interconnection. Day-Ahead Scheduling Reserve Preliminary Billing Data. http://www.pjm.com/markets-and-operations/market-settlements/preliminary-billing-reports/dsr-pjm.aspx (2014). Accessed August 2014.

[15] Sullivan, Michael J. Estimated Value of Service Reliability for Electric Utility Customers in the United States. Lawrence Berkeley National Laboratory (2009). http://certs.lbl.gov/pdf/lbnl-2132e.pdf (accessed September 2014).

D Appendix: Detailed results

Scheduling planned outages and maintenance outages

We schedule each plant's planned outages and maintenance outages with the following process:

1. Find the total planned outage hours (POH) and forced outage hours (FOH) for each plant
2. Divide plants into two categories: peaking plants (<100 MW) and non-peaking plants
3. Schedule peaking outages such that the total offline capacity is roughly equal for all hours of the year. Each plant is assumed to undergo one outage, of duration POH + FOH. ~1.7 GW of peaking capacity is scheduled offline each hour.
4. Schedule non-peaking outages to occur during the spring (March, April, May) and fall (September, October, November). Each plant is assumed to undergo one outage, of duration POH + FOH. ~35 GW of non-peaking capacity is scheduled offline each spring and fall hour.

By scheduling outages in this manner, we minimize the likelihood of a supply shortage. We also mimic the actual scheduling of outages in PJM, in which baseload coal and combined cycle plants are primarily offline during the spring and fall, and combustion turbines are offline throughout the year (Figure D-1).

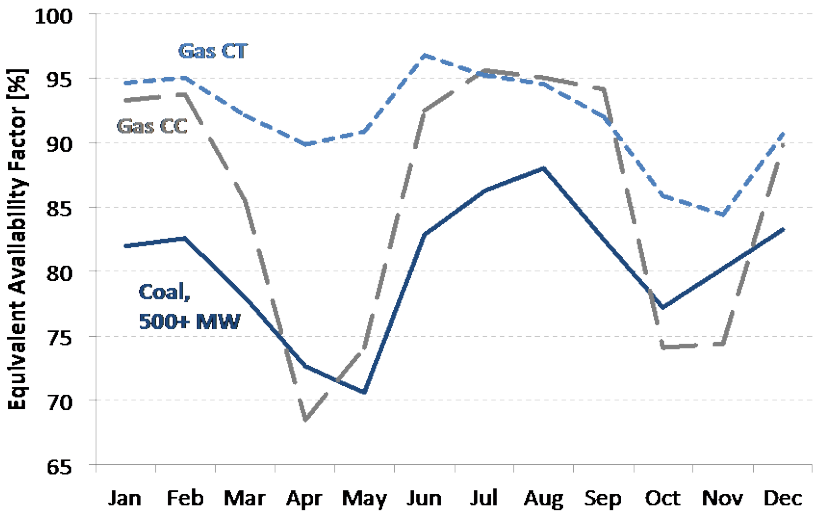

Figure D-1. Equivalent availability factor, PJM generators, 2010 [1].

Detailed Regression Results

Table D-1 provides detailed regression results for the PJM Classic region. We find that the significant results have the expected sign in most cases. For example, signs are negative for holidays, reflecting that load are lower on these days. Signs are also negative for low-load hours during the night and positive for high-load hours during the day and evening.

Table D-1. Detailed regression results for the PJM Classic region.

Note: Dependent variable is residuals from the long-term trend regression (see main paper, step 1).
*Significance codes: '***' (P < 0.001); '**' (P < 0.01); '*' (P < 0.05); '.' (P < 0.1); ' ' (P < 1)*

Variable	Estimate	Std. Error	t value	Significance	Notes
(Intercept)	1.81E-01	2.82E-02	6.42	***	
isTue	1.06E-02	6.83E-04	15.551	***	
isWed	1.39E-02	6.84E-04	20.32	***	
isThu	1.46E-02	6.87E-04	21.199	***	
isFri	1.67E-03	6.92E-04	2.417	*	
isSat	-8.53E-02	6.86E-04	-124.412	***	
isSun	-1.15E-01	6.87E-04	-167.982	***	
isMLK	-1.07E-02	3.53E-03	-3.036	**	
isPresidentsDay	3.24E-03	3.55E-03	0.913		
isGoodFriday	-5.23E-02	3.50E-03	-14.933	***	
isMemorialDay	-1.01E-01	4.28E-03	-23.616	***	
isMemorialDayWeekend	-2.92E-02	2.73E-03	-10.701	***	
isJuly4	-1.14E-01	3.57E-03	-31.912	***	
isLaborDay	-1.13E-01	4.26E-03	-26.464	***	
isLaborDayWeekend	-2.25E-02	2.63E-03	-8.572	***	
isChristmas	-1.41E-01	4.65E-03	-30.313	***	
isXmasEveEve	-1.56E-03	4.65E-03	-0.335		Dec 23
isChristmasEve	-7.55E-02	4.65E-03	-16.234	***	Dec 24
isXMasWk	-2.49E-02	3.51E-03	-7.091	***	Dec 26 - 30
XMasLights	1.39E-02	2.65E-03	5.256	***	Dec 4 - Dec 22
isThanksgiving	-1.50E-01	3.80E-03	-39.4	***	
isThanksgivingFriday	-1.01E-01	3.80E-03	-26.556	***	Day after Thanksgiving
isNewYearsDay	-9.74E-02	3.62E-03	-26.935	***	
isNewYearsEve	-5.05E-02	4.55E-03	-11.086	***	
isThanksgivingWeek	-4.39E-03	1.95E-03	-2.249	*	Mon - Sun, Thanksgiving week
isXmasDayAfter	-4.66E-02	3.84E-03	-12.129	***	Dec 26
isFeb	5.69E-01	3.58E-02	15.918	***	

Variable	Estimate	Std. Error	t value	Significance	Notes
isH1	-1.27E-01	3.18E-03	-40.034	***	
isH2	-1.58E-01	3.18E-03	-49.564	***	
isH3	-1.71E-01	3.18E-03	-53.732	***	
isH4	-1.72E-01	3.18E-03	-53.952	***	
isH5	-1.52E-01	3.18E-03	-47.793	***	
isH6	-9.37E-02	3.18E-03	-29.479	***	
isH7	1.63E-04	3.18E-03	0.051		
isH8	5.40E-02	3.18E-03	16.975	***	
isH9	6.73E-02	3.18E-03	21.169	***	
isH10	7.31E-02	3.18E-03	23.001	***	
isH11	7.34E-02	3.18E-03	23.104	***	
isH12	6.48E-02	3.18E-03	20.401	***	
isH13	5.12E-02	3.18E-03	16.099	***	
isH14	3.93E-02	3.18E-03	12.356	***	
isH15	2.67E-02	3.18E-03	8.407	***	
isH16	2.58E-02	3.18E-03	8.13	***	
isH17	5.70E-02	3.18E-03	17.928	***	
isH18	1.31E-01	3.18E-03	41.196	***	
isH19	1.45E-01	3.18E-03	45.666	***	
isH20	1.32E-01	3.18E-03	41.475	***	
isH21	1.11E-01	3.18E-03	34.75	***	
isH22	6.89E-02	3.18E-03	21.672	***	
isH23	3.30E-03	3.18E-03	1.039		
isH24	-6.95E-02	3.18E-03	-21.878	***	
isMar	7.45E-01	3.44E-02	21.642	***	
isApr	6.17E-01	3.65E-02	16.902	***	
isMay	1.35E-02	4.38E-02	0.309		
isJun	-2.49E+00	1.18E-01	-21.184	***	
isJul	1.13E+00	6.13E-02	18.502	***	
isAug	1.88E-02	3.87E-02	0.486		
isSep	1.85E-02	3.64E-02	0.51		
isOct	3.60E-01	3.41E-02	10.542	***	
isNov	5.39E-01	3.87E-02	13.929	***	
isDec	1.57E+00	1.08E-01	14.539	***	
sun.hours	6.30E-04	4.99E-05	12.617	***	Daily daylight length, DC [mins]
isFeb:isH1	2.94E-02	4.54E-03	6.474	***	
isFeb:isH2	3.16E-02	4.54E-03	6.966	***	
isFeb:isH3	3.40E-02	4.54E-03	7.483	***	
isFeb:isH4	3.58E-02	4.54E-03	7.88	***	
isFeb:isH5	3.75E-02	4.54E-03	8.259	***	
isFeb:isH6	4.06E-02	4.54E-03	8.939	***	

Variable	Estimate	Std. Error	t value	Significance	Notes
isFeb:isH7	4.15E-02	4.54E-03	9.139	***	
isFeb:isH8	3.38E-02	4.54E-03	7.456	***	
isFeb:isH9	3.47E-02	4.54E-03	7.645	***	
isFeb:isH10	3.13E-02	4.54E-03	6.888	***	
isFeb:isH11	2.77E-02	4.54E-03	6.106	***	
isFeb:isH12	2.42E-02	4.54E-03	5.324	***	
isFeb:isH13	2.12E-02	4.54E-03	4.675	***	
isFeb:isH14	1.90E-02	4.54E-03	4.179	***	
isFeb:isH15	1.67E-02	4.54E-03	3.678	***	
isFeb:isH16	1.22E-02	4.54E-03	2.695	**	
isFeb:isH17	-1.80E-03	4.54E-03	-0.396		
isFeb:isH18	-2.08E-02	4.54E-03	-4.584	***	
isFeb:isH19	1.29E-02	4.54E-03	2.848	**	
isFeb:isH20	1.84E-02	4.54E-03	4.051	***	
isFeb:isH21	2.00E-02	4.54E-03	4.403	***	
isFeb:isH22	2.13E-02	4.54E-03	4.693	***	
isFeb:isH23	2.30E-02	4.54E-03	5.076	***	
isFeb:isH24	2.53E-02	4.54E-03	5.569	***	
isH1:isMar	2.86E-02	4.42E-03	6.465	***	
isH2:isMar	2.71E-02	4.42E-03	6.126	***	
isH3:isMar	2.66E-02	4.43E-03	6.004	***	
isH4:isMar	2.71E-02	4.42E-03	6.143	***	
isH5:isMar	2.91E-02	4.42E-03	6.59	***	
isH6:isMar	3.70E-02	4.42E-03	8.378	***	
isH7:isMar	3.87E-02	4.42E-03	8.766	***	
isH8:isMar	4.10E-02	4.42E-03	9.294	***	
isH9:isMar	4.69E-02	4.42E-03	10.619	***	
isH10:isMar	4.77E-02	4.42E-03	10.795	***	
isH11:isMar	4.78E-02	4.42E-03	10.816	***	
isH12:isMar	4.71E-02	4.42E-03	10.674	***	
isH13:isMar	4.68E-02	4.42E-03	10.593	***	
isH14:isMar	4.64E-02	4.42E-03	10.498	***	
isH15:isMar	4.38E-02	4.42E-03	9.908	***	
isH16:isMar	3.60E-02	4.42E-03	8.163	***	
isH17:isMar	1.15E-02	4.42E-03	2.605	**	
isH18:isMar	-3.91E-02	4.42E-03	-8.847	***	
isH19:isMar	-4.31E-03	4.42E-03	-0.977		
isH20:isMar	2.86E-02	4.42E-03	6.465	***	
isH21:isMar	3.68E-02	4.42E-03	8.326	***	
isH22:isMar	3.57E-02	4.42E-03	8.073	***	
isH23:isMar	3.13E-02	4.42E-03	7.093	***	

Variable	Estimate	Std. Error	t value	Significance	Notes
isH24:isMar	2.67E-02	4.42E-03	6.045	***	
isH1:isApr	1.16E-02	4.48E-03	2.599	**	
isH2:isApr	-8.57E-04	4.48E-03	-0.191		
isH3:isApr	-1.03E-02	4.51E-03	-2.291	*	
isH4:isApr	-1.44E-02	4.48E-03	-3.209	**	
isH5:isApr	-1.68E-02	4.48E-03	-3.74	***	
isH6:isApr	-9.50E-03	4.48E-03	-2.122	*	
isH7:isApr	-4.69E-03	4.48E-03	-1.048		
isH8:isApr	9.13E-03	4.48E-03	2.039	*	
isH9:isApr	3.21E-02	4.48E-03	7.178	***	
isH10:isApr	4.73E-02	4.48E-03	10.555	***	
isH11:isApr	5.98E-02	4.48E-03	13.365	***	
isH12:isApr	6.93E-02	4.48E-03	15.469	***	
isH13:isApr	7.69E-02	4.48E-03	17.172	***	
isH14:isApr	8.28E-02	4.48E-03	18.502	***	
isH15:isApr	8.44E-02	4.48E-03	18.859	***	
isH16:isApr	7.70E-02	4.48E-03	17.194	***	
isH17:isApr	4.43E-02	4.48E-03	9.89	***	
isH18:isApr	-2.95E-02	4.48E-03	-6.597	***	
isH19:isApr	-4.54E-02	4.48E-03	-10.138	***	
isH20:isApr	-1.11E-02	4.48E-03	-2.486	*	
isH21:isApr	4.66E-02	4.48E-03	10.399	***	
isH22:isApr	5.28E-02	4.48E-03	11.788	***	
isH23:isApr	4.11E-02	4.48E-03	9.186	***	
isH24:isApr	2.47E-02	4.48E-03	5.521	***	
isH1:isMay	-2.65E-02	4.56E-03	-5.812	***	
isH2:isMay	-4.77E-02	4.56E-03	-10.455	***	
isH3:isMay	-6.37E-02	4.56E-03	-13.978	***	
isH4:isMay	-7.67E-02	4.56E-03	-16.82	***	
isH5:isMay	-8.53E-02	4.56E-03	-18.709	***	
isH6:isMay	-8.81E-02	4.56E-03	-19.331	***	
isH7:isMay	-9.21E-02	4.56E-03	-20.197	***	
isH8:isMay	-6.09E-02	4.56E-03	-13.356	***	
isH9:isMay	-2.11E-02	4.56E-03	-4.626	***	
isH10:isMay	1.01E-02	4.56E-03	2.223	*	
isH11:isMay	3.71E-02	4.56E-03	8.13	***	
isH12:isMay	5.92E-02	4.56E-03	12.994	***	
isH13:isMay	7.75E-02	4.56E-03	17.009	***	
isH14:isMay	9.32E-02	4.56E-03	20.442	***	
isH15:isMay	1.04E-01	4.56E-03	22.723	***	
isH16:isMay	1.03E-01	4.56E-03	22.628	***	

Variable	Estimate	Std. Error	t value	Significance	Notes
isH17:isMay	7.35E-02	4.56E-03	16.118	***	
isH18:isMay	-4.76E-03	4.56E-03	-1.045		
isH19:isMay	-3.53E-02	4.56E-03	-7.745	***	
isH20:isMay	-3.06E-02	4.56E-03	-6.721	***	
isH21:isMay	1.95E-02	4.56E-03	4.27	***	
isH22:isMay	4.21E-02	4.56E-03	9.243	***	
isH23:isMay	2.59E-02	4.56E-03	5.685	***	
isH24:isMay	1.37E-03	4.56E-03	0.3		
isH1:isJun	-1.33E-01	6.46E-03	-20.594	***	
isH2:isJun	-1.63E-01	6.46E-03	-25.214	***	
isH3:isJun	-1.88E-01	6.46E-03	-29.167	***	
isH4:isJun	-2.10E-01	6.46E-03	-32.541	***	
isH5:isJun	-2.28E-01	6.46E-03	-35.239	***	
isH6:isJun	-2.49E-01	6.46E-03	-38.536	***	
isH7:isJun	-2.67E-01	6.46E-03	-41.394	***	
isH8:isJun	-2.28E-01	6.46E-03	-35.286	***	
isH9:isJun	-1.68E-01	6.46E-03	-26.041	***	
isH10:isJun	-1.18E-01	6.46E-03	-18.229	***	
isH11:isJun	-7.30E-02	6.46E-03	-11.307	***	
isH12:isJun	-3.42E-02	6.46E-03	-5.288	***	
isH13:isJun	-1.52E-03	6.46E-03	-0.234		
isH14:isJun	2.60E-02	6.46E-03	4.024	***	
isH15:isJun	4.75E-02	6.46E-03	7.355	***	
isH16:isJun	5.42E-02	6.46E-03	8.385	***	
isH17:isJun	2.65E-02	6.46E-03	4.101	***	
isH18:isJun	-5.42E-02	6.46E-03	-8.397	***	
isH19:isJun	-9.27E-02	6.46E-03	-14.353	***	
isH20:isJun	-1.07E-01	6.46E-03	-16.592	***	
isH21:isJun	-9.39E-02	6.46E-03	-14.533	***	
isH22:isJun	-6.30E-02	6.46E-03	-9.746	***	
isH23:isJun	-7.39E-02	6.46E-03	-11.446	***	
isH24:isJun	-9.86E-02	6.46E-03	-15.263	***	
isH1:isJul	3.13E-02	4.90E-03	6.4	***	
isH2:isJul	-9.19E-04	4.90E-03	-0.188		
isH3:isJul	-2.99E-02	4.90E-03	-6.107	***	
isH4:isJul	-5.57E-02	4.90E-03	-11.372	***	
isH5:isJul	-7.88E-02	4.90E-03	-16.098	***	
isH6:isJul	-1.07E-01	4.90E-03	-21.945	***	
isH7:isJul	-1.48E-01	4.90E-03	-30.185	***	
isH8:isJul	-1.16E-01	4.90E-03	-23.785	***	
isH9:isJul	-4.95E-02	4.90E-03	-10.106	***	

Variable	Estimate	Std. Error	t value	Significance	Notes
isH10:isJul	1.15E-02	4.90E-03	2.349	*	
isH11:isJul	6.66E-02	4.90E-03	13.598	***	
isH12:isJul	1.15E-01	4.90E-03	23.4	***	
isH13:isJul	1.55E-01	4.90E-03	31.573	***	
isH14:isJul	1.87E-01	4.90E-03	38.222	***	
isH15:isJul	2.12E-01	4.90E-03	43.326	***	
isH16:isJul	2.21E-01	4.90E-03	45.119	***	
isH17:isJul	1.94E-01	4.90E-03	39.662	***	
isH18:isJul	1.14E-01	4.90E-03	23.296	***	
isH19:isJul	7.45E-02	4.90E-03	15.213	***	
isH20:isJul	5.32E-02	4.90E-03	10.871	***	
isH21:isJul	5.90E-02	4.90E-03	12.056	***	
isH22:isJul	8.59E-02	4.90E-03	17.552	***	
isH23:isJul	7.95E-02	4.90E-03	16.23	***	
isH24:isJul	6.15E-02	4.90E-03	12.557	***	
isH1:isAug	-1.60E-02	4.48E-03	-3.57	***	
isH2:isAug	-4.49E-02	4.48E-03	-10.022	***	
isH3:isAug	-7.22E-02	4.48E-03	-16.118	***	
isH4:isAug	-9.64E-02	4.48E-03	-21.53	***	
isH5:isAug	-1.18E-01	4.48E-03	-26.299	***	
isH6:isAug	-1.39E-01	4.48E-03	-31.018	***	
isH7:isAug	-1.74E-01	4.48E-03	-38.891	***	
isH8:isAug	-1.57E-01	4.48E-03	-35.129	***	
isH9:isAug	-9.56E-02	4.48E-03	-21.352	***	
isH10:isAug	-3.69E-02	4.48E-03	-8.232	***	
isH11:isAug	1.73E-02	4.48E-03	3.853	***	
isH12:isAug	6.52E-02	4.48E-03	14.567	***	
isH13:isAug	1.05E-01	4.48E-03	23.494	***	
isH14:isAug	1.38E-01	4.48E-03	30.847	***	
isH15:isAug	1.63E-01	4.48E-03	36.395	***	
isH16:isAug	1.71E-01	4.48E-03	38.156	***	
isH17:isAug	1.43E-01	4.48E-03	31.836	***	
isH18:isAug	6.06E-02	4.48E-03	13.53	***	
isH19:isAug	1.92E-02	4.48E-03	4.299	***	
isH20:isAug	4.13E-03	4.48E-03	0.922		
isH21:isAug	2.70E-02	4.48E-03	6.029	***	
isH22:isAug	3.24E-02	4.48E-03	7.246	***	
isH23:isAug	2.01E-02	4.48E-03	4.48	***	
isH24:isAug	3.15E-03	4.48E-03	0.704		
isH1:isSep	-2.96E-02	4.48E-03	-6.603	***	
isH2:isSep	-5.28E-02	4.48E-03	-11.8	***	

Variable	Estimate	Std. Error	t value	Significance	Notes
isH3:isSep	-7.29E-02	4.48E-03	-16.288	***	
isH4:isSep	-9.00E-02	4.48E-03	-20.102	***	
isH5:isSep	-1.04E-01	4.48E-03	-23.172	***	
isH6:isSep	-1.09E-01	4.48E-03	-24.309	***	
isH7:isSep	-1.06E-01	4.48E-03	-23.76	***	
isH8:isSep	-1.00E-01	4.48E-03	-22.41	***	
isH9:isSep	-5.75E-02	4.48E-03	-12.845	***	
isH10:isSep	-1.41E-02	4.48E-03	-3.152	**	
isH11:isSep	2.48E-02	4.48E-03	5.534	***	
isH12:isSep	5.79E-02	4.48E-03	12.928	***	
isH13:isSep	8.69E-02	4.48E-03	19.415	***	
isH14:isSep	1.12E-01	4.48E-03	25.011	***	
isH15:isSep	1.31E-01	4.48E-03	29.165	***	
isH16:isSep	1.35E-01	4.48E-03	30.26	***	
isH17:isSep	1.07E-01	4.48E-03	23.929	***	
isH18:isSep	2.63E-02	4.48E-03	5.865	***	
isH19:isSep	-5.96E-03	4.48E-03	-1.332		
isH20:isSep	2.19E-02	4.48E-03	4.892	***	
isH21:isSep	3.78E-02	4.48E-03	8.452	***	
isH22:isSep	2.63E-02	4.48E-03	5.871	***	
isH23:isSep	7.17E-03	4.48E-03	1.603		
isH24:isSep	-1.35E-02	4.48E-03	-3.014	**	
isH1:isOct	-1.58E-02	4.41E-03	-3.572	***	
isH2:isOct	-3.00E-02	4.39E-03	-6.834	***	
isH3:isOct	-4.09E-02	4.41E-03	-9.264	***	
isH4:isOct	-4.90E-02	4.41E-03	-11.094	***	
isH5:isOct	-5.28E-02	4.41E-03	-11.971	***	
isH6:isOct	-4.45E-02	4.41E-03	-10.078	***	
isH7:isOct	-2.13E-02	4.41E-03	-4.818	***	
isH8:isOct	-7.60E-03	4.41E-03	-1.723	.	
isH9:isOct	1.05E-02	4.41E-03	2.39	*	
isH10:isOct	2.83E-02	4.41E-03	6.42	***	
isH11:isOct	4.42E-02	4.41E-03	10.024	***	
isH12:isOct	5.70E-02	4.41E-03	12.915	***	
isH13:isOct	6.85E-02	4.41E-03	15.525	***	
isH14:isOct	7.82E-02	4.41E-03	17.723	***	
isH15:isOct	8.39E-02	4.41E-03	19.011	***	
isH16:isOct	8.04E-02	4.41E-03	18.219	***	
isH17:isOct	5.33E-02	4.41E-03	12.073	***	
isH18:isOct	-9.01E-03	4.41E-03	-2.043	*	
isH19:isOct	6.71E-03	4.41E-03	1.522		

Variable	Estimate	Std. Error	t value	Significance	Notes
isH20:isOct	3.96E-02	4.41E-03	8.976	***	
isH21:isOct	3.67E-02	4.41E-03	8.307	***	
isH22:isOct	2.87E-02	4.41E-03	6.505	***	
isH23:isOct	1.46E-02	4.41E-03	3.311	***	
isH24:isOct	-7.66E-05	4.41E-03	-0.017		
isH1:isNov	2.41E-03	4.51E-03	0.535		
isH2:isNov	-4.85E-03	4.50E-03	-1.076		
isH3:isNov	-9.05E-03	4.51E-03	-2.008	*	
isH4:isNov	-1.14E-02	4.51E-03	-2.529	*	
isH5:isNov	-9.98E-03	4.51E-03	-2.214	*	
isH6:isNov	-1.68E-03	4.51E-03	-0.372		
isH7:isNov	5.75E-03	4.51E-03	1.274		
isH8:isNov	6.81E-03	4.51E-03	1.511		
isH9:isNov	2.07E-02	4.51E-03	4.589	***	
isH10:isNov	2.84E-02	4.51E-03	6.288	***	
isH11:isNov	3.27E-02	4.51E-03	7.243	***	
isH12:isNov	3.67E-02	4.51E-03	8.132	***	
isH13:isNov	4.00E-02	4.51E-03	8.865	***	
isH14:isNov	4.29E-02	4.51E-03	9.508	***	
isH15:isNov	4.50E-02	4.51E-03	9.968	***	
isH16:isNov	4.59E-02	4.51E-03	10.186	***	
isH17:isNov	5.32E-02	4.51E-03	11.807	***	
isH18:isNov	5.24E-02	4.51E-03	11.63	***	
isH19:isNov	3.94E-02	4.51E-03	8.739	***	
isH20:isNov	3.54E-02	4.51E-03	7.86	***	
isH21:isNov	3.14E-02	4.51E-03	6.966	***	
isH22:isNov	2.61E-02	4.51E-03	5.798	***	
isH23:isNov	1.94E-02	4.51E-03	4.306	***	
isH24:isNov	1.15E-02	4.51E-03	2.553	*	
isH1:isDec	6.61E-02	6.13E-03	10.793	***	
isH2:isDec	5.80E-02	6.13E-03	9.457	***	
isH3:isDec	5.33E-02	6.13E-03	8.701	***	
isH4:isDec	5.13E-02	6.13E-03	8.377	***	
isH5:isDec	5.10E-02	6.13E-03	8.319	***	
isH6:isDec	5.08E-02	6.13E-03	8.289	***	
isH7:isDec	4.80E-02	6.13E-03	7.832	***	
isH8:isDec	4.83E-02	6.13E-03	7.879	***	
isH9:isDec	5.57E-02	6.13E-03	9.082	***	
isH10:isDec	5.85E-02	6.13E-03	9.54	***	
isH11:isDec	5.69E-02	6.13E-03	9.284	***	
isH12:isDec	5.56E-02	6.13E-03	9.073	***	

Variable	Estimate	Std. Error	t value	Significance	Notes
isH13:isDec	5.51E-02	6.13E-03	8.985	***	
isH14:isDec	5.54E-02	6.13E-03	9.048	***	
isH15:isDec	5.78E-02	6.13E-03	9.44	***	
isH16:isDec	6.27E-02	6.13E-03	10.231	***	
isH17:isDec	8.43E-02	6.13E-03	13.749	***	
isH18:isDec	9.31E-02	6.13E-03	15.199	***	
isH19:isDec	8.20E-02	6.13E-03	13.376	***	
isH20:isDec	8.16E-02	6.13E-03	13.31	***	
isH21:isDec	8.43E-02	6.13E-03	13.757	***	
isH22:isDec	8.79E-02	6.13E-03	14.35	***	
isH23:isDec	8.79E-02	6.13E-03	14.34	***	
isH24:isDec	7.92E-02	6.13E-03	12.922	***	
isFeb:sun.hours	-9.88E-04	6.12E-05	-16.132	***	
isMar:sun.hours	-1.26E-03	5.78E-05	-21.739	***	
isApr:sun.hours	-1.08E-03	5.87E-05	-18.32	***	
isMay:sun.hours	-3.03E-04	6.47E-05	-4.684	***	
isJun:sun.hours	2.66E-03	1.43E-04	18.647	***	
isJul:sun.hours	-1.58E-03	8.15E-05	-19.384	***	
isAug:sun.hours	-2.29E-04	6.01E-05	-3.82	***	
isSep:sun.hours	-2.20E-04	5.93E-05	-3.715	***	
isOct:sun.hours	-7.31E-04	5.81E-05	-12.582	***	
isNov:sun.hours	-1.02E-03	6.72E-05	-15.176	***	
isDec:sun.hours	-2.85E-03	1.93E-04	-14.738	***	

Linear model results

We use a non-parametric, additive model to account for the relationship between adjusted average daily temperature and hourly load (see Methods - Step 2). However, we also investigated the potential of using a linear model to account for the relationship. As discussed below, we found that using a linear fit worked well for the majority of hours, but considerably over-predicted loads during high temperature days. This over prediction led to the linear model over-estimating the probability of a supply shortage.

The linear model we used in the second step considered the maximum and minimum daily temperature (5–19). We divided days into heating degree days (HDD) and cooling degree days

(CDD), as is common in literature (5–20). The split temperature between HDD/CDD was set to minimize model error: for Tmax terms, the temperature was 20.6 °C. For Tmin terms, temperature was 7.2 °C. We then used a linear and quadratic term for both HDD and CDD temperatures in the regression (5–21).

Table D-2. Temperature calculations

$$Tmax_D = max\ Tadj_h, \quad \forall h \in D$$
$$Tmin_D = min\ Tadj_h \quad \forall h \in D \qquad (5–19)$$

$$Tmax.HDD = max(69 – Tmax_D, 0)$$
$$Tmax.CDD = max(Tmax_D - 69, 0)$$
$$Tmin.HDD = max(45 – Tmin_D, 0)$$
$$Tmin.CDD = max(Tmin_D – 45, 0) \qquad (5–20)$$

h = hour of the day
D = day of the year
$Tadj_h$ = hourly adjusted temperature
$Tmax_D$, $Tmin_D$ = daily max and min temperature [°F]

$$X = weekday + hour*month + holidays + Tmax.HDD + Tmax.CDD + Tmin.HDD + Tmin.CDD + Tmax.HDD^2 + Tmax.CDD^2 + Tmin.HDD^2 + Tmin.CDD^2 + daylightHours*month + Y \qquad (5–21)$$

As shown in Figure D-2 - Figure D-4, the linear model significantly over-predicts load during high-temperature days. This is because the linear model predicts exponential growth in load with increasing temperatures. However, load growth actually begins to slow once a average daily temperatures of ~27 °C are reached (Figure 5-2). This is likely because air conditioning loads start to saturate once temperatures are high enough. This overprediction of peak load hours causes the linear model to overstate LOLE (Figure D-5). Due to this bias in the linear model, we use a non-linear model in our main analysis.

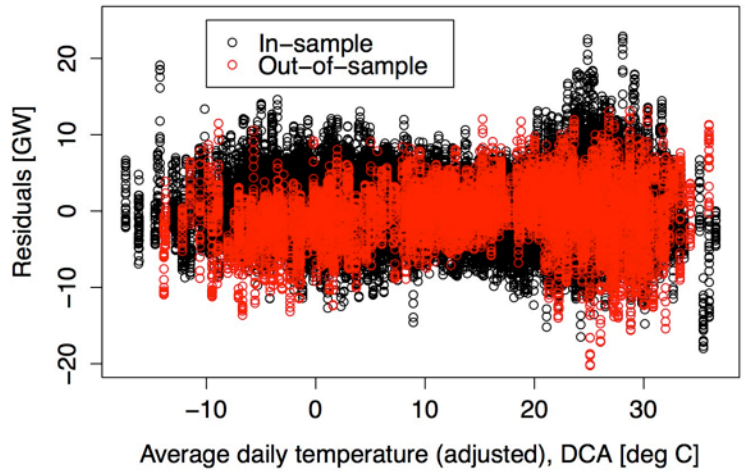

Figure D-2. In-sample and out-of-sample residuals for PJM, linear model. Residuals are large at high temperature days.

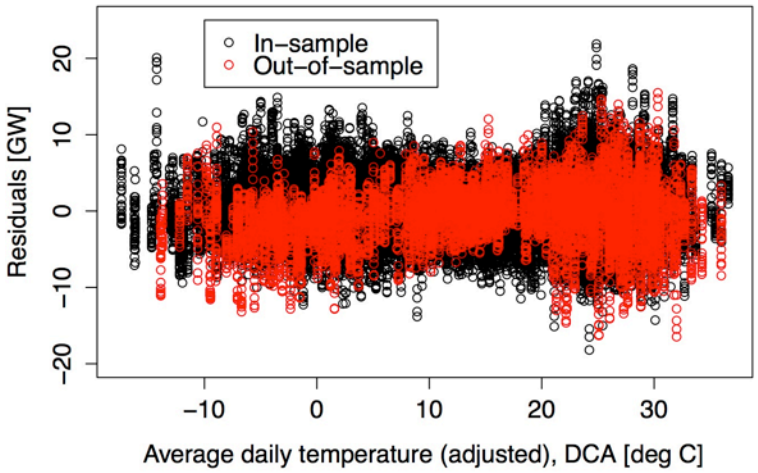

Figure D-3. In-sample and out-of-sample residuals for PJM, non-linear model. The model is more accurate at predicting load during high temperature days than the linear model.

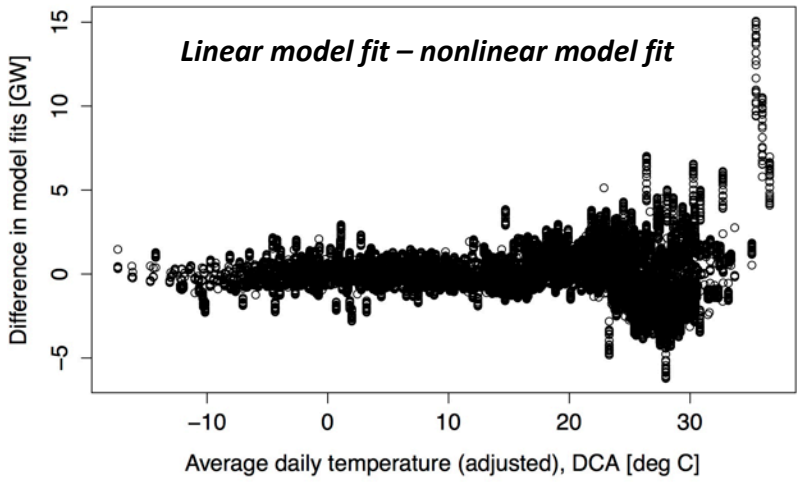

Figure D-4. Difference in linear and nonlinear model fits, when predicting load out-of-sample.

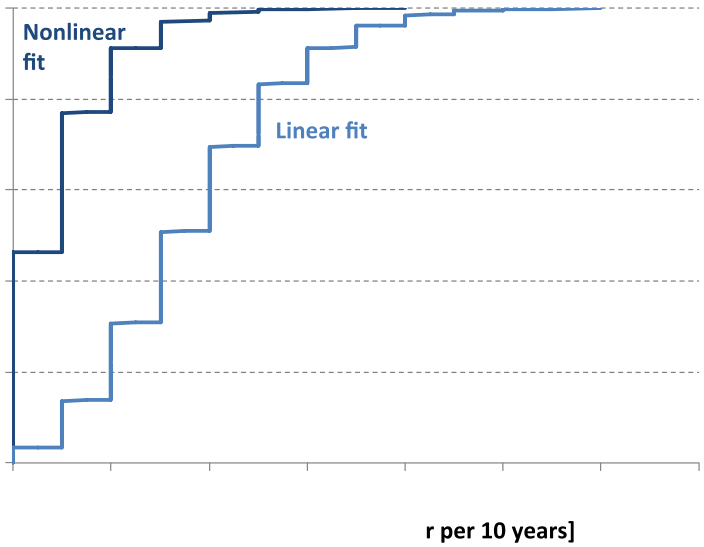

Figure D-5. Calculated LOLE for linear and nonlinear models

Temperature analysis

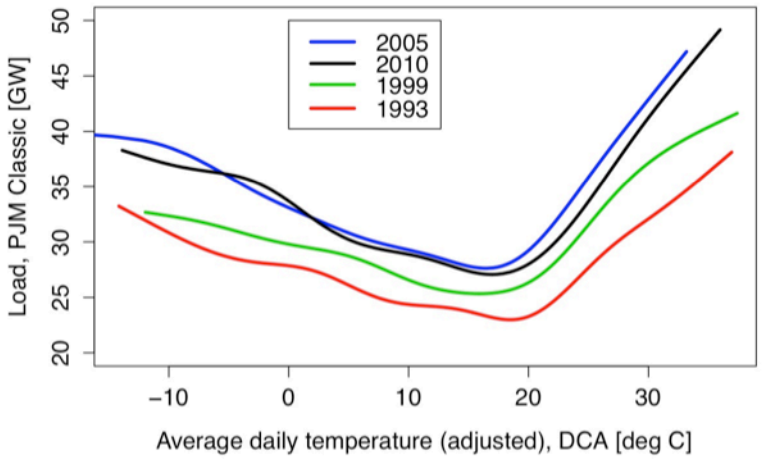

Figure D-6. Relationship between temperature and load, different years. Load in PJM has become increasingly responsive to high temperatures.

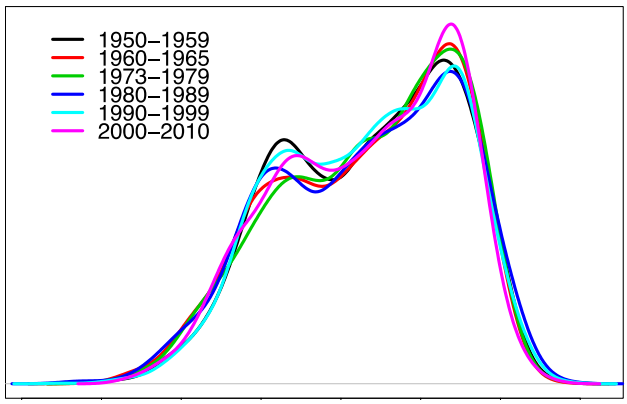

Figure D-7. Distribution of average adjusted daily temperature, by decade. Distributions are very similar across decade and show no evidence of a trend over time.

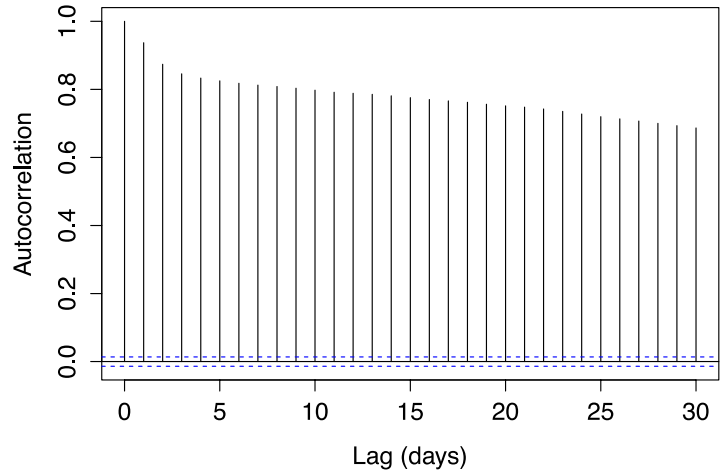

Figure D-8. Autocorrelation function, average adjusted daily temperature. Data is for years 1949 – 2010, except 1966 – 1972.

Residuals analysis

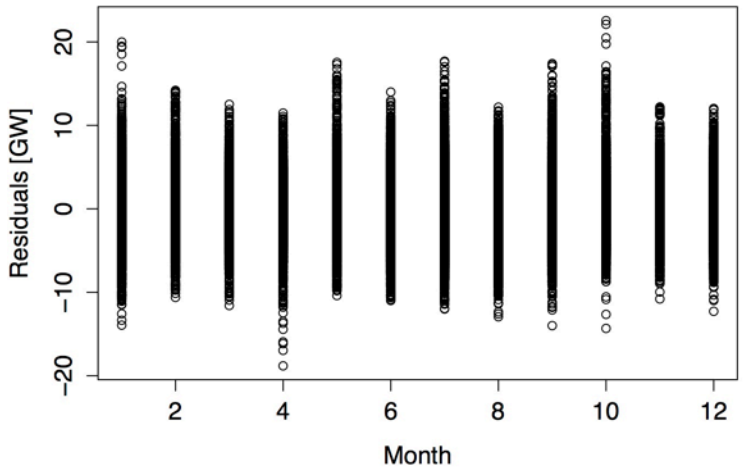

Figure D-9. In-sample residuals, by month

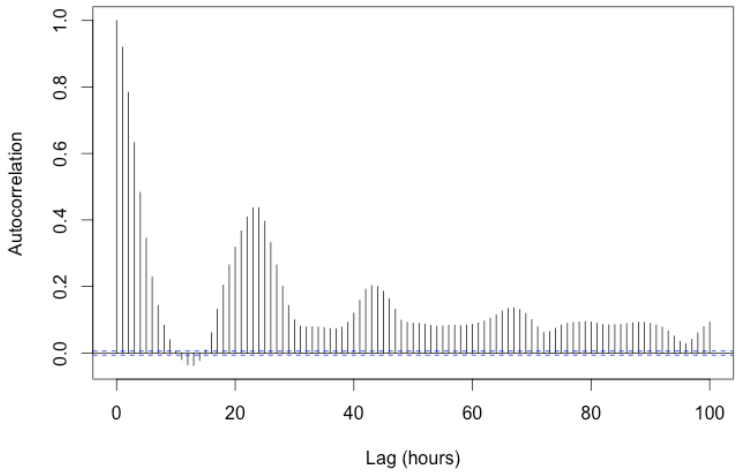

Figure D-10. Autocorrelation of in-sample residuals

LOLE sensitivity to forced outage rate

In our regressions, we hold each plant's forced outage rate (EFORd) constant throughout the year. Here we test the effects on LOLE of EFORd being sensitive to ambient temperature, rising 50% in the warmest 6 months (April – September) and dropping 50% in the coolest 6 months (October – March). To be clear, there is no evidence that EFORd does vary significantly from month to month or is correlated to ambient temperature. However, Figure D-11 shows varying EFORd in this extreme manner more than doubles the expected value of LOLE.

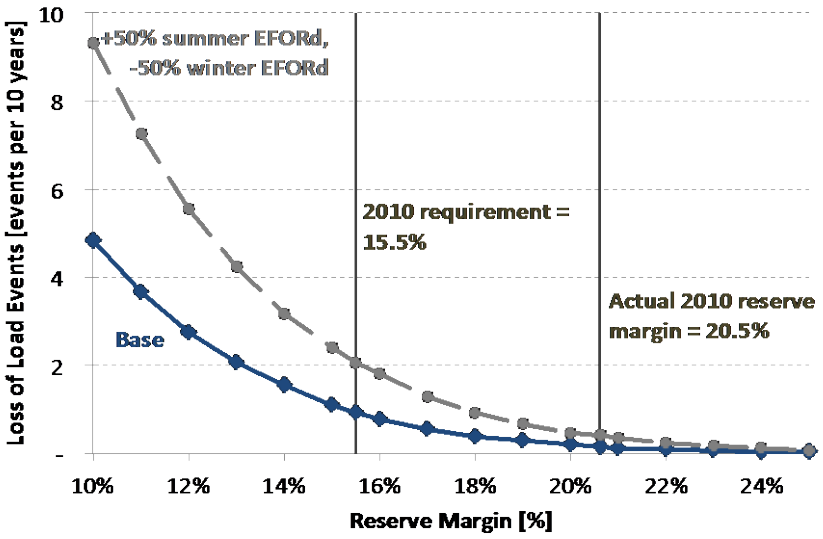

Figure D-11. Sensitivity of LOLE expected value to forced outage rate (EFORd).

Correlated outages

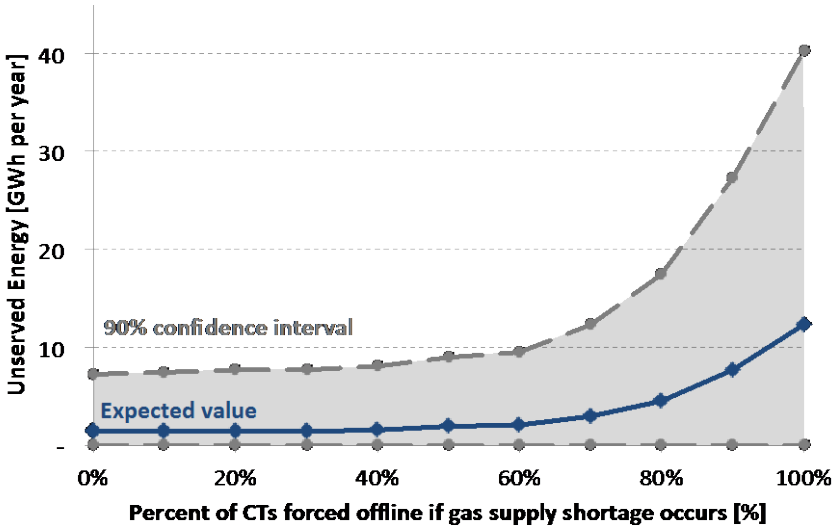

Figure D-12. Sensitivity of unserved energy to natural gas supply shortages that occur on average once per year. Evaluated at 15.5% IRM.

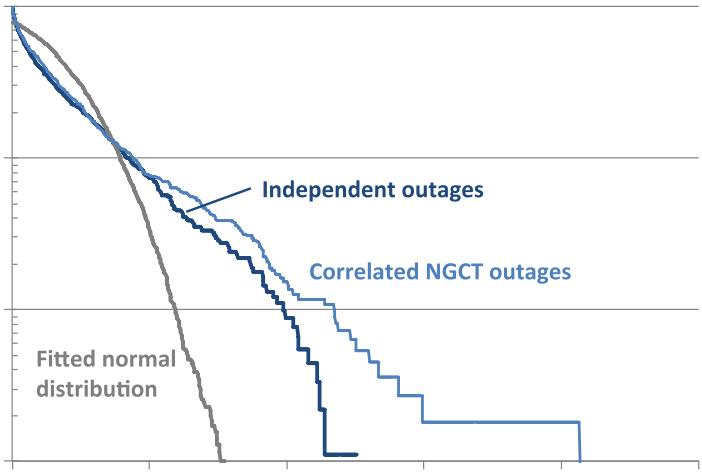

Figure D-13. Distribution of outage size, in terms of unserved energy. Shown are both scenario in which outages are independent, and a scenario in which a natural gas supply shortage occurs on average once per year, forcing 50% of NGCTs offline at once. Assumed reserve margin is 15.5%.

References

[1] Bresler, S. PJM. Personal communication, 2012.